# Influence of Green Corridor and Bridge Piers on River turbulence by Experimental and Numerical investigation

*Thesis submitted in partial fulfilment of the requirements for the award of the degree of*

Doctor of Philosophy

*in*

Centre for the Environment

*by*

MODALAVALASA SURESH

*with the supervision of*

Prof. Subashisa Dutta

&

Prof. Vinayak Kulkarni

Centre for the Environment
Indian Institute of Technology Guwahati
Guwahati – 781039, Assam, India

November, 2021

TH-2690_166152105

# Influence of Green Corridor and Bridge Piers on River turbulence by Experimental and Numerical investigation

MODALAVALASA SURESH

Indian Institute of Technology Guwahati

Centre for the Environment, Guwahati, Assam 781039

TH-2690_166152105


To

# The Indian Peninsular Rivers

TH-2690_166152105

# ACKNOWLEDGEMENTS

I feel delighted to present the dissertation on “Influence of green corridor and bridge piers on river turbulence by experimental and numerical investigation”. I want to convey my profound sense of gratitude to my supervisors, Prof. Subashisa Dutta and Prof. Vinayak Kulkarni, for the opportunity, support, guidance, and the trust they have conferred upon me to pursue research in this exciting field. Their advice and help have been of high value throughout the whole Ph.D. program. During my research, both the supervisors have provided me with the most precious ideas and resources that played a vital role in completing the thesis successfully. I enjoyed every moment working under their supervision and learned many things from them, which will be an asset for my future research.

I would also like to extend my heartful thanks to my doctoral committee members, Prof. Bimlesh Kumar (Chairman, Doctoral committee), Dr. Rishikesh Bharti, and Dr. Swarup Bag. Their constant support, and constructive criticism that has helped me to progress in my research work. I would also thank Prof. Utpal Bora, present Head of Centre for the Environment and past HOC’s Prof. Mihir Kumar Purkait and Prof. Vikash Kumar Dubey under whose administration I was able to carry out my research work in a collegial environment.

I thank my professor, Subashisa Dutta for not just introducing me to the field of hydraulics but also for great support throughout my PhD and especially in my difficult times. I have a full respect and affection towards him at every stage of my life. My sincere thanks to Vinay Chembolu, for staying my side for these 4 years and giving me emotional support and helping me in completing this research. Also big heartful thanks to lab members, Satish, Suman, Sridevi, Vinay, Anjaneyulu, Chandan, Riddick, Ketan, Lasya and Mridu Pawan for friendly cooperation and togetherness. And I also extended my sincere thanks to Lasya and Mridu Pawan for their helping hand. I would like to thank Bazal da for helping me in my experimental work. And also thank to Pankaj Lawande and Indian Flow3D team for supporting me when I struck in simulation work.

TH-2690_166152105

I would like to acknowledge Department of Civil Engineering at IIT Guwahati for giving the opportunity to do my research work and particularly experimental work carried out in the Fluvial hydro-ecological laboratory.

Thanks to my friends Mukesh, Viswanth, Venkatesh Reddy and Muni Raja for their friendship and affection towards me. Special thanks to Hemanth, Maharshi for your friendly love. Thanks to Amma, Nanna, Chelli, and my beloved wife and my children (little champs) Devashish and Dithya for their unconditional love and affection on me. Finally, I owe it all to God for granting me the wisdom, health and strength to undertake this research task and enabling me to its completion.

MODALAVALASA SURESH

TH-2690_166152105

# DECLARATION

I, Modalavalasa Suresh, author of the Ph. D. thesis "Influence of Green Corridor and Bridge Piers on River turbulence by Experimental and Numerical investigation" would like to certify that

- The work presented in this thesis is original research work carried out by me.
- The research work has not been submitted for any degree or diploma or any other qualification either in this institute or in any other university.
- Whenever I have used resources [theory, concepts, texts, data, graphs, figures or any other similar nature] from other sources, a due credit by citing in the text of the thesis is clearly made.
- The work presented here is free from plagiarism to the best of my knowledge, and I take the responsibility for any issues.
- I also affirm that thesis supervisor is not responsible for any possible instance of plagiarism within this submitted work.

Date: MODALAVALASA SURESH

Place: [166152105]

TH-2690_166152105

# Indian Institute of Technology Guwahati

Centre for the Environment, Guwahati, Assam 781039


Dr. Subashisa Dutta
Professor
Department of Civil Engineering
Email : subashisa@iitg.ac.in
Phone : +91-361-258-2415

Dr. Vinayak Kulkarni
Professor
Department of Mechanical Engineering
Email : vinayak@iitg.ac.in
Phone : +91-361-258-2655


## CERTIFICATE

This is to certify that thesis entitled "Influence of Green Corridor and Bridge Piers on River turbulence by Experimental and Numerical investigation" submitted by Modalavalasa Suresh, in partial fulfilment of the requirements for the award of degree of Doctor of Philosophy, to Indian Institute of Technology Guwahati, Assam, India, is a record of the bonafide research work carried out by him under my guidance and supervision at the Centre for the Environment, Indian Institute of Technology Guwahati, Assam, India. To the best of my knowledge, no part of the work reported in this thesis has been presented for the ward of any degree at any other institution.

Date: November 12th, 2021
Place: Guwahati

Prof. Subashisa Dutta

Prof. Vinayak Kulkarni

TH-2690_166152105

# ABSTRACT

Most of the Indian peninsular rivers are generally low sinuous rivers. The three-dimensional flow structures in curved channels control the hydrodynamic and morphological adjustments of the river system. In addition, physio-hydrological characteristics of the river, engineering interventions and river corridor vegetation alter the flow structure in these rivers. The flow-vegetation-sediment interactions and management of flood-plain vegetation can be helpful for morphological stability and ecological maintenance of the rivers. The present thesis aims to understand the hydraulics of the compound meandering channel of low sinuosity with the different cases of flood-plain vegetation under varying flow conditions. An experimental methodology is framed to investigate the (a) effect of flood-plain vegetation grasses of varying densities; (b) effect of heterogeneous forms of flood-plain vegetation; (c) combined effect of bridge pier and flood-plain vegetation; on turbulent structure in the main channel under emergent and submerged vegetation conditions. Further, an inter-comparison study is carried out between numerical model simulations and experimental results for evaluating the performance of CFD model in predicting the hydrodynamics structure with the influence of flood-plain vegetation in the meandering channel.

The first objective deals with the investigation of the effect of natural flood-plain vegetation grasses of varying densities (100, 150, 200 and 400 plants/$m^2$) under submerged vegetation conditions. The presence of higher density of flood-plain vegetation resulted in increased streamwise velocity up to 25% as compared to other vegetation layouts. The turbulent shear production near the channel-floodplain interface is observed to increase with increasing vegetation density. This resulted in an increase in turbulence parameters such as turbulence intensity, Reynold's stress and turbulent kinetic energy showing peak near the inner bank. Further, the floodplain vegetation shifts the flow structure into the

TH-2690_166152105

mainstream and thus creating more turbulence and altering distribution of velocity profiles. The variability of flow angle at cross-section apex, bend and crossover region is dominant under different flow conditions and vegetation densities. These findings provide better understanding of the effect of shear layer mechanism and momentum transfer in the main channel with the effect of floodplain vegetation.

The vegetation is often observed as patches of reeds, grasses and other heterogeneous plant forms in natural river environments. In the second objective, an experimental investigation on the turbulent flow characteristics in flood-plain vegetation patches of varying plant forms (leafy, grass, and cylindrical forms) in a staggered pattern. The results show that the presence of leafy vegetation patches increases the main channel velocities compared to other vegetation forms. The additional drag due to leafy vegetation increases the shear generated turbulence at the channel floodplain transition. The different floodplain vegetation forms are observed to change the cross-section distribution of velocity and turbulent fields at apex, bend and cross-over regions of the channel. Specifically, different plant forms significantly altered the velocity increments and momentum transfer between the floodplain-vegetation interface. Further, the flow angle is observed as 11°, 9°, 7.3° and 5.5° for leafy, mixed, grass and cylindrical vegetation respectively. However, the transverse flow motion and transverse surface gradient in the region of leading edge of the outer bank is enhanced by strengthening of secondary flows.

The understanding of flow and floodplain vegetation interaction is extended to study the hydrodynamic response of the sinuous river subjected to combined effect of bridge piers and vegetation cover over the floodplain. The results reveal the presence of bridge piers and vegetation roughness tends to cause more turbulence in the main channel of a river. At the channel-floodplain interface, the velocity gradient in the lateral direction increased with addition of bridge piers, thus forming a strong shear layer at that location. The provision of the large diameter pier additionally causes more secondary circulations in the main channel due to the combination of horseshoe vortex, shear vortex and curvature vortex resulting from bridge pier, vegetation elements and channel curvature. Further, the large diameter pier increases the main channel velocity up to 36% compared to smaller diameter pier, only vegetation and no-obstruction conditions on the floodplain.

The turbulence characteristics of sinuous channel with floodplain vegetation have been studied through laboratory experiments and numerical computations. Vegetation cover and bridge piers are incorporated in the CFD model, and hydrodynamic simulations are carried out for the turbulence characteristics. The results reveal the hydraulic parameters

TH-2690_166152105

such as primary and secondary flow velocities, and turbulent kinetic energy behavior in the main channel were captured by FLOW3D solver using the RNG (Renormalization-Group) turbulence model. Moreover, the analysis of turbulence statistics reveal the interaction of the main channel and floodplain flow were predicted well. These results obtained from the study have shown the capability of the RNG model to capture the shear layer mechanism and momentum transfer phenomenon at the channel-floodplain transition. The vegetation-bridge pier-flow response can be extended further by monitoring the process at field scale for river corridor management. The present thesis work provides a comprehensive understanding on the effect of floodplain vegetation of various scenarios on main channel turbulent characteristics of sinuous rivers.




TH-2690_166152105

# CONTENTS





TH-2690_166152105

TH-2690_166152105

TH-2690_166152105

# LIST OF FIGURES





TH-2690_166152105

TH-2690_166152105

TH-2690_166152105

# LIST OF TABLES





TH-2690_166152105

# LIST OF SYMBOLS

| Symbol | Description |
|---|---|
| $D_{50}$ | Representative diameter |
| Q | Discharge |
| H | Total flow depth |
| h | Floodplain depth |
| $F_r$ | Froud's number |
| g | Gravitational acceleration |
| Re | Reynold's number |
| R | Hydraulic radius |
| $A_{mc}$ | Area of the main channel |
| $R_{mc}$ | Main channel hydraulic radius |
| ν | Kinematic viscosity |
| $S_o$ | Slope |
| s | Sinuosity |
| α | Relative width ratio |
| β , $D_r$ | Relative flow depth |
| Θ | Flow angle |
| U, V, W | Time averaged velocity in streamwise, spanwise and vertical directions |
| u', v', w' | Fluctuating velocity in streamwise, spanwise and vertical directions |
| $U_m$ | Mean velocity |
| $U_*$ | Shear velocity |
| -u'w' or $RS_{u'w'}$ | Reynold stress in vertical direction |
| -u'v' or $RS_{u'v'}$ | Reynold stress in spanwise direction |
| -v'w' or $RS_{v'w'}$ | Reynold stress in streamwise direction |
| $u_{rms}$, $w_{rms}$ | Turbulence intensity in streamwise and vertical directions |
| $R_{mc}$ | Main channel hydraulic radius |



TH-2690_166152105

# LIST OF ABBREVIATIONS

| Terms | Description |
|---|---|
| ADV | Acoustic Doppler Velocimeter |
| CFD | Computational Fluid Dynamics |
| COR | Cross-over region |
| DNS | Direct Numerical Simulation |
| FAVOR | Fractional Area/Volume Obstacle Representation |
| LES | Large Eddy Simulation |
| RANS | Reynold's Averaged Navier-Stokes |
| RMS | Root Mean Square |
| RSS | Reynold's Shear Stress |
| RNG | Renormalization-Group |
| SCC | Secondary Current Cell |
| STL | Stereo Lithography |
| TI | Turbulence Intensity |
| TKE | Turbulent Kinetic Energy |



TH-2690_166152105

# 1

# INTRODUCTION

Most of the Indian peninsular rivers are generally low sinuous rivers (Pradhan et al., 2017). Determining the three-dimensional structures in curved channels has become one of the key challenges in river engineering. Natural river characteristics, including the protection of riverbank and floodplain vegetation, have further complicated the hydraulic design process. Moreover, channel-floodplain vegetation interactions are considered a fundamental part of the fluvial ecosystem (e.g., Newson 1992, Brookes 1996) to maintain the ecological health of waterways. In a river, the study of turbulence characteristics in the channel with the effect of floodplain vegetation is important to stabilize bank erosion control and maintain ecological balance. This thesis aims to work for understanding the river turbulence with the effect of floodplain roughness.

## 1.1 GREEN CORRIDOR OF THE RIVER SYSTEM

The riparian green corridor is a fundamental feature of natural riverine systems, and it has a significant impact on the river ecological system. In general, the vegetation is rigid or flexible depending on the plant characteristics and the flow conditions. The presence of floodplain vegetation significantly alters the flow field in terms of drag variation, changes in velocity distribution, and turbulence structures. Further, the flow structure in emergent and submerged vegetation widely differs due to vegetation interaction with flow depth at different scales (Shucksmith et al., 2010). Vegetation also alters local velocities, turbulence

TH-2690_166152105

intensities, turbulent Reynold's stresses, and vertical and horizontal distributions (Liu et al. 2008, 2010; Kubrak et al. 2008; Wilson 2007; Garcia et al. 2004; Stone and Shen 2002; Nepf 1999; Shimizu 1994). Many past studies focused on the flow structure affected by riparian vegetation zone; however, limited efforts were made to understand the impact of plant density on spatial turbulence features in a partially vegetated river with gradually changing flow conditions. Generally, the riparian vegetation consists of emergent aquatic plants, shrubs, and trees in the riparian zone. The majority of the research has been done in laboratory flumes with artificial, rigid (e.g., Bennett et al., 2002; Liu et al., 2008; King et al., 2012) or flexible type (e.g., Velasco et al., 2008; Chen et al., 2011) cylindrical vegetation, where flow complexities arising from plant morphology were ignored (Nepf, 1999; Tanino and Nepf, 2008; Siniscalchi et al., 2012). To study the effect of plant morphology on turbulence structure, Wilson et al. (2003) have conducted laboratory experiments on flexible vegetation with and without fronds. The present study attempts to understand the flow behavior with the effect of different floodplain vegetation layouts such as cylindrical vegetation, flexible grasses, leafy vegetation and mixed of above plant forms, which are mainly focused.

The design of bridge piers mainly depended upon the economic and structural point of view. But nobody considers the effect of bridge pier and surrounded with floodplain vegetation on main channel flow structures. Several authors like Kothayari et al.,1992; Koken 2008, Keshavarzi et al., 2014; Morales 2013; Lee 2019 have discussed about the turbulent flow and scour around the bridge piers. When bridge piers restrict the flow in an alluvial channel, dynamic pressure rises in front of the pier, resulting in an adverse pressure gradient from the free surface to the channel's bottom. As a result, flow separation occurs near the pier, resulting in the creation of vortices surrounding the pier (Narayana et al., 2021). Present study mainly focuses on how the main channel flow structures will get affected by the bridge piers along with floodplain vegetation.

The understanding of experimental results became easier using quasi measurement techniques. However, it comes with costs and the technological advantage of linked interdisciplinary expertise. In these cases, computational fluid dynamics plays a pivotal role. Previously, researchers have detailed studies on turbulence closure models, which have eased the process of turbulence modelling (Ferziger et al., 2002; Morvan et al., 2002; Morvan 2005). Furthermore, the major approach of these models on open channel flow has intimidated researchers with producing better results for a wide range of channels including complex geometries like meandering, gravel bed and complex flows in vegetation (Singh



TH-2690_166152105

et al., 2021; Rahimi et al., 2020; Cacqueray et al., 2009). Present study, numerical study on turbulence characteristics in the main channel effected by the presence of bridge piers and floodplain vegetation have been examined.

The main objective of this study is to provide comprehensive details of the low sinuous river of different flow depths by analyzing the relationship between secondary flow structures, turbulence intensities, turbulent kinetic energy and Reynold's shear stresses of a river. Also, most of the flow structure studies along the cross-section of the channel describe the flow structure within the layer of vegetation. The effects of the vegetated layer on the channel, however, are limited to the vegetated portion. Hence the study is motivated to investigate the flow features in the main channel with the effect of the green corridor with different vegetation densities with respect to spacing between them. From the results, to attain the optimum density of vegetation, our study has chosen four different configurations of vegetation. This research comprises various cross-sections of flow due to curvature of the channel and, with the impact of the green corridor, suits the best for studying the river channel behavior. This research contributes to understanding the hydrodynamic behavior of a sinuous river with different densities of homogeneous vegetation, flow through different vegetation patches, with the effect of obstructions (bridge pier) on the floodplain. In this study, an experimental investigation is conducted and analyzed the data measurements, and a computational fluid dynamic model is used for the hydrodynamic understanding of the river and green corridor.

## 1.2 AIMS AND SCOPE OF THE THESIS

Considering the research needs in flow-vegetation interactions with emphasis to sinuous river the following are the objectives outlined for the present research study.

- To study the effect of the homogeneous natural green corridor on hydrodynamic characteristics under emergent and submerged flow conditions in a sinuous river experimentally.
- To study the impact of the natural vegetation patches on hydrodynamic characteristics under submerged flow conditions investigated in an experimental flume.
- To study the combined effect of bridge piers and floodplain vegetation on main channel hydraulics and turbulence structures.



TH-2690_166152105

- To study the numerical investigation of effect of green corridor and bridge piers on river turbulence characteristics

## 1.3 ORGANISATION OF THE THESIS

The research work in this thesis is presented in seven chapters. The thesis focuses on understanding the hydrodynamic behavior of a sinuous river with different densities of homogeneous vegetation, natural vegetation patches, obstructions (bridge pier) on the floodplain through lab and modeling-based approaches. The thesis is separated into chapters based on the objectives of the current study. Primarily, the effect of the homogeneous green corridor on a hydrodynamic system of the river is studied through experimental analysis. This is followed by understanding the river turbulence characteristics with the effect of the natural vegetation patches by experimental study. The later chapter investigates the flow-bridge pier-vegetation interaction through a lab-based experimental study. Lastly, numerical modeling is carried out to evaluate the performance evaluation of the CFD model to predict hydrodynamic changes due to the presence of green corridor. The chapter-wise description of the thesis is

- *Chapter 1* discussed the overview of the green corridor system and hydrodynamic characteristics followed by aims and scope of the thesis.
- *Chapter 2* reports the review of literature carried on hydrodynamics and flow-vegetation interaction essential for the present investigation.
- *Chapter 3* deals with the experimental study on homogeneous natural green corridor on hydrodynamic characteristics under emergent and submerged flow conditions of the complex sinuous river system.
- *Chapter 4* deals with flow through vegetation patches on hydrodynamic characteristics under submerged flow conditions investigated in an experimental flume.
- *Chapter 5* deals with the experimental study on combined effect of bridge piers and floodplain vegetation on main channel hydraulics.
- *Chapter 6* deals with numerical investigation of effect of green corridor and bridge piers on river turbulence using a computational fluid dynamic model.
- *Chapter 7* summarizes the present research and suggests the future scope of the present work.



TH-2690_166152105

# 2

# REVIEW OF LITERATURE

The green corridor is an important component of dynamic river systems. Vegetation exerts influences on flow resistance, flood prevention, sediment transport and riverbed evolution. When flow passes through vegetation, the flow characteristics will be affected on the floodplain and main channel of the river. The drag forces cause the stem of vegetation to change its location via bending or vibrating. On the other hand, depending on the roughness and shape of the body and the configuration of vegetation densities, the drag force changes the velocity around them. Shape, rigidity, configuration and the height of the vegetation cover have a significant effect on the flow properties.

## 2.1 FLOW THROUGH GREEN CORRIDOR

The Green corridor changes flow structure and sediment transport and acts as a natural treatment facility by helping to purify the polluted water and maintain a good environment. The physical interaction of vegetation with water is usually considered at three different locations. i.e., the canopy height of the vegetation, just below the canopy and the stem of the plant and these locations are totally affected the velocity profile occurs in the channel. The vegetation is generally classified according to the flow conditions as emergent vegetation and submerged vegetation conditions in the water, and they create an interface for velocity profiles. Above the vegetation, the flow is similar as there is no friction or drag, whereas, within the vegetation, the velocity profile changes (Wu, Shen, & Chou, 1999). It is very well known that during flooding (fast flow), the

TH-2690_166152105

resuspension of sediment particles is unavoidable, primarily when the vegetation cover is sparsely distributed. On the other hand, dense vegetation will help to minimize the erosion of river banks and beds; thus, keeping river morphology as stable as possible.

In nature, rivers are in the form of a compound cross-section with one deep main channel and one or two adjacent floodplains at the sides (Myers 1978). The structure of flow around the vegetation was widely studied by laboratory and field experiments (Gambi, Nowell, & Jumars, 1990; Liu et al., 2008; Sand-Jensen & Pedersen, 1999). Hu et al., 2008 and Pujol et al., 2010 show in their experiment that the vegetation can considerably decrease the water flow velocity and the turbulence, respectively, as compared with that in non-vegetation zones (Ackerman & Okubo, 1993; Gambi et al., 1990; Pujol, Colomer, Serra, & Casamitjana, 2010). For open channels like rivers and streams with both smooth and rough beds, the power and/or logarithmic velocity distribution with different forms agrees well with the real cases in most of the studies. Mostly, the vertical velocity distribution is connected directly to the bed shear stress for the non-vegetation stream, while for a vegetated stream, it's mainly defined by the vegetation drag force since the vegetation roughness is much more than river bed roughness (Huai, Zeng, Xu, & Yang, 2009; Klopstra, Barneveld, Van Noortwijk, & Van Velzen, 1996; Righetti, 2008; Wilson, 2007). The resistance to flow due to vegetation cover has been studied by many researchers. The initial studies were based on adapting the Manning's roughness coefficient, n, to the flow parameters and attaining a value to "n" for representing the vegetation resistance (Petryk & Bosmajian, 1975).

Later, further studies on the effect of resistance or drag on flow structures are performed. Most of these studies were experimental and were focused on analyzing the impact of both rigid and flexible vegetation elements of flow structures (Cameron et al., 2013; Carollo, Ferro, & Termini, 2002; Hu et al., 2008; Stone & Shen, 2002; Türker, Yagci, & Kabdaşlı, 2006). In most of these studies the resistance to flow and the variations on velocity profile is defined by the help of drag coefficient via the empirical relationships. On the other hand, the flow characteristics of vegetal regions are also described by using the velocity and turbulent intensity profiles at a single point or at an average of several points (Nepf, 1999). The effect of bank vegetation on channel flow is recognized to be confusing hydrodynamics since the lateral exchange of momentum from banks to the mainstream generates interface flow between flow in the main channel and lateral effect of flow from banks (Shiono & Knight, 1991). The impact of bank vegetation changes with respect to the flow discharge, bank slope, vegetation density and etc.



TH-2690_166152105

However, these studies have provided an understanding of flow through the green corridor, limited their work to flow parameters surrounding floodplain vegetation.

## 2.2 FLOW - GREEN CORRIDOR - INTERACTIONS

Riparian green corridor development has a significant influence on river morphodynamics and plays a significant role in improving the river ecosystem (Gurnell et al., 2012). The importance of the riparian green corridor is recognized and is broadly used for river management. Vegetation causes the shear layer mechanism at the interface of the main channel and floodplain due to the velocity gradient and a significant momentum is exchange that leads to the generation of vortices and secondary current circulations (Shiono and Knight 1991, Tominaga and Nezu 1991, Myers et al., 2001, Bousmar 2002). When the flow exceeds the bankfull condition of the main channel, the faster flow interacts with the slow velocity in the floodplain vegetation, generating mixing shear layers near the interface between the main channel and the floodplain, which creates additional resistance. Many of the studies highlighted the vegetation arrangement, pattern (Nezu and Sanjou 2008, Chen et al., 2011) and effects of vegetation density (Li et al., 2014, Chembolu et al., 2019, Devi et al., 2016) on flow and turbulent structure. Experimental data from the U.S. Army and the UK Flood Channel Facility (FCF), (Ervine et al. 1993) discussed the determining factors in curved compound channels for conveyance capability. Shiono et al., 1999, Khatua et al., 2011, Shan et al., 2015 and Liu et al., (2014, 2016) proposed methods to estimate discharge and distribution of lateral velocity, including flow interaction between the main channel and the floodplain of a meandering channel. The secondary motions strongly rely on the geometry of the waterway; both the sinuosity of the channel and the cross-sectional shape influence these motions. The secondary cell circulation and their effects on the streamwise velocity distribution (Moncho Esteve et al., 2017, Sun and Shiono 2009) emphasize that the option of vegetation spacing when the vegetation is planted for bank safety at the edge of the floodplain is very critical for flood risk management. (Wang et al., 2015) studied vegetation and its effects on flow and sediment transport. Researchers highlighted that vegetation characteristics such as shape, height and flexibility have important impact on the structure of the flow, however, limited their work to artificial floodplain vegetation. These studies have provided an understanding of flow-green corridor interactions. However, they limited their work to presence of vegetation cover in a straight channel and one particular flow condition.



TH-2690_166152105

## 2.3 FLOW THROUGH HETEROGENEOUS GREEN CORRIDOR

Vegetation is the key component in a river-floodplain corridor which has a vital role in influencing the hydrodynamics, morphology and ecological characteristics of river systems (Brachet 2015). And vegetation can be found in a variety of forms on natural river corridors, and it is very significant for hydrologists and hydraulic engineers when conducting flood risk assessments, sediment transport studies, and designing river restoration plans (Bennett and Simon 2004, Aberle and Jarvela 2013, D'Ippolito et al., 2013, and Vargas-Luna et al., 2016). The investigation on the interaction between fluid flow and vegetation is a quite complex subject, due to both the different physical mechanisms that play a role in the phenomenon, and the biomechanical properties that characterize the diverse type of vegetation. The interactions between flow, vegetation, and sediment involve several fluvio-hydro-ecological variables (Hupp 2000, Hughes et al., 2001). In natural river-floodplain corridor, the vegetation is often observed as patches of reeds, shrubs, grasses of varying densities. The heterogeneous vegetation on floodplain plays an important role in planform stability by increasing the flow resistance and also provide spatial heterogeneity in the flow and turbulence field helpful for river ecology (Chembolu et al., 2019).

The recognition of importance of vegetation on planform stability and river ecological aspects has started in the recent decades (Gurnell 2014). Neary et al., 2012 stated that vegetation can significantly alter the bulk, time-averaged and instantaneous flow characteristics of turbulent flows, and these changes have major effects on sediment transport and morphology of the rivers. Chembolu et al., 2019 observed the clear distinction of velocity profile characteristics in flow through homogeneous and heterogeneous vegetation in straight channels. Further, the local and patch scale turbulent structure, variability in turbulence parameters like Reynolds stresses and turbulence intensities were also influenced by vegetation (Liu et al., 2008, 2010; Kubrak et al. 2008; Wilson 2007; Garcia et al., 2004; Stone and Shen 2002; Nepf 1999; Shimizu 1994). Gorrick and Rodriguez 2014, conducted series of laboratory experiments on low-sinuous and varying width channel to observe the changes in flow and turbulence structure with and without vegetation on outer banks. Literature review suggests that previous works present a good process-based understanding of flow and vegetation interactions. However, most of the works focused on reporting the flow results through homogeneous



TH-2690_166152105

vegetation in straight channels and further limited works on using natural heterogeneous vegetation for experiments.

## 2.4 FLOW- BRIDGE PIER- GREEN CORRIDOR INTERACTIONS

Generally, bridges will be seen on rivers with the surrounding green corridor system. However, the hydraulic engineers do not include the green corridor as a part of the river system. Evidently, these people considered the effect of bridge pier only but not assess the impact of the green corridor on turbulence characteristics of the mainstream. Further, the favorable conditions for constructing a bridge, the river should be straight at its upstream. When the river banks are stable and non-erodible, the bridge piers can also be placed at a curving part of the river. Although many studies were carried out the individual effect of flow resistance of green corridor and flow characteristics around bridge piers, none considered the combined effect of green corridor and bridge pier on flow features of a river. This study aims to estimate the shear layer mechanism resulting from green corridor and pier-like obstacles and the effect on the stream channel.

The flow around the bridge pier is completely three-dimensional and it is quite complex to predict the coherent structures (Raudkivi and Ettema 1983; Melville and Chiew 1999; Kirkil and Constantinesu 2008). On river bars and floodplains, vegetation is ubiquitous, and it can have a significant impact on flow, sediment transport rates, stream temperature, bank stability, and aquatic ecology. (e.g., Ormerod et al., 1993; McKenney et al., 1995; Abernethy and Rutherfurd 1998; Simon and Collison 2002; Pollen 2007). And the presence of floodplain vegetation plays an important role in the river system by improving the biological characteristics (Brachet 2015). Basic physical properties of vegetation, such as variations in drag, changes in streamwise velocity, turbulence patterns, the occurrence of periodic vortices, deposition distributions, increased flow resistance, and lower conveyance capacities, were discovered in their investigations (e.g., Nepf 1999, Lopez and Garcia 2001, Bennett et al., 2002, James and Makoa 2006 and Zong and Nepf 2011). Different flow fields are generated due to the interaction of approach flow with bridge piers, including downflow, horse-shoe vortex, wake vortices and bow waves, which result a complex flow field in the stream channel. Several authors like Kothayari et al.,1992, Koken 2008, Keshavarzi et al., 2014, Morales 2013, Lee 2019 have discussed about the turbulent flow and scour around the bridge piers. When bridge piers restrict the flow in an alluvial channel, dynamic pressure rises in front of the pier, resulting in an adverse pressure gradient from the free surface to the channel bottom. As a



TH-2690_166152105

result, flow separation occurs near the pier, resulting in the creation of vortices surrounding the pier (Narayana et al., 2021). The three-dimensional separated flows are typically composed of a complex system of vortices. Dargahi 1989 stated that the magnitudes of the vortices present around the vicinity of the cylinder are independent of Reynold's number, and it is mainly influenced by the diameter of the pier. Goutam et al., 2019 reported that compared to pier with and without pile cap, the flow structures such as mean velocities, turbulence intensities and Reynold's shear stresses are lower than the simple pier. However, most of the works focused on reporting the results of scour and turbulence structures around the pier and further very limited works focused on turbulence behavior in the main channel with the effect of floodplain obstructions for the experimental investigation.

## 2.5 NUMERICAL MODEL APPROACH

Numerical study is increased in past 10 years to better understand the hydrodynamic behavior of the fluvial studies. Development of 2D and 3D CFD models can be helpful for the investigation of hydrodynamic changes in a sinuous river along with different hydraulic structures and green corridor, at various cross-sections of the river. Abad et al., 2008 study is to assess the hydraulic performance of bendway weirs in a natural river at several flow stages. The three-dimensional velocity data collected at low flow depth within a meander bend containing bendway weirs are used to evaluate predictions of flow structure through the bend using a FLOW-3D 9.0 model. The validated model is then used to forecast the flow structure through the bend for medium and high-stage conditions. Flow structures in the meandering channel is more complex than the regular channels, though its complex three-dimensional nature. Vegetation in the riverine environment plays an important role in changes in the velocity distribution, turbulence patterns, formation of vortices, spreading deposition, extra flow resistance, and decreased conveyance efficiency. Several past studies have investigated the interaction between flow and flexible vegetation (Kouwen and Unny 1973; Temple 1986; Fathi-Moghadam and Kouwen 1997; Wu et al. 1999; Kouwen and Fathi-Moghadam 2000; Jarvela 2002; Carollo et al. 2002; Jarvela 2004; Armanini et al. 2005; Carollo et al. 2005; Righetti 2008; Aberle and Jarvela 2013). Liu et al. (2008) conducted the experiments to determine the velocity distributions and turbulence properties in vegetated channels. The experimental and numerical studies on flow through vegetation in open channels were



TH-2690_166152105

investigated by Shimizu 1994, Nepf 1999, Nepf and Vivoni 2000, Stephan and Gutknecht 2002, Neary 2003, Erduran and Kutija 2003, Stoesser et al., 2003, Defina and Bixio 2005, Choi and Kang 2004, Stoesser et al., 2010.

Nikora et al., 2007 stated that the main turbulent models for hydrodynamic applications can be divided into three categories:1) no averaging Direct Numerical Simulation (DNS) models; 2) spatial averaging of the Navier-Stokes equations of Large Eddy Simulation (LES) models; and 3) Reynolds Averaged Navier-Stokes (RANS) models with temporal averaging of the Navier-Stokes equations. And also mentioned that the DNS method is extremely expensive, particularly for complex geometries and heterogeneous cases at higher Reynolds numbers. Cui and Neary 2008 and Stoesser et al., 2009 used the LES approach to simulate flows influenced by aquatic vegetation. Huang et al., 2009 obtained the LES experimental results, which studied the effect of plant density on large-scale coherent structures inside the canopy sublayer. The $k$-$\varepsilon$ turbulence model has been used to simulate flows impacted by vegetation by Choi and Kang 2004, Fischer-Antze et al., 2001, López and García 2001, and Neary 2003. These studies demonstrate the model capabilities. However, the model still has some limitations due to configurable parameters and coefficients for flows with vegetation cover. Turbulent flow around a bridge pier is quite complex and that has been analyzed both computationally and experimentally by Melville and Raudkivi 1977; Dargahi 1990; Ahmed and Rajarantnam 1998; Ettema et al., 2006; Unger and Hager 2006; Dey and Raikar 2007; Kirkil et al., 2008. Chang et al., 1999 solved the flow equations around a bridge pier with a fixed bed and no scour using a large-eddy simulation (LES) model. Tseng et al., 2000 used the LES to run a numerical simulation for square and circular pier conditions. The flow patterns around a bridge pier with and without the scour hole were modeled by Richardson et al., 1998. And reported that the FLOW-3D fluid dynamic model accurately predicts the complicated flow patterns around the bridge pier when they analyzed the simulated and experimental data. However, most of the works focused on reporting the results of hydrodynamic change due to presence of vegetation cover in a straight channel is studied using three-dimensional computational fluid dynamic model and further very limited works focused on the development of numerical models applicable to simulate the turbulent characteristics in a sinuous channel



TH-2690_166152105

## 2.6 CHAPTER SUMMARY

The literature review on green corridor and river hydro-dynamics exposed that while studying the flow structure, earlier studies limited to understand the process mechanisms of a sinuous river with the green corridor. However, the river behavior and response of influence of green corridor with varying vegetation configurations and plant forms are yet to be understood. The knowledge of river behavior is limited and remained challenging. The literature review on flow-vegetation interactions reveals the necessity of understanding the flow structure in heterogeneous green corridors which are frequently observed over the riverine corridor. Different flow fields are generated due to the interaction of approach flow with bridge piers, resulting in a complex flow field in the stream channel.



TH-2690_166152105

# 3

# FLOW IN HOMOGENEOUS GREEN RIVER CORRIDOR

The Green corridor is an essential component of fluvial systems that comprises various socio-ecological mechanisms (Dufour et al., 2019) such as to maintain the ecological health of waterways since it helps to balance the oxygen ($O_2$), nutrients and sediment while also creating habitat and food for species. This green corridor nurtures along the banks of an estuary that extends to the floodplain's edge. The riparian zones of a river are covered with vegetation patches and this makes important to study vegetation influence on river turbulence. This chapter addresses the following questions through experimental study.

- How the flow features are get affected in a river with the impact of different configurations of homogeneous flexible vegetation?
- How do the turbulent structures behavior in the main channel for different flow and vegetation corridor conditions?

## 3.1 INTRODUCTION

Vegetation plays a significant role on ecology of a river corridor system. And also helpful for enhancing the physical features and ecological standards of the river corridor system (Wilson et al., 2003; Bennett and Simon 2004; Nepf and Ghisalberti 2008; Kondolf et al., 2013; Brachet et al., 2015; Gurbisz et al., 2016, 2017; Vargas-Luna et al., 2018; Lera et al., 2019). Bornette and Puijalon (2011) found that aquatic or riparian vegetation has a

TH-2690_166152105

substantial impact on riverine habitat, water quality (Dosskey et al., 2010), and pollutant and nutrient distribution (Perucca et al., 2009; Shucksmith et al., 2010), and sediment transport (Lopez and Gracia 1998; Jordanova and Jame 2003; Baptist 2003; Kothyari et al., 2009).

Rivers generate energy on the bed of their channel while water flows downstream. A cross section of a meander would show the channel is very deep and concave on the outside bend. This is because the outer bend is where the river flows more rapidly and is more energetic so there is a lot of erosion and abrasion takes place. Here the vegetation supports the ecology of a river corridor system in different aspects such as drag variation, changes in the velocity distribution, turbulence structures, incidence of periodic vortices, spreading deposition, extra flow resistance and decreased the conveyance efficiency. As a result of the velocity gradient and large momentum exchange, a shear layer forms at the interface of the main channel and floodplain, resulting in the formation of vortices and secondary current circulation (Shiono and Knight 1991, Tominaga and Nezu 1991, Myers et al., 2001 and Bousmar 2002). Floodplains are generally rougher than main channels. Owing to the development of various types of vegetation in different alignments and configurations, such as one-line, double layered vegetation and fully vegetated floodplain. When the flow in the main channel exceeds the bankfull condition, the faster flow interacts with the slower flow on the floodplain, generating mixing shear layers near the main channel-floodplain contact, which causes additional resistance. Many of the studies highlighted the vegetation arrangement, pattern (Nezu and Sanjou 2008, Chen et al., 2011) and effects of density of vegetation (Li et al., 2014, Devi et al., 2016) on flow and turbulent structure. According to Neary et al., 2012, a taxonomy that defines vegetated flows as dense, sparse, or isolated based on threshold criteria such as stem diameter and stem spacing ratio is useful for comparing studies among researchers and anticipating possible morphological trajectories. The flow in a meandering channel and a straight compound channel completely differs from each other. Ervine et al., 1993 examined the determining elements in curved compound channels for conveyance capabilities based on experimental data from the US Army and the UK Flood Channel Facility (FCF). Shiono et al., 1999, Khatua et al., 2011, Shan et al., 2015 and Liu et al., (2014, 2016) proposed methods to estimate discharge and distribution of lateral velocity including flow interaction between main channel and the floodplain of a meandering channel. The secondary motions strongly rely on the geometry of the waterway; both the sinuosity of the channel and the cross-



TH-2690_166152105

sectional shape, influence these motions. The secondary cell circulation and their effects on the streamwise velocity distribution is discussed by Moncho Esteve et al., 2017. Sun and Shiono 2009 highlighted that the option of vegetation spacing when the vegetation is planted for bank safety at the edge of the floodplain is very critical for flood risk management. Wang et al., 2015 studied about the vegetation and its effects on the flow and the sediment transport. They highlighted the characteristics of vegetation such as shape, height and flexibility have important effects on the structure of the flow. The main objective of this study is to provide an experimentally more comprehensive details of flow of low sinuous channel for different flow depths by analyzing the relationship between streamwise velocities, secondary flow structures, turbulence intensities, turbulent kinetic energy and Reynold's shear stresses of the channel. In addition, that the most of the flow structure studies along the cross-section of the channel describe the flow structure within the layer of vegetation. The effects of the vegetated layer on the channel, however, are limited to vegetated portion. Hence the study is motivated towards the investigation of the flow features in the main channel with the effect of floodplain vegetation with different densities with respect to spacing between the vegetation. From the result, to attain the optimum density of vegetation our study chosen four different configurations of vegetation layout.

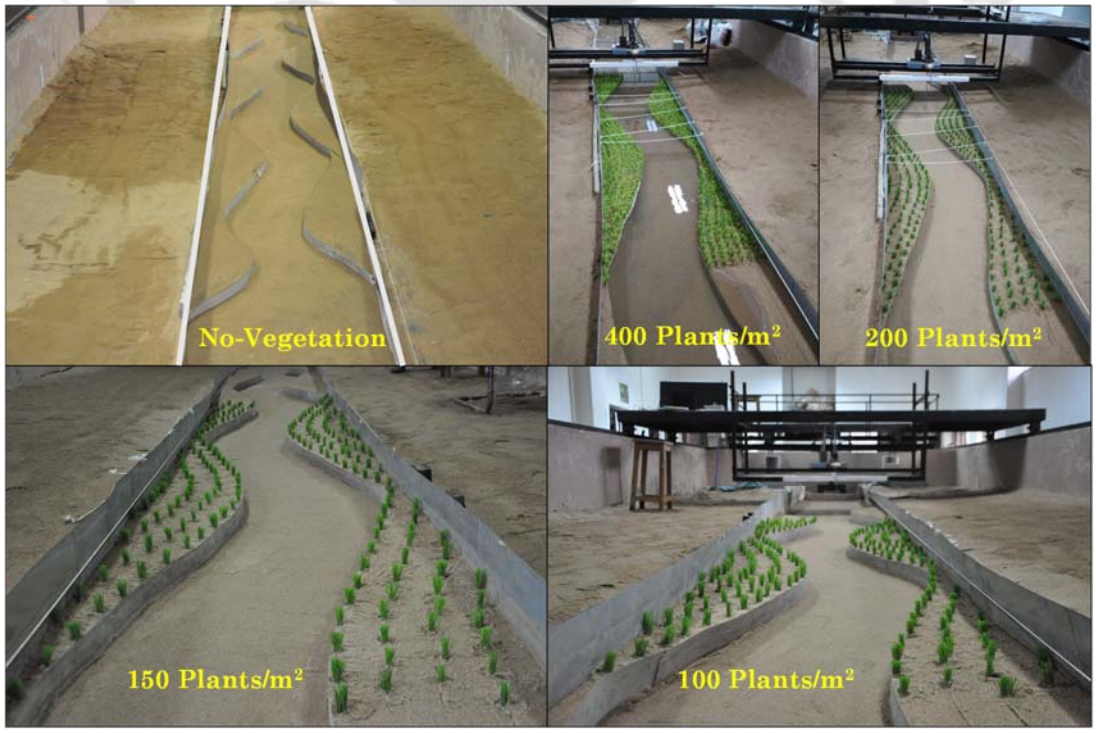


*Figure 3.1* Different experimental layouts used in the Fluvial hydro-ecological laboratory



TH-2690_166152105

## 3.2 MATERIALS AND METHODS

### 3.2.1 Experimental Setup

A series of experiments were conducted at the Fluvial hydro-ecological laboratory (Civil engineering department, IIT Guwahati) in 18 m long, 1 m wide and 0.3 m deep reinforced concrete flume filled with 1 m layer of river sand (Figure 3.1 (i)). Two 15 HP and one 3HP pumps were used to drive and recirculate the flow between 10,000 litres capacity of sump and the channel. Bed slope of the flume was maintained 0.001 throughout the experiments. The flume primarily consists of inlet chamber, stream channel, outlet chamber and recirculating system. A 4 m long, 1.5 m wide, and 1.5 m deep collecting chamber with concrete walls and roughness features was built upstream to reduce turbulence and straighten the incoming flow into the channel. Sinuosity has been taken for the channel is 1.1. Flow discharge is controlled by 3 pumps with 2-15 HP Pumps and 1-3HP pump with a maximum discharge of 35 litres/sec. The $D_{50}$ used for the sand distribution was 0.37 mm. The discharge was measured using a V-notch at the inlet of the flume, and the flow depth was measured using a digital point gauge. At a sampling frequency of 100 Hz, a three-dimensional acoustic Doppler velocimeter (4 probe, 10 MHz Vectrino ADV designed by Nortek) was used to get instantaneous velocity measurements. The duration of data acquisition was fixed to 2 minute and in total 10,000 samples were collected. The time series velocity data was post-processed using an accelerating threshold (Goring and Nikora, 2002) to remove the spikes. The 1.2 m long test segment was placed in the middle of the flume to reduce the impacts of upstream and downstream entry and exit. Natural rice plants (Oryza Sativa) were planted in various configurations along the test section, and laboratory experiments were conducted to determine the turbulence features.



TH-2690_166152105

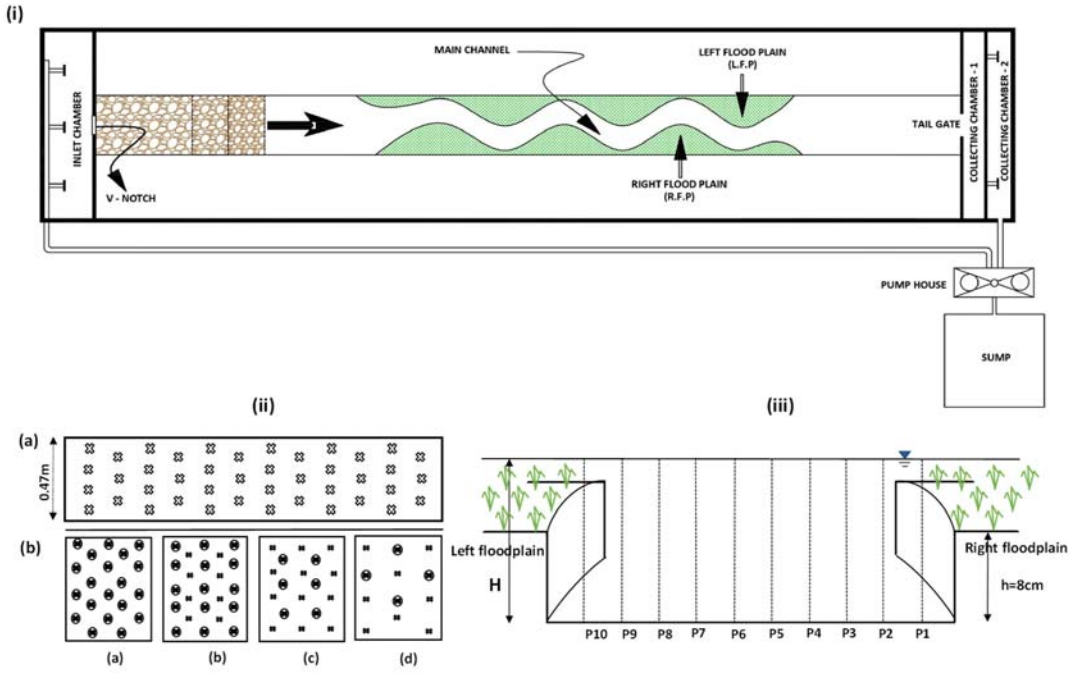


*Figure 3.2* (i) Flow chart of the water supply system presents in the Fluvial laboratory at IIT Guwahati, (ii) type of vegetation layouts/configurations experiments conducted, (iii) measurement locations at each cross-section.

### 3.2.2 Vegetation Types and Arrangement

Natural vegetation of rice grass (*Oryza sativa*-young rice plants of bladed type) was used in experiments. In total 8 experiments with different vegetation configurations (Figure 3.2 (ii)) and 2 experiments without vegetation were performed. All the plants were placed in a staggered pattern along the test section with a different density of 400, 200, 150, 100 plants/$m^2$. To carry out the experiments, four different vegetation layouts (Figure 3.1) were setup.

### 3.2.3 Flow Conditions and Measurement Locations

Experiments were carried out in both emergent and submerged flow conditions. Table 3.1 lists the hydraulic conditions are maintained in the channel, Table 3.2 shows the plant bio-physical properties and Figure 3.2 (ii) shows for different vegetation layouts. Figure 3.3, flow measurements were carried at 5 cross-sections like apex, bend and cross-over regions along 1.2m as a test section in the channel to study the effect of vegetation on flow and turbulent behavior. For experiments the measurement locations were positioned and shown in the Figure 3.1 (iii) these measurement locations are change in each cross-



TH-2690_166152105

section. Instantaneous velocity components were measured along the flow depth at an increment of 1 cm from the near bed at each measurement point in the main channel in every cross-section in the test section. Thus, more than 14 measurement points at each vertical profile were obtained.

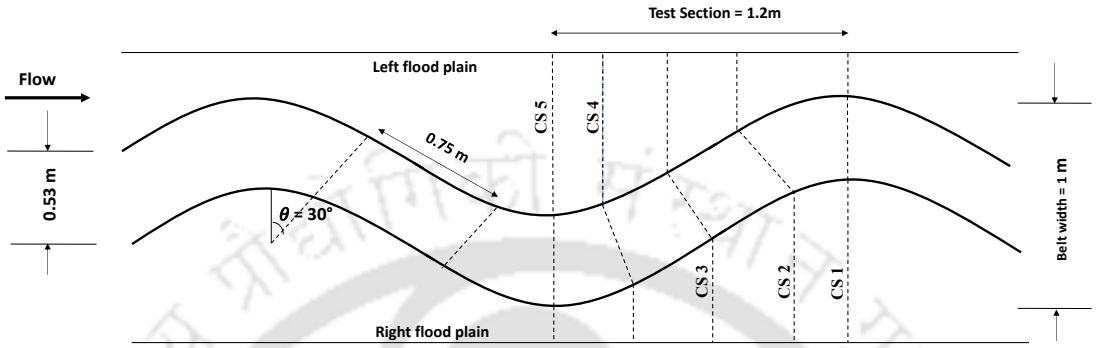


*Figure. 3.3* Plan view of the low sinuous channel and measurement sections for the test section

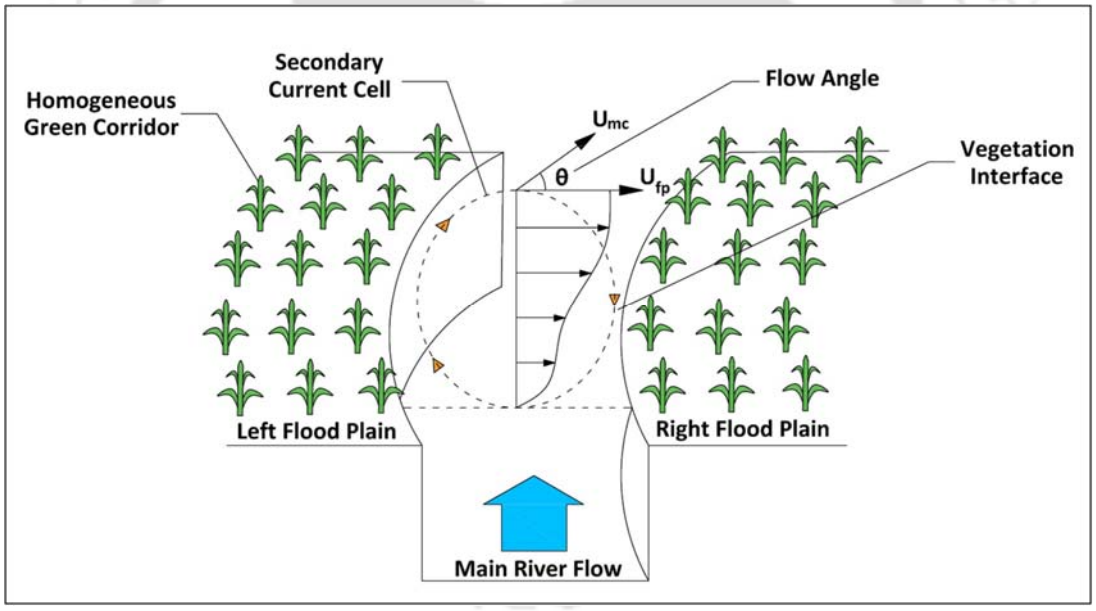


*Figure 3.4* Schematic diagram of secondary flow in the experimental channel



TH-2690_166152105

*Table 3.1:* Summary of the experiments

| H(cm) | h(cm) | α | β | Q (cumecs) | $A_{mc}$ ($m^2$) | $R_{mc}$ (m) | $u_*$ (m/s) | $U_m$ (m/s) | $F_r$ | Re |
|---|---|---|---|---|---|---|---|---|---|---|
| **11** | 8 | 1.88 | 0.27 | 0.008688 | 0.06 | 0.07 | 0.026 | 0.14 | 0.17 | 11000 |
| **14** | 8 | 1.88 | 0.43 | 0.01536 | 0.07 | 0.09 | 0.029 | 0.20 | 0.21 | 18000 |

Note: Q is the total discharge, α = B/b, Relative flow depth β = (H-h)/h, Sinuosity- 1.1, H is the total flow depth of the main channel, $U_m$ is the mean streamwise velocity at the apex section, $u_* = \sqrt{gR_{mc}(\frac{S_o}{s})}$ is the shear velocity in the main channel, where 'g' gravitational acceleration, '$R_{mc}$' main channel hydraulic radius, '$S_o$' averaged bed slope and '$s$' is the channel sinuosity. $F_r = U_m/\sqrt{gR}$, $Re = U_m R/\nu$, ν is Kinematic viscosity = 0.01$cm^2/s$. 'R' hydraulic radius at apex (Liu et al., 2016).

*Table 3.2*: Plant Parameters/ Bio- Physical properties

| S. No. | Plant form | Plant Parameter | Value |
|---|---|---|---|
| **1** |  | Average Plant Height | 6cm |
| **2** | | Average blade width | 2mm |
| **3** | | Approx. No. of Strands per plant | 12 |
| **4** | | Average Deflected Height ($h_d$) | 0.5cm |
| **5** | | Projected Area | 7.2$cm^2$ |
| **6** | | Plant flexibility ($h_d$/h) | 0.0625 |



TH-2690_166152105

*Table 3.3*: Details of channel geometry

| S. No. | Parameter | Description |
|---|---|---|
| **1** | Type of Channel | Simple meandering |
| **2** | Flume dimensions (m) | 18 X 1 X 0.3 |
| **3** | Meandering Channel geometry | Compound section with side slopes 1:1 |
| **4** | Type of bed surface | (No transport condition) Rigid and Main channel- Smooth, FP- rough |
| **5** | Section of channel | Compound channel |
| **6** | Bankfull Depth (m) | 0.08 |
| **7** | Bed Slope of the channel | 0.001 |
| **8** | Sinuosity of the channel | 1.1 |
| **9** | Angle of arc Φ (°) | 60 |
| **10** | Meander wavelength $L_w$ (m) | 2.4 |
| **12** | Flood plain Width $B_w$ (m) | 0.47 |
| **13** | Bend radius $r_c$ (m) | 0.40 |
| **14** | Crossover length $L_{co}$ (m) | 0.75 |
| **15** | Channel width $B_{mc}$ (m) | 0.53 |
| **16** | Amplitude/Width (R) | 0.40 |
| **17** | Belt width (m) | 1 |
| **18** | Radius of curvature(m) | 0.665 |
| **19** | Bend length (m) | 1.21 |



TH-2690_166152105

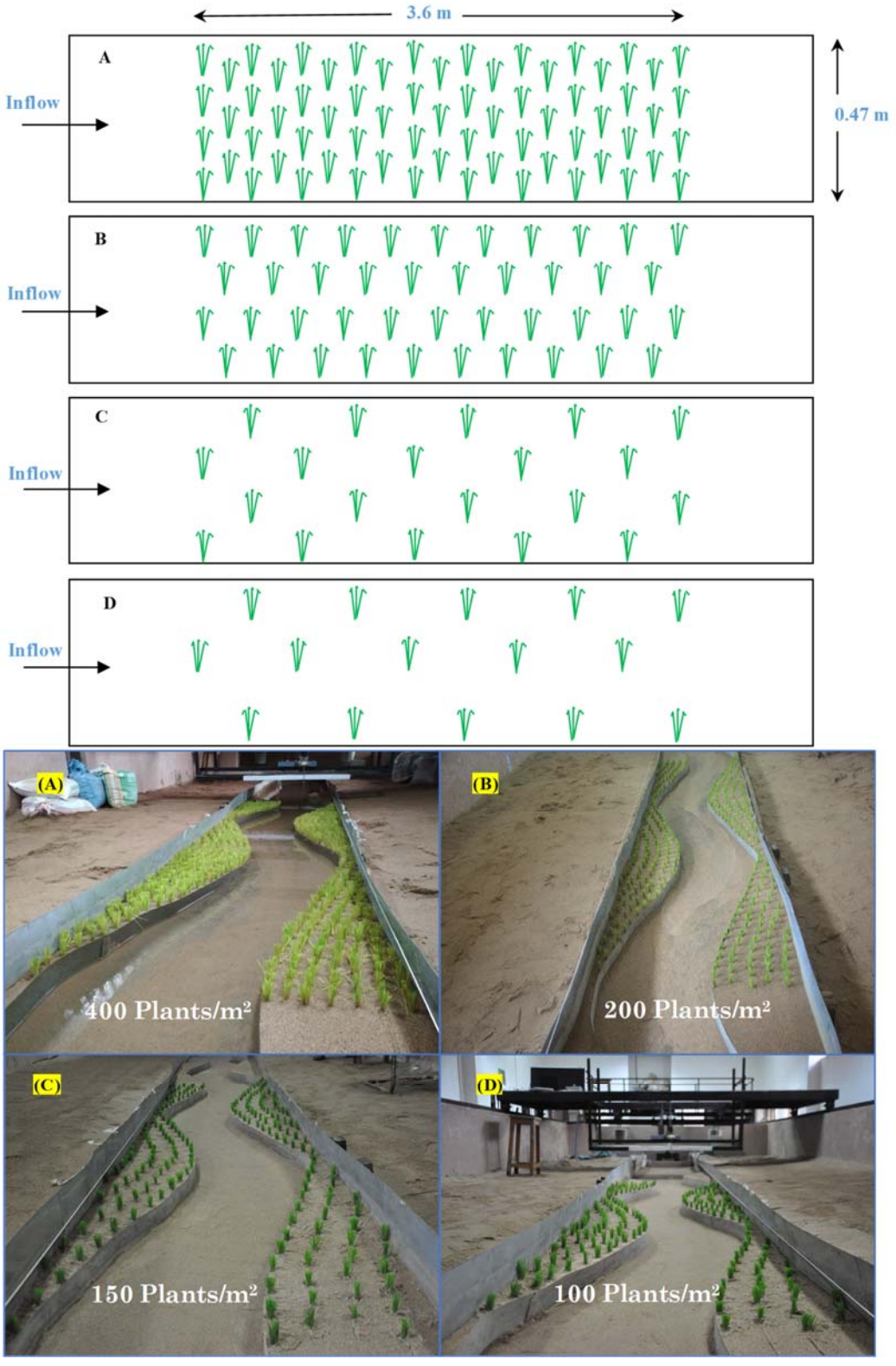


*Figure 3.5* Sketch for representation of vegetation patch layouts.



TH-2690_166152105

*Table 3.4*: Trend of turbulence parameters for submerged condition

| Turbulence characteristics | 100 Plants/m$^2$ | 150 Plants/m$^2$ | 200 Plants/m$^2$ | 400 Plants/m$^2$ |
|---|---|---|---|---|
| Streamwise velocity | 10% | 16% | 18% | 23% |
| Secondary velocity | 16% | 19% | 20% | 22% |
| Turbulence Intensity ($u_{rms}$) | 5% | 9% | 11% | 18% |
| Reynold's shear stress (-$u'w'$) | 11% | 21% | 27% | 39% |
| Turbulent kinetic energy | 12% | 15% | 19% | 25% |

### 3.2.4 Turbulence term definitions

A representative selection of velocities from despiked and ADV measurements of streamwise (u), cross-stream (v) and vertical velocity (w) were used to calculate time averaged components $\overline{U}$, $\overline{V}$ and $\overline{W}$ from which fluctuating components ($u'$, $v'$and $w'$) were determined. Liu et al. (2016) utilizes the turbulence parameters followed by the turbulence intensities (σ) in a specific direction can be calculated $\sigma_x = \sqrt{\overline{u'^2}}$. Where $\sqrt{\overline{u'^2}}$ (root-mean square of the time series of stream wise velocity fluctuations). Reynold's shear stresses were calculated with fluctuated averaged velocities using the equation $\tau_{xz} = -\overline{\rho u' w'}$. Here ρ is the density of water; u′and $w'$are the fluctuating velocities in $x$ and $z$ direction, respectively. The factor TKE was estimated by using the formula, $TKE = \frac{1}{2}\left(\overline{u'}^2 + \overline{v'}^2 + \overline{w'}^2\right)$.

## 3.3 RESULTS

### 3.3.1 Homogeneous Flexible Green Corridor

#### Streamwise velocities

This section discusses the variability in longitudinal streamwise velocity profiles of a sinuous channel with flood-plain vegetation of different densities and without vegetation. The velocity measurements were measured using ADV at different cross-sections (CS1 to CS5) along test section. Figure 3.6 shows the normalized velocity ($u/u_*$) contours at apex (CS1) with flood-plain vegetation of different densities for two flow depth scenarios of



TH-2690_166152105

$D_r$=0.27 and 0.43. In both the depth scenarios, the maximum core magnitude is found near the inner bank (Y/h= 5) at apex section. For submerged floodplain vegetation ($D_r$=0.43), the velocity magnitude increases by 10%, 16%, 18% and 23% with increase in vegetation densities from 100, 150, 200 and 400 plants/m$^2$ relative to no-vegetation scenario (Table 3.4). Under emergent conditions ($D_r$=0.27), this difference in velocity magnitude was less predominant with increased vegetation densities. The mean velocity of streamwise velocity is around $7u_*$ for higher floodplain depth with all the vegetation densities with increasing order from 100 to 400 plants/m$^2$. The average streamwise velocity for higher floodplain depth increases with increasing density of vegetation. However, in the higher floodplain depth the mean velocity in no-vegetation condition is less than to the vegetation cases. A strong velocity gradient is observed in the high vegetation density scenario *i.e.,* 400 plants/m$^2$ because of flow diversion from floodplain to the main channel. Figure 3.6 (II) shows the increased magnitude of velocity in main channel with increasing vegetation densities under submerged conditions. In emergent condition ($D_r$=0.27), there is no significant difference in velocity contours observed among varying densities. However, in general trend, there is increase in velocity with increase in flood-plain vegetation densities. The presence of lower velocity zones at the outer bank and maximum velocity cores at inner bank were observed to be similar for all the cases of flood-plain densities. Further, throughout the channel the large regions of maximum velocity are observed which indicates that the flow in meandering channel with lower flood-plain depth is dominant in longitudinal direction. In both the cases of emergent ($D_r$=0.27) and submerged ($D_r$=0.43) case, the increased flood-plain resistance is created with increase in vegetation density resulted in higher velocity magnitude in the main channel.



TH-2690_166152105

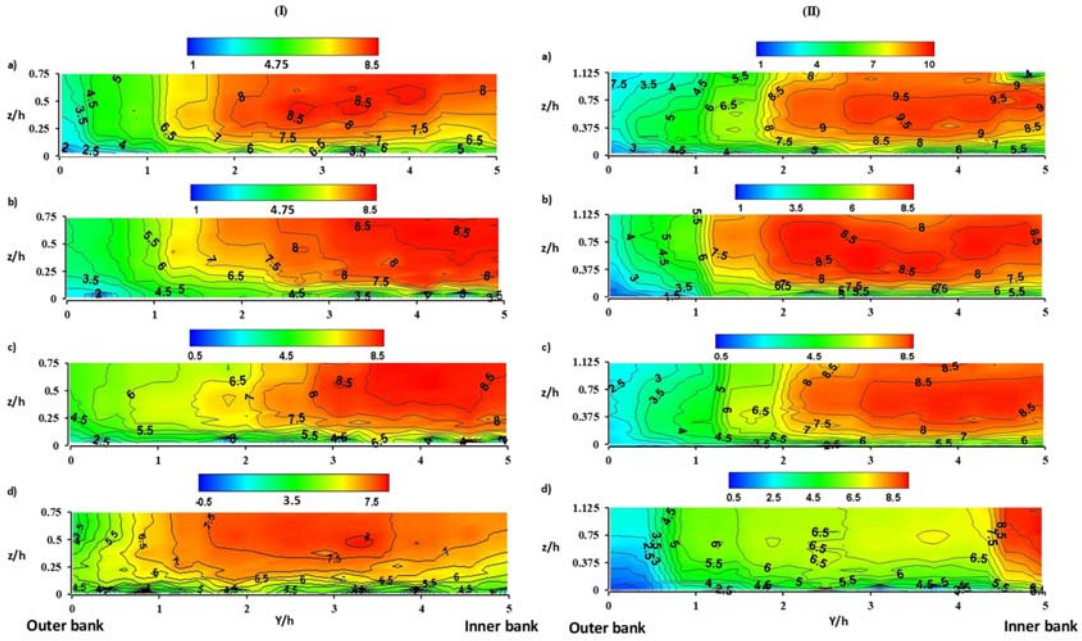


*Figure 3.6* Normalized contour plots of streamwise velocities ($u/u_*$) for the relative flow depths *(I)* $D_r$=0.27 and *(II)* $D_r$=0.43 of apex section (CS1) *a)* 400 plants/m$^2$ *b)* 200 plants/m$^2$ *c)* 150 plants/m$^2$ *d)* 100 plants/m$^2$

## Secondary Velocities

Figure 3.7 shows the velocity vectors ($v'$, $w'$) of the secondary currents and the background color represent the cross-stream velocity ($v'$) in the experimental channel under submerged conditions ($D_r$= 0.43) with vegetated and non-vegetated flood plain. It is observed that the magnitude of secondary velocity vectors increases with increase in vegetation densities. Further, this magnitude of secondary velocity vector is greater at cross-over regions followed by bend and apex regions for any vegetation density. On the other hand, the secondary circulations the scenario is quite different. In no-vegetation case, because of the free flood-plain surface and side bank, there was a turbulence anisotropy along the side wall of the main channel that transfers the flow into the main channel and the pair of vortices were created at the free surface and at the bottom of the channel. As the presence of flood-plain vegetation imposes the flow resistance and increases turbulence, in compare to non-vegetated condition the pattern of secondary flow has changed significantly in vegetation cases. Figure 3.8 (I, II) shows the secondary flow in $D_r$ = 0.27 and 0.43 conditions at apex-section for different densities. In both the scenarios, the magnitude of secondary velocity is observed higher at the outer bank for all the vegetation densities. However, the secondary cell circulations are noticed mostly near the outer bank for high



TH-2690_166152105

density flood-plain vegetation conditions (400 and 200 plants/$m^2$). Further, the experiments were conducted in low sinuous channel that resulted in reduced the strength of secondary circulation cells as compared to the high sinuous channel.

The cross-stream velocity ($v'$) and vertical component ($w'$) of velocities were smaller compared to streamwise velocities. In compared to no-vegetated channels the fluctuating component of cross-stream velocity ($v'$) has increased in emergent condition ($D_r$=0.27), and at submerged condition ($D_r$=0.43) the fluctuated values were low. In submerged condition ($D_r$=0.43), the maximum magnitude of secondary velocity vectors are 22%, 19%, 18%, 16% and 12% of the maximum streamwise velocity for 400, 200, 150, 100 plants/$m^2$ and no-vegetation respectively. That is, the magnitude of secondary currents is strengthened as the vegetation density increases in higher floodplain flow depth. Further, the angle of inclination of secondary currents in higher floodplain flow condition are about 2°, 6°, 6.5° and 7.3° for 100, 150, 200 and 400 plants/$m^2$, respectively. The inclination angle of the flexible grasses increases with the increasing of the density of vegetation. The arrangement of vegetation on the floodplain has significant influence on the flow distribution in the channel.



TH-2690_166152105

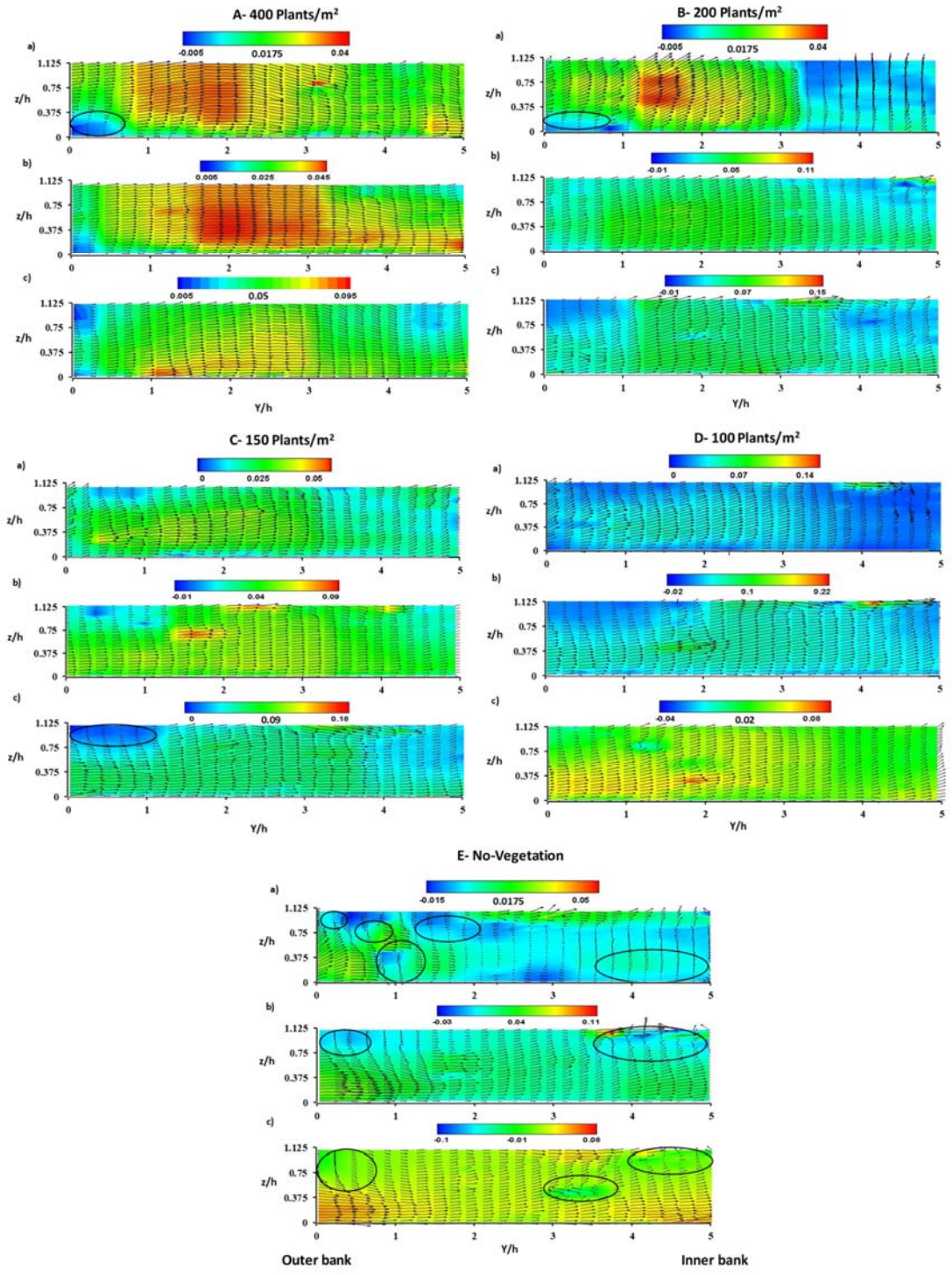


*Figure 3.7* Secondary velocity plots for the flow depth of 14 cm ($D_r$ = 0.43) vegetation with different densities and non-vegetated condition at *a)* apex section (CS1); *b)* bend section (CS2); *c)* cross over region (CS3)



TH-2690_166152105

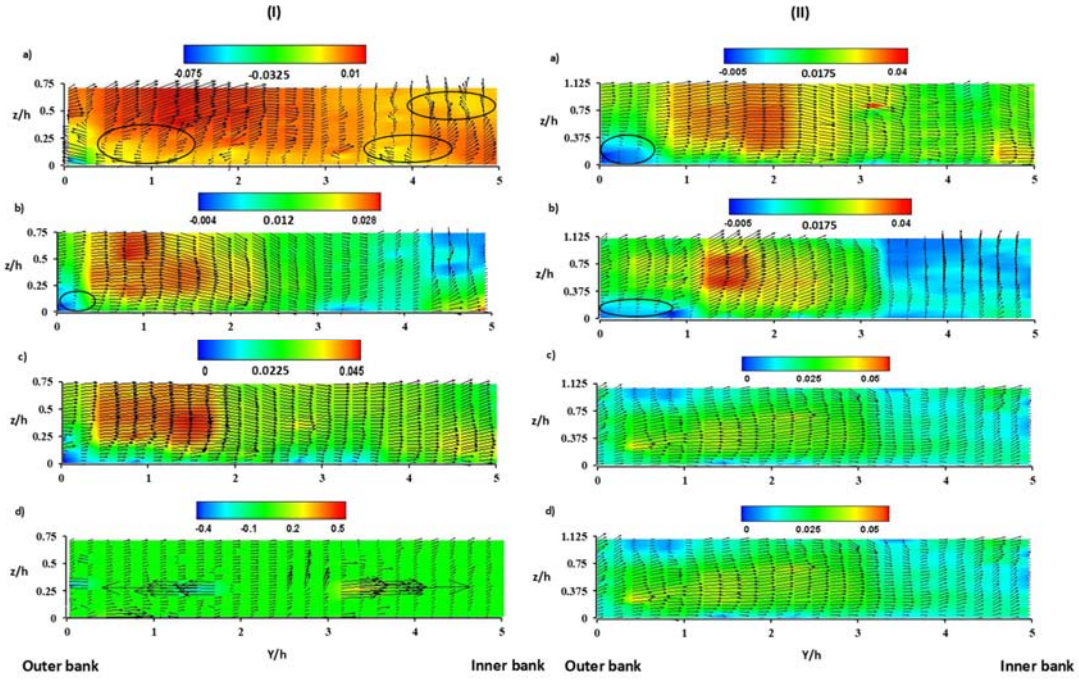


*Figure 3.8* Secondary velocity plots for $D_r$= 0.27 *(I)* and 0.43 *(II)* at apex section (CS1) *a)* 400 plants/m$^2$ *b)* 200 plants/m$^2$ *c)* 150 plants/m$^2$ *d)* 100 plants/m$^2$

## Turbulent Intensity

Figure 3.9 shows the contour plot of turbulence intensity (TI) normalized by the shear velocity ($u_*$) for different vegetation cases of two different relative depths *i.e.*, $D_r$ = 0.27 and 0.43. For emergent floodplain vegetation $D_r$ = 0.27 (Figure 3.9(I)), the high turbulence values were recorded near the bed (z/h = 0 to 0.25) of the channel. Further, with increase in vegetation densities, the turbulence intensity is higher and relatively uniform throughout the cross-section. At lower vegetation densities, the turbulence intensity is lesser and varies across the cross-section. For all the vegetation densities under emergent condition, the turbulence intensity shows peak near the outer bank (Y/h~0). In the case of submerged floodplain vegetation ($D_r$ = 0.43, Figure 3.9(II)), the turbulence intensity core region is found near inner bank for all the vegetation densities. However, for higher density case (400 plants/m$^2$), the turbulence core spreads across Y/h ~ 4 to 5 and z/h is 0.375. Further, this core region is deeper in the main channel which may be due to the more surface area occupied by the higher density of vegetation compared to other vegetation configurations. In other cases (200,150 and 100 plants/m$^2$), the turbulence intensity is maximum at the inner bank water surface and then observed to decrease towards the bed which may be due to velocity dip phenomena. For submerged condition, the percentage



TH-2690_166152105

increase in turbulence intensity in the main channel by 5%, 9%, 11% and 18% with increase in vegetation densities from 100, 150, 200 and 400 plants/m$^2$ relative to no-vegetation scenario. The maximum TI values highly dependent on the density of the vegetation. This is due to the turbulence shear production generated near the vegetation interface (channel floodplain transition) increasing with vegetation density in the submerged condition.

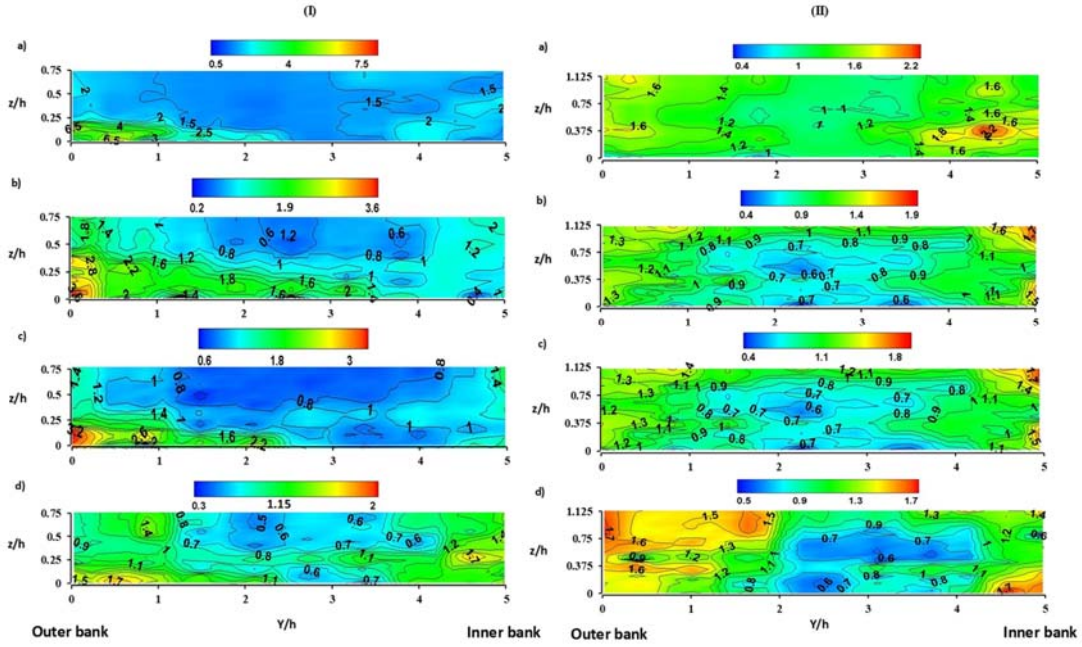


*Figure 3.9* Normalized contour plots of turbulence intensity ($TI/u_*$) for $D_r$= 0.27 *(I)* and 0.43 *(II)* at apex section (CS1) *a)* 400 plants/m$^2$ *b)* 200 plants/m$^2$ *c)* 150 plants/m$^2$ *d)* 100 plants/m$^2$

## Reynolds Stresses

Figure 3.10 shows the normalized Reynold's shear stress distribution ($-u'w'/{u_*}^2$) in the sinuous channel with the effect of different vegetation densities. For $D_r$=0.43 (submerged condition), the percentage increase in Reynold's shear stress by 11%, 21%, 27% and 39% with increase in vegetation densities from 100, 150, 200 and 400 plants/m$^2$ relative to no-vegetation scenario. For $D_r$=0.27 (emergent condition), this difference in Reynold's shear stress was less predominant with increased vegetation densities.

For submerged condition (Figure 3.10 (II)) the results reported that the maximum positive Reynold's stresses occur at the interface of main channel and floodplain vegetated region in between the range of z/h~0.75 to 1.125 (h is floodplain depth), which indicates that the shear becomes dominant and the maximum along the inner bend apex of the main



TH-2690_166152105

channel. The Reynold's stress is found to be zero along the cross-section line (Figure 3.10), which is observed to vary with different vegetation densities. The Reynold's stress is negative and positive at the below and above of the zero-line. This can be anticipated from the lateral gradient of the streamwise mean velocity (Figure 3.6). Under emergent conditions (Figure 3.10 (I), the zero-Reynold's stress line is deformed and moves up to the water surface with decreasing vegetation density. Figure 3.10 shows that for both $D_r = 0.27$ and 0.43 conditions, the values were negative below the zero-Reynold's stress line. This is due to the negative Reynold's shear stress originates through the momentum transfer from the side wall into the center of the main channel. However, in a sinuous channel for different cross-sections, the momentum exchange is relatively different.

Reynold's shear stress provides us an understanding of the momentum fluxes produced by turbulent variations. The findings showed that in the main channel (Figure 3.10), floodplain vegetation affects the Reynold's shear stresses, producing strong lateral shear stresses at a higher floodplain flow depth. In comparison, the distribution of the interface shear stresses changed entirely at low flow depth, although its magnitude nearly same. Due to the velocity gradient and secondary circulations in the main channel there are broad transverse shear stresses along the vegetated area (Figure 3.10 (II)). The turbulence dissipation caused by the momentum is significantly related to exchange. Thus, the floodplain vegetation shifts the flow structure into the main stream, creates the more turbulence and alters the distribution of velocity profiles.



TH-2690_166152105

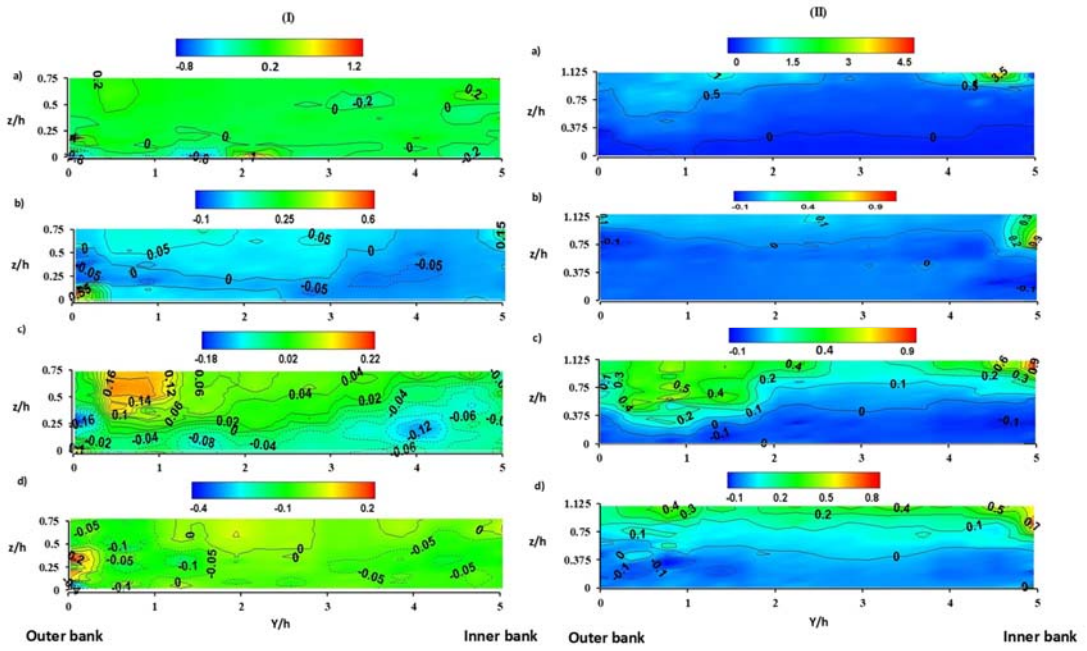


*Figure 3.10* Normalized contour plots of Reynold's shear stress ($RSS/u_*^2$) for $D_r$= 0.27 *(I)* and 0.43 *(II)* at apex section (CS1) *a)* 400 plants/m$^2$ *b)* 200 plants/m$^2$ *c)* 150 plants/m$^2$ *d)* 100 plants/m$^2$

### Turbulent Kinetic Energy (TKE)

Figure 3.12 shows the normalized turbulent kinetic energy ($TKE/u_*^2$) contours. In the case of emergent condition ($D_r$=0.27, Figure 3.11(I)), the TKE originates at the outer bank and spreads toward the inner bank. The maximum TKE values were observed at outer bank bottom (*i.e.*, Y/h~ 0 to 1). And the scenario is relatively different in submerged condition where TKE originates at top of the inner bank and migrate towards outer bank. Further, the percentage increase in TKE 12%, 15%, 19% and 25% with increase in vegetation densities from 100, 150, 200 and 400plants/m$^2$ relative to no-vegetation condition. Under higher vegetation densities, the maximum TKE is formed as waves (Figure 3.11 (II)) created near the floodplain-channel transition (Y/h~5) due to the vegetation structure interactions. This may be due to the discontinuity of the drag force at that region resulting a high velocity gradient near the vegetation interface. In this study, we are trying to correlate the distribution of TKE related to the secondary circulation cell produced in the channel. In emergent condition (Figure 3.8 (I)), the circulation of cells at apex section for different densities of vegetation correlates with the higher values of TKE (Figure 3.11(I)). This indicates the development of TKE is associated with recirculation cell generated by the local curvature. Figure 3.8 (II) shows the submerged condition, where



TH-2690_166152105

the minimum turbulent kinetic energy occurs underneath the water surface in the main channel, which is associated to the velocity dip feature causes due to the secondary currents. From the results, in the main channel the higher vegetation density causes to increase in TKE values observed in Figure 3.8 (II). Similar to the Reynolds stress, the turbulent kinetic energy shows a maximum near the interface, which increases with increase of vegetation density. This is due to the turbulence shear production generated near the interface. Finally, the density of vegetation has a noteworthy influence on flow structures.

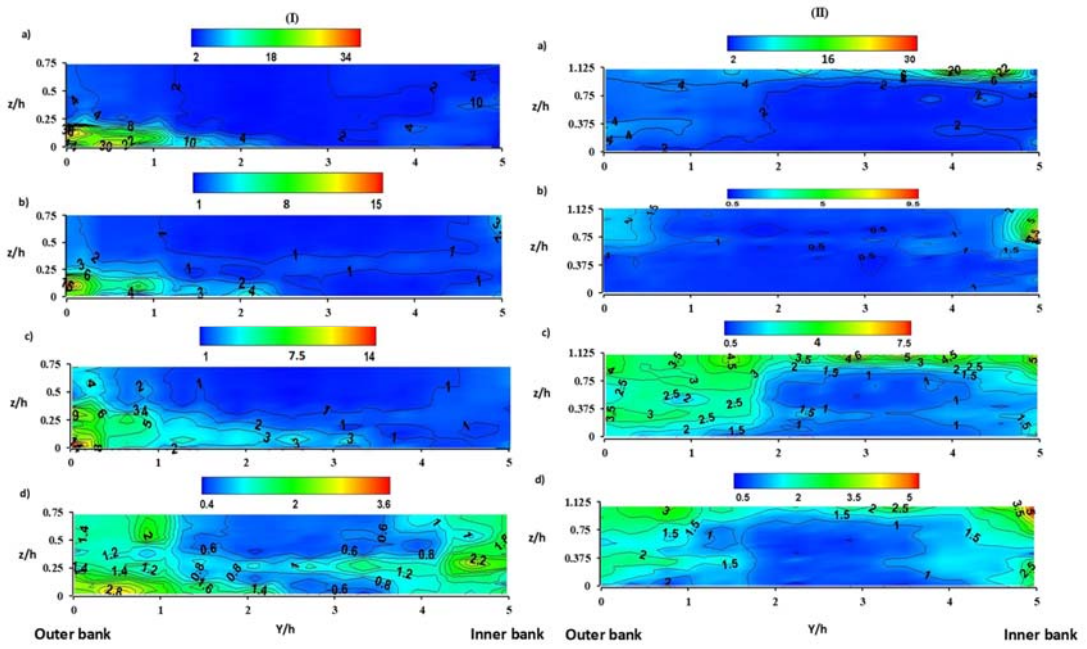


*Figure 3.11* Normalized contour plots of turbulent kinetic energy ($TKE/u_*^2$) for $D_r$= 0.27 (I) and 0.43 (II) at apex section (CS1) a) 400 plants/m$^2$ b) 200 plants/m$^2$ c) 150 plants/m$^2$ d) 100 plants/m$^2$

### 3.3.2 Flow Angle

The flow angle can be resolved into components with an angle 'Θ'. Where angle Θ is obtained as $\Theta = \tan^{-1}(\overline{v'}/\overline{u'})$ . Figure 3.12 shows the vertical ratio (Θ) distributions at apex, bend and cross-over regions in main channel with no-vegetation and varying vegetation densities on flood-plain (400 plants/m$^2$ and 100 plants/m$^2$). The experimental configurations of no-vegetation, higher (400 plants/m$^2$) and lower (100 plants/m$^2$) vegetation densities were chosen for discussion for better understanding at varying conditions. The flow angle is calculated with in the main channel to understand the variation of velocity gradient in each layer of the flow. This velocity gradient at the



TH-2690_166152105

interface results in shear layer generation and its consequence effects were discussed in above sections. It is observed that the maximum flow angle (Θ = 25°) is reported for lower flood-plain depth ($D_r$ = 0.27, emergent vegetation) condition at cross-over region for vegetation density of 100 plants/$m^2$. At other cross-section of bend (Θ = 25°) and apex region (Θ =4°), relatively lower flow angle is observed. Further, at the apex section the flow angle variability can be observed from near bed to the top surface in comparison to other two sections. In the case of higher flood-plain depth ($D_r$ = 0.43, submerged vegetation), the maximum flow angle is Θ = 20°, which is observed for vegetation density of 400 plants/$m^2$ at COR and bend region. This analysis indicates the flow angle parameter also has similar response at lower and higher flood-plain depths like other turbulent parameters. In the case of no flood-plain vegetation condition, the effect on flow angle is insignificant in compared to other vegetated floodplain conditions.

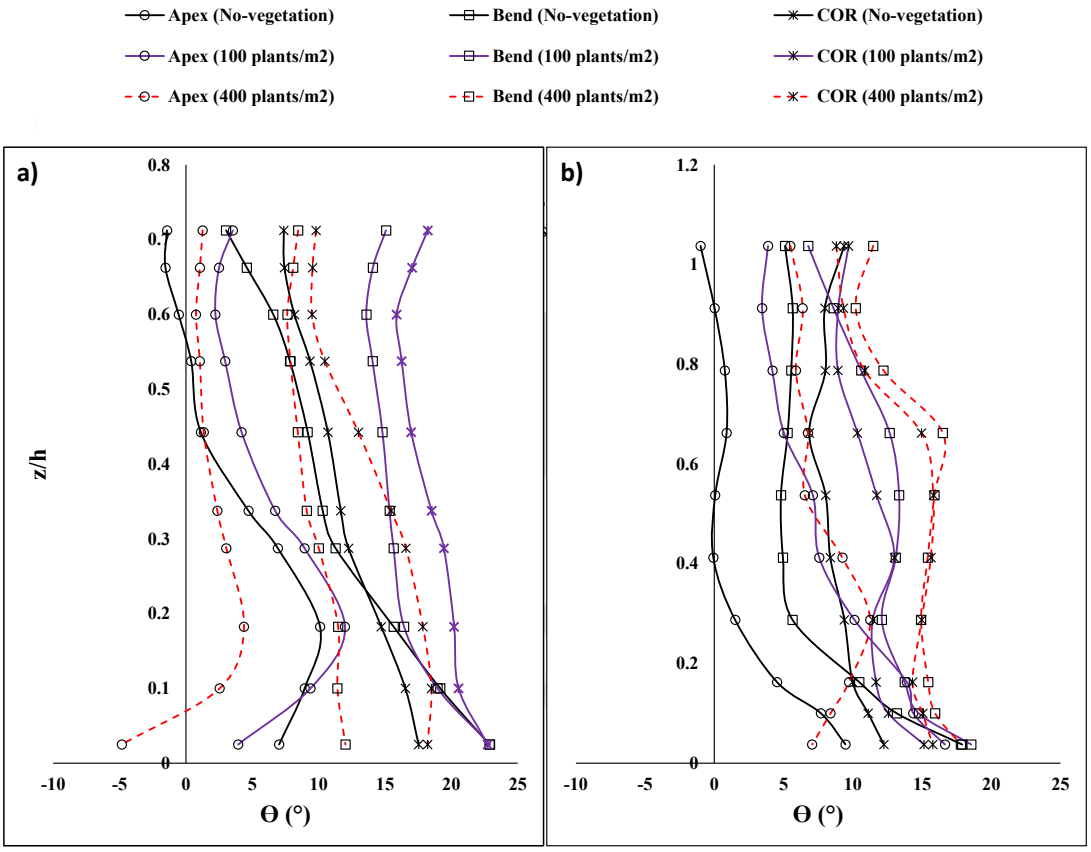


*Figure 3.12* Flow angle for the relative flow depths of *a)* $D_r$ = 0.27 and *b)* 0.43, no-vegetation case and vegetation with two different densities at apex section (CS1); bend section (CS2); and cross over region (CS3)



TH-2690_166152105

## 3.4 DISCUSSIONS

In this section, the shear layer generation mechanism and impact of vegetation density is discussed. Figure 3.6 represents the shear layer generation along the edge of the vegetated region which is laterally moving from inner bank to outer bank. It is pushed away from the vegetated zone to become a free shear layer with higher turbulence energy. Due to the vegetation drag effect, the shear layer at the interface of the vegetated floodplain was seen to be less elongated and wider than the non-vegetated case. Figure 3.6 (I), shows the emergent condition the maximum streamwise velocity increases with increase of vegetation density and shear layer width is extended to outer bank (Y/h~ 1.2) as the vegetation density increases and also noticed that among the vegetation densities there is no significant difference in their streamwise velocities. In the context of submerged condition, the streamwise velocities grows with increase of vegetation density. In addition to that the core velocity region and shear layer width is extended to outer bank (Y/h ~ 0.8) as the vegetation density increases. Yang et al., 2007 stated that in a flow-through compound channel, the flow interaction between the main channel and the flood plain occurs, and a shear layer forms as a result of the flow in the main channel moving faster than the flow in the vegetated flood plain. The development of the shear layer produces additional turbulence due to the mixing layer between floodplain and the meandering channel flow (Moncho- Esteve et al., 2018).

At the floodplain vegetation interface, the velocity gradient in the crosswise direction increases with increasing vegetation density, generating a strong shear layer at that position. The wavy isovel lines (Figure 3.6) were deepens as the vegetation density increases and these lines were occurred due to strong secondary currents. As the secondary circulation strength increases at the outer bank, it is helpful to restrict the wavy isovel lines extended to outer bank in the vegetated condition. In such cases, the velocity distribution in the channel appears to be uniform in the lateral direction unlike that in the non-vegetated zone. The water surface gradient increases with the increasing of density of vegetation. Jahra 2010 reported that the mass and momentum exchange between the main channel and the floodplain of a compound meandering channel is a complicated process and this will be the primary significance in the formation of secondary currents. Moncho-Esteve et al., 2018 stated that secondary flow motions are highly influenced by the geometry of waterway, both by the sinuosity of the channel and by the cross-sectional form. Further, Rozoviskii, 1961 stated that the fully developed secondary current cell can be observed at



TH-2690_166152105

bend section having an angle of 220° leading to the fact of rare possibility in the development of secondary flow in a meandering channel. Muto 1999 reported that the behavior of the secondary circulation structures changes with increasing sinuosity from 1.09 to 1.59 for $D_r$= 0.15. In this study, the experimental channel is having low sinuosity (bend angle of 60°), which reduced the strength of secondary circulation cells as compared to the high sinuous channel.

Figure 3.10(II) shows the higher flood condition, the result reported that the maximum positive Reynold's stresses occur at the interface of main channel and vegetated zone in between the range of z/h=0.75 to 1.125 (h is floodplain depth), which indicates that the shear becomes dominant and the maximum along the inner bend apex of the main channel. This may be due to the impact of vegetation density and shear layer effect. The maximum positive and negative values of Reynold's stresses are observed at the interface of main channel and vegetated zone. The values were negative in the main channel. Azevedo et al., 2017 reported that the negative RSS originates through the momentum transfer from the side wall into the mid of the main channel. Jahra 2010, study for the emergent condition, the spanwise distribution of Reynolds shear stress, observed that with the increase of vegetation density the spanwise Reynold's stress increases in terms of positive and negative along the two-inner apex of the meandering wave. In the present study for emergent condition ($D_r$=0.27), the Reynold's shear stress also increase with increase of vegetation density (Figure 3.10 (I)). Kang 2006, found the Reynolds stress is zero along the vertical line and the values were negative and positive at the right-hand side and left-hand side of the line, respectively. This can also be expected from the lateral gradient of the mean streamwise velocity. With increasing vegetation density, the zero-Reynold's stress line deforms and travels to the right bank.

Figure 3.11 (II) represents, at the high flow flood water depth, the turbulent shear layer causes to give more TKE values at upper layer (z/h = 0.75 to 1.125) of the inner bank, whereas in the case of low flow flood water depth (Figure 3.12 (I)) the maximum values of TKE are at the outer wall (z/h= 0 to 0.25). Zhang et al., 2020 stated that the high value of TKE was observed at the top of the vegetation due to the discontinuity of the drag force at that region resulting a high velocity gradient near the vegetation interface. In submerged condition, the turbulent kinetic energy shows a peak near the inner bank and the maximum value increases as the vegetation density increases. Note that a minimum turbulent kinetic energy occurs underneath the water surface in the main channel, which is related to the



TH-2690_166152105

velocity dip produced due to the secondary currents. Similar to the turbulent kinetic energy, the Reynolds stress shows a maximum near the main channel and floodplain transition, which increases with vegetation density. When it comes to turbulence in a compound channel, it involves complex processes like the momentum transfer between the main channel and flood plain, vortex shedding, shear-driven instability, etc. For a vegetated flood plain, these processes are more complicated as vegetation canopy scale turbulence comes in picture. In present study, the vegetation density and different flow conditions have shown a significant effect on main channel flow structure. The response of the flow to varying vegetation densities and its characteristics certainly influences the flow structures.

## 3.5 CHAPTER SUMMARY

In the present study, an analysis of laboratory experiments was conducted to investigate the effect of emergent and submerged homogeneous green corridor on flow structures. For this purpose, Oryza Sativa (young rice plants) of 400, 200, 150, 100 plants/$m^2$ were arranged in four different layouts (Figure 3.3). The results of the study provided the understanding of effect of homogeneous green corridor on flow characteristics.

The following conclusions are the major observations in the study.

i) A strong velocity gradient is observed in the high vegetation density scenario *i.e.,* 400 plants/$m^2$ because of flow diversion from floodplain to the main channel, which resulted in increases the main channel velocity by 23% compared to the no-vegetation scenario.
ii) The angle of inclination of secondary currents in higher floodplain flow condition are about 2°, 6°, 6.5° and 7.3° for 100, 150, 200 and 400 plants/$m^2$, respectively. This indicates the arrangement of vegetation on the floodplain has significant influence on the flow distribution in the channel.
iii) The turbulence core region is mainly observed towards the inner bank (Y/h ~ 4 to 5) and z/h is 0.375. Further, this core region is deeper in the main channel which may be due to more surface area occupied by the higher density of vegetation compared to other vegetation configurations.
iv) The maximum positive Reynold's stresses occur at the interface of main channel and vegetated zone in between the range of z/h~0.75 to 1.125 (h is floodplain



TH-2690_166152105

depth), which indicates that the shear becomes dominant and the maximum along the inner bend apex of the main channel.

v) The findings showed the floodplain vegetation affects the Reynold's shear stresses in the main channel, producing strong lateral shear stresses at a higher floodplain flow depth condition. Thus, the floodplain vegetation shifts the flow structure into the main stream, creates the more turbulence and alters the distribution of velocity profiles that play an important role in stabilizing the bank and ecological regeneration.

The presence of high vegetation density on the floodplain of the river, increases the flow velocity and turbulent characteristics in the main channel. The variation of vegetation densities on floodplain provides appropriate feedback for river ecological restoration and bank erosion control. This work can be further extended to study on floodplain under the same flow conditions. To investigate further, comprehensive measurements in longitudinal and traverse directions of floodplain will, however, be helpful for better understanding and interpretation of the turbulent behavior in a river.



TH-2690_166152105

# 4

# FLOW THROUGH VEGETATION PATCHES

The green corridor functions as an active component of the floodplain ecological dynamics and interacts with fluvial mechanisms such as flow hydraulics and ecological processes and river morphological dynamics controlling river-riparian system functioning (Robertson and Augspurger 1999, Hupp 2000). River corridor vegetation consists of reeds, shrubs, grasses under emergent and submerged flow conditions. This heterogeneity in riparian vegetation influences hydraulics, sediment transport and nutrient distribution in main channel and floodplain transport. This chapter attempts to address the following questions concerning flow in heterogeneous vegetation corridor through experimental investigations.

- What kind of the flow structure is observed in the main river with the effect of heterogeneous green corridor on floodplain? How is its influence on main channel hydraulics?
- How heterogeneous vegetation zones on floodplain can be helpful for river and ecological restoration measures?

## 4.1 INTRODUCTION

Vegetation is the key component in river-floodplain corridor which has a vital role in influencing the hydrodynamics, morphology and ecological characteristics of river systems (Brachet 2015). On natural river corridors, vegetation can be found in a variety of

TH-2690_166152105

forms (e.g., Figure 4.1), and it is very significant for researchers and hydraulic engineers when conducting flood risk impact assessments, bank erosion investigations, and planning of flood management (Bennett and Simon 2004, Aberle and Jarvela 2013, D'Ippolito et al., 2013, and Vargas-Luna et al., 2016). The investigation on the interaction between fluid flow and vegetation is a quite complex subject, due to both the different physical mechanisms that play a role in the phenomenon, and the biomechanical properties that characterize the diverse type of vegetation. The interactions between flow, vegetation and sediment involves changes in several fluvio-hydro-ecological variables (Hupp, 2000; Hughes et al., 2001). In natural river-floodplain corridor, the vegetation is often observed as patches of reeds, shrubs, grasses of varying densities. The heterogeneous vegetation on floodplain contributes to planform stability by increasing the flow resistance and providing spatial variability in the flow and turbulence field, both of which are beneficial to river ecology (Chembolu et al., 2019).

The recognition of importance of vegetation on planform stability and river ecological aspects has started in the recent decades (Gurnell 2014). Neary et al., 2012 stated that vegetation can significantly alter the bulk, time-averaged and instantaneous flow characteristics of turbulent flows, and these changes have major effects on sediment transport and morphology of the rivers. Chembolu et al., 2019 observed the clear distinction of velocity profile characteristics in flow through homogeneous and heterogeneous vegetation in straight channels. Further, the local and patch scale turbulent structure, variability in turbulence parameters like Reynolds stresses and turbulence intensities were also influenced by vegetation (Garcia et al., 2013; Liu et al. 2008, 2010; Kubrak et al., 2008; Wilson 2007; Stone and Shen 2002; Nepf 1999; Shimizu 1994). Gorrick and Rodriguez 2014, conducted series of laboratory experiments on low-sinuous and varying width channel to observe the changes in flow and turbulence structure with and without vegetation on outer banks. Literature review suggests that a good process-based understanding of flow and vegetation interactions is presented by previous works. However, most of the works focused on reporting the results of flow through homogeneous vegetation in straight channels and further very limited works on using natural vegetation for experiments (e.g., Devi 2016).

The current study examines the impacts of plant heterogeneity on flow and turbulence structure in a low sinuous channel, which is the primary goal of this study. The objectives of this study include: (a) investigate the main channel flow structures with the effect of different vegetation forms on flood-plain in a low-sinuous compound channel;



TH-2690_166152105

(b) Understand the flow behavior on different vegetation forms and organize the flow characteristics. To obtain these objectives, we conducted laboratory experiments with different vegetation forms and detailed flow measurements were taken to brief the heterogeneous characteristics. A series of laboratory experiments was carried out in a submerged flow condition, where the flow depth was equal to the height of the vegetation canopy. The findings provide better understanding on the impact of diverse features such as plant form on flow behavior.

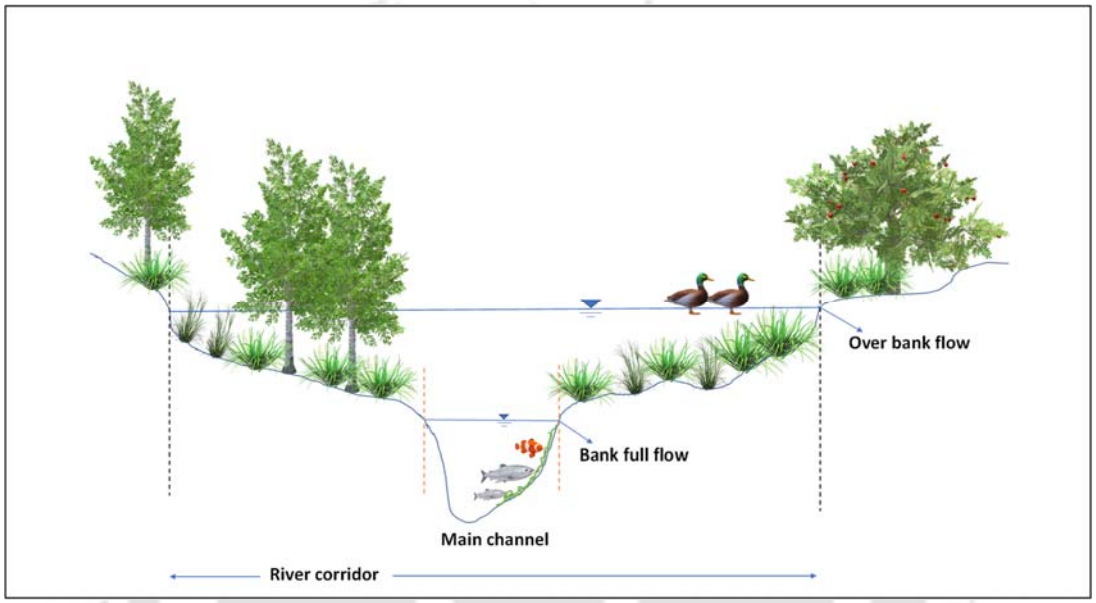


*Figure 4.1* Riparian green corridor along the river bank system

## 4.2 MATERIALS AND METHODS

### 4.2.1 Experimental Setup

A series of experiments were conducted at the Fluvial hydro-ecological laboratory (Civil Engineering Department, IIT Guwahati) in an 18 m long, 4 m wide (flow constricts to 1 m wide) and 0.3 m deep flume. Two 15 HP and one 3 HP pumps were utilised to drive and recirculate the flow between the channel and the 10,000 litres capacity of underground sump (10x10 m). A 4 m long, 1.5 m wide, 1.5 m deep collecting chamber with pebbles as roughness components was built upstream to reduce turbulence, and iron mesh screens were employed to straighten the incoming flow to the channel. Slope of the flume was fixed to 0.001 throughout the experiments. The discharge was measured using a triangular notch at the channel inlet, and the flow depth was measured using a digital point gauge. At each measuring point, the data was collected for up to two minutes using



TH-2690_166152105

a three-dimensional Acoustic Doppler Velocimeter (ADV) (4 probes, 10 MHz Vectrino ADV manufactured by Nortek) with a sample frequency of 100 Hz. To remove the spikes from the time series velocity data, the accelerating threshold method was utilised (Goring and Nikora, 2002; Dey et al., 2012; Devi, 2016). The signal-to-noise ratio of the measurements is maintained above 15, to ensure the quality of the data collected. To conduct the laboratory experiments, a 1.2-meter-long test section was chosen at a distance of 10.6 metres from the flume entrance to reduce the impacts of upstream entry and downstream exit. Natural plants with heterogeneous plant forms were planted in a staggered pattern along the test section, and studies were conducted to examine turbulence flow structures.

### 4.2.2 Vegetation Types and Arrangement

In the experimental studies, three different types of natural vegetation such as leafy, cylindrical and bladed vegetation were used to bring out the diverse characteristics of flow behavior. Sprigs of Duranta erecta for leafy type, the stems (without leaves) of Sphagneticola trilobata for rigid cylinders, and Oryza sativa (young rice plants) to represent bladed type were used. This vegetation morphologically illustrates the real species like leafy bushes, reedy vegetation and flexible grasses along the floodplain of the river (Figure 4.2). Certain plants reflect heterogeneity in terms of structure, swaying motion, and the drag effect. The leafy vegetation was semi-flexible with the stem being rigid and leaves, the cylindrical was rigid in nature, and, flexible bladed vegetation form was flexible to sway motion. Moreover, the canopy porosity and projected area occupied by these plants also vary differently. Table 4.1 describe the physical characteristics of the plant forms used in the work. To carry out the experiments, four different vegetation layouts (Figure 4.2) were designed along the floodplain of the river. All the plants were placed in a staggered pattern along the test section with a density of 400 plants/$m^2$. The plant biomechanical properties have been reported from the study (Chembolu et al., 2019)

### 4.2.3 Flow Conditions and Measurement Locations

Experiments were conducted in submerged flow conditions in which flow depth is at the vegetation height. In the present work, considering the no bed load transport condition, the main channel depths were maintained lesser than the incipient motion depths (Devi et al., 2016). The median sand diameter was taken as $D_{50}$ =0.37 mm. The corresponding flow depth (H) and discharge (Q) were 14 cm and 0.0153 $m^3/s$. Table 4.2 shows the



TH-2690_166152105

hydraulic conditions maintained in the channel for different vegetation layouts. Flow measurements were taken at several points of the test section to investigate the impact of varied vegetation types on flow and turbulence behavior. In all of the experiments, the number of plants per square metre remained constant regardless of plant type. Measurement locations in the experiments were positioned in main channel form P1 to P10. Figure 3.3 shows the measurement locations along each cross-section of the channel. ADV was used to collect instantaneous velocity components along the flow depth in 1 cm increments from the near bed. As a result, for each measuring point, 14-16 depth wise measurements were obtained.

*Table 4.1*: Summary of plant parameters

| S. No. | Plant form | Plant parameter | Value |
|---|---|---|---|
| **1** |  | *Bladed vegetation* | |
| | | Average plant height (h) | 6 cm |
| | | Average deflected height ($h_d$) | 4 cm |
| | | Average blade width | 2 mm |
| | | Approx. no. of blades in one plant | 6 |
| | | Relative canopy porosity | Medium |
| | | Projected area | 7.2 $cm^2$ |
| | | Plant flexibility ($h_d/h$) | 0.67 |
| **2** |  | *Leafy vegetation* | |
| | | Average plant height (h) | 6 cm |
| | | Average deflected height ($h_d$) | 5.4cm |
| | | Diameter of the stem | 0.1 cm |
| | | Approx. no. of leaves in each stem | 9 |
| | | Average width of leaf | 1.5cm |
| | | Average length of leaf | 2 cm |
| | | Relative canopy porosity | Low |
| | | Projected area | 21.795 $cm^2$ |
| | | Plant flexibility ($h_d/h$) | 0.90 |
| **3** |  | *Cylindrical vegetation* | |
| | | Average plant height (h) | 6 cm |
| | | Average deflected height ($h_d$) | 5.8 cm |
| | | Diameter of the stem | 0.25 cm |
| | | Relative canopy porosity | High |
| | | Projected area | 1.5 $cm^2$ |
| | | Plant flexibility ($h_d/h$) | 0.97 |



TH-2690_166152105

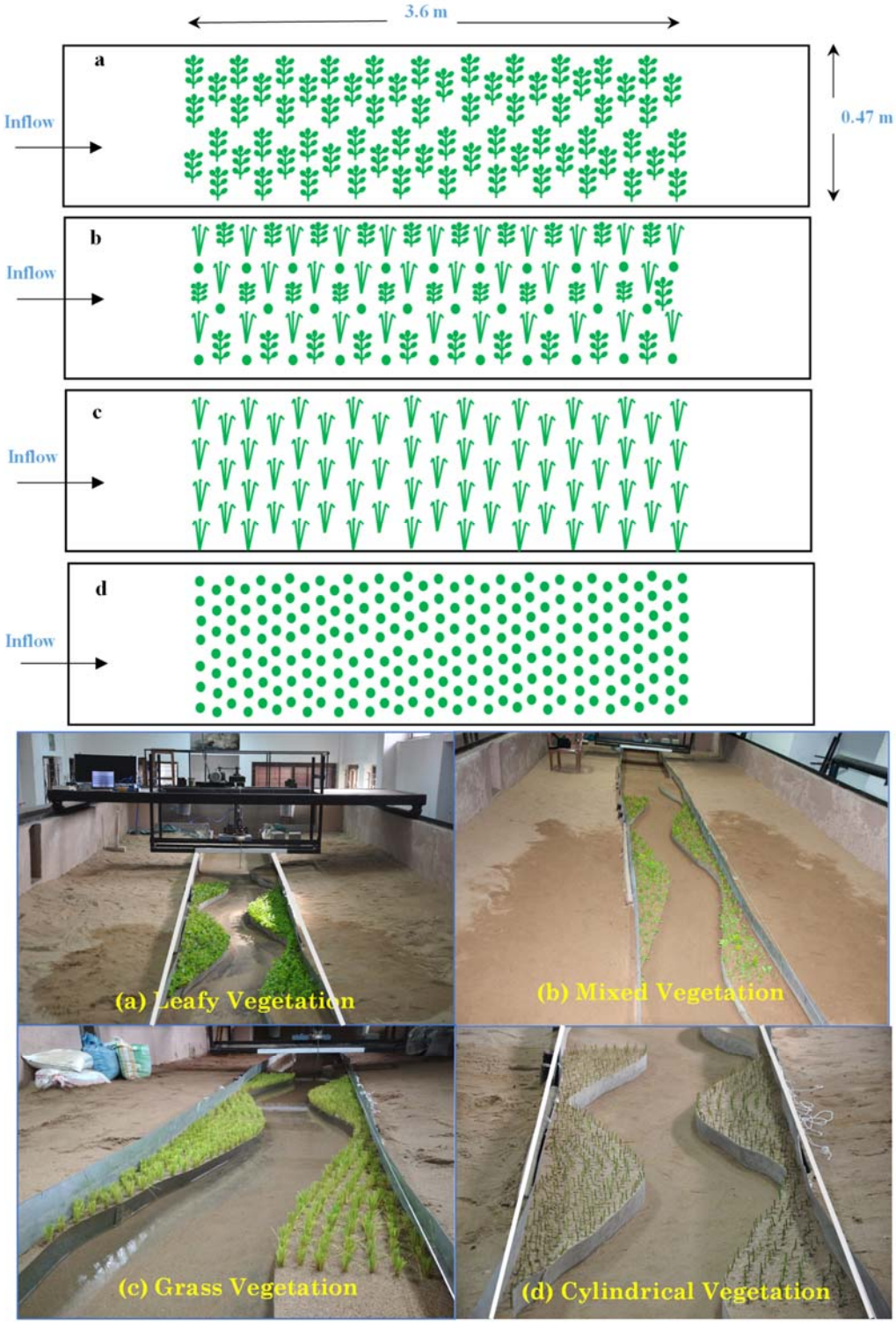


*Figure 4.2* Sketch for representation of different experimental floodplain vegetation patches layout.



TH-2690_166152105

*Table 4.2:* Summary of the experiments

| S. No. | Vegetation layout | Pattern | Flow Depth (cm) | $F_r$ | Re |
|---|---|---|---|---|---|
| 1 | Leafy vegetation | Figure 5.3a | 14 | 0.270 | 23127 |
| 2 | Mixed heterogeneous vegetation | Figure 5.3b | 14 | 0.229 | 19597 |
| 3 | Flexible bladed vegetation | Figure 5.3c | 14 | 0.213 | 18200 |
| 4 | Cylindrical vegetation | Figure 5.3d | 14 | 0.192 | 16380 |

*Table 4.3*: Trend of turbulence parameters

| Characteristics | Cylindrical Vegetation | Grass Vegetation | Mixed Vegetation | Leafy Vegetation |
|---|---|---|---|---|
| Streamwise velocity | 21% | 23% | 27% | 38% |
| Secondary velocity | 14% | 22% | 24% | 26% |
| Turbulence Intensity ($u_{rms}$) | 2% | 18% | 24% | 31% |
| Reynold's shear stress ($-u'w'$) | 17% | 39% | 45% | 56% |
| Turbulent kinetic energy | 9% | 25% | 29% | 35% |



TH-2690_166152105

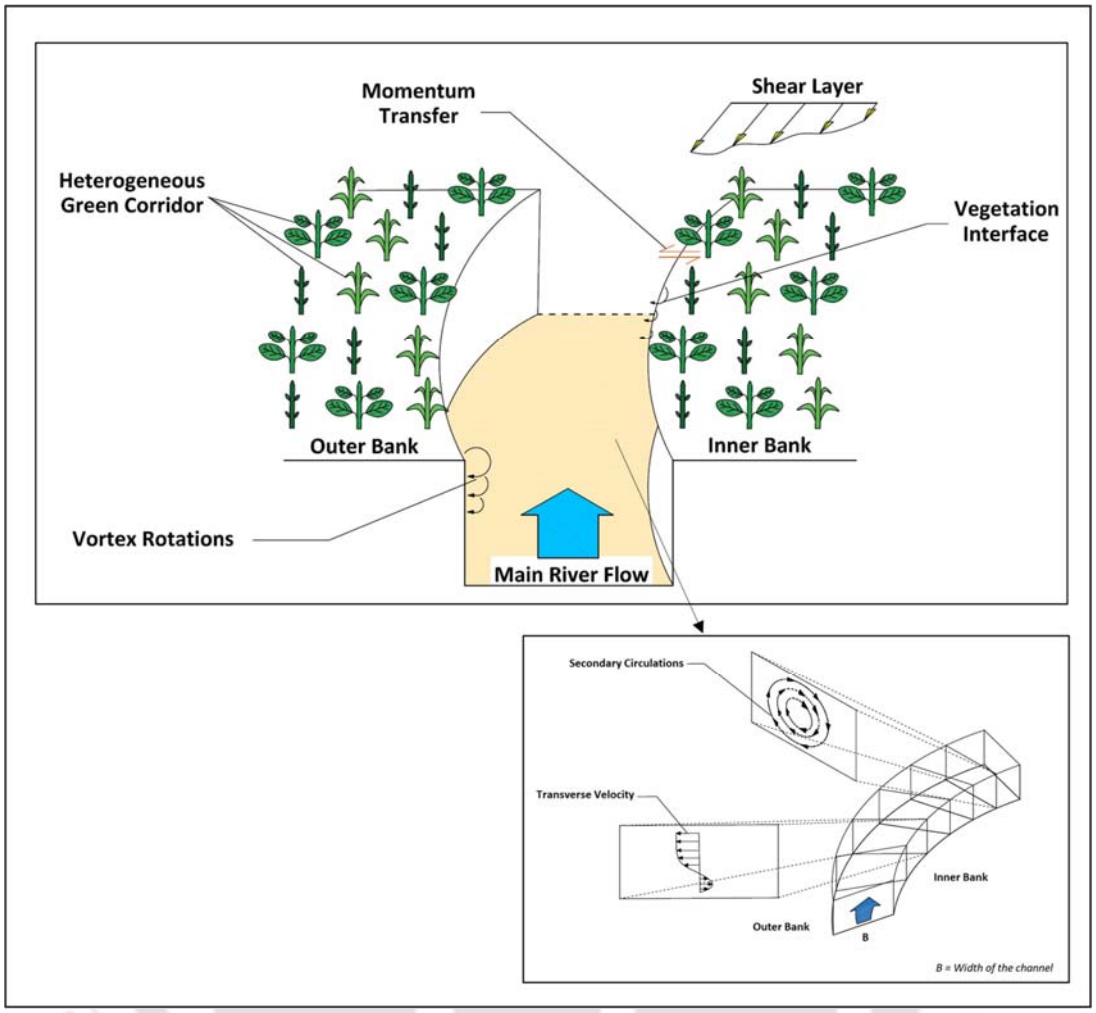


*Figure. 4.3* Conceptual diagram of heterogeneous green river corridor

## 4.3 RESULTS

### 4.3.1 Floodplain vegetation patches effect on flow velocity distribution:

#### Streamwise Velocity

Figure 4.4a represents the vertical distribution profiles showing the variation of streamwise velocity in the main channel with effect of floodplain vegetation. The velocity profiles were observed to be logarithmic in nature in all the conditions. In apex region, the magnitude of cross-sectional average velocity vary as leafy> mixed> grass> cylindrical> no vegetation. At the measurement location P1, the velocity magnitude in the main channel vary as 0.14 to 0.25 m/s in flexible grasses, 0.18 to 0.25 m/s in cylindrical vegetation, 0.20 to 0.27 m/s in mixed vegetation layout, 0.22 to 0.29 m/s in leafy



TH-2690_166152105

vegetation and 0.07 to 0.21 m/s in no-vegetation case. It is clear that the leafy vegetation and mixed vegetation layouts increased the velocity in main channel than other vegetation forms, which is due to higher resistance offered by leafy forms over the flood plain. The highly resistant vegetation layouts such as leafy and mixed vegetation conditions enhanced the flood-plain flow obstruction and diverted the flow towards the main channel causing increased velocities and better streamlining effect.

Figure 4.5 shows the normalized stream wise velocity ($u/u_*$) contour plots for different vegetation layouts. In the no-vegetation condition the velocity core region is observed at top region of inner bank. While in vegetation influenced scenarios, the velocity core extended from inner bank towards outer bank depending on type of vegetation. The mean velocity is observed in the order of $9u_*$ for leafy vegetation and $7.5u_*$ for mixed vegetation layouts, which is relatively higher than flexible grass ($7u_*$) and cylindrical ($6u_*$) layouts. Further, the percentage difference in primary velocities is observed as 38%, 27%, 23% and 21% for leafy, mixed vegetation, grasses and cylindrical layouts as compared with no-vegetation condition. The effect of shear layer is also observed to different for varying conditions, which increased from inner bank to outer bank. In cylindrical layout, the horizontal shear layer is observed at Y/h ~ 4.8 close to the inner bank, while in higher resistant leafy layout it is at Y/h ~ 1.5. In the case of leafy vegetation, the reduction in velocity in the channel from P1 to P10 is observed as 51% at vegetation canopy height.



TH-2690_166152105

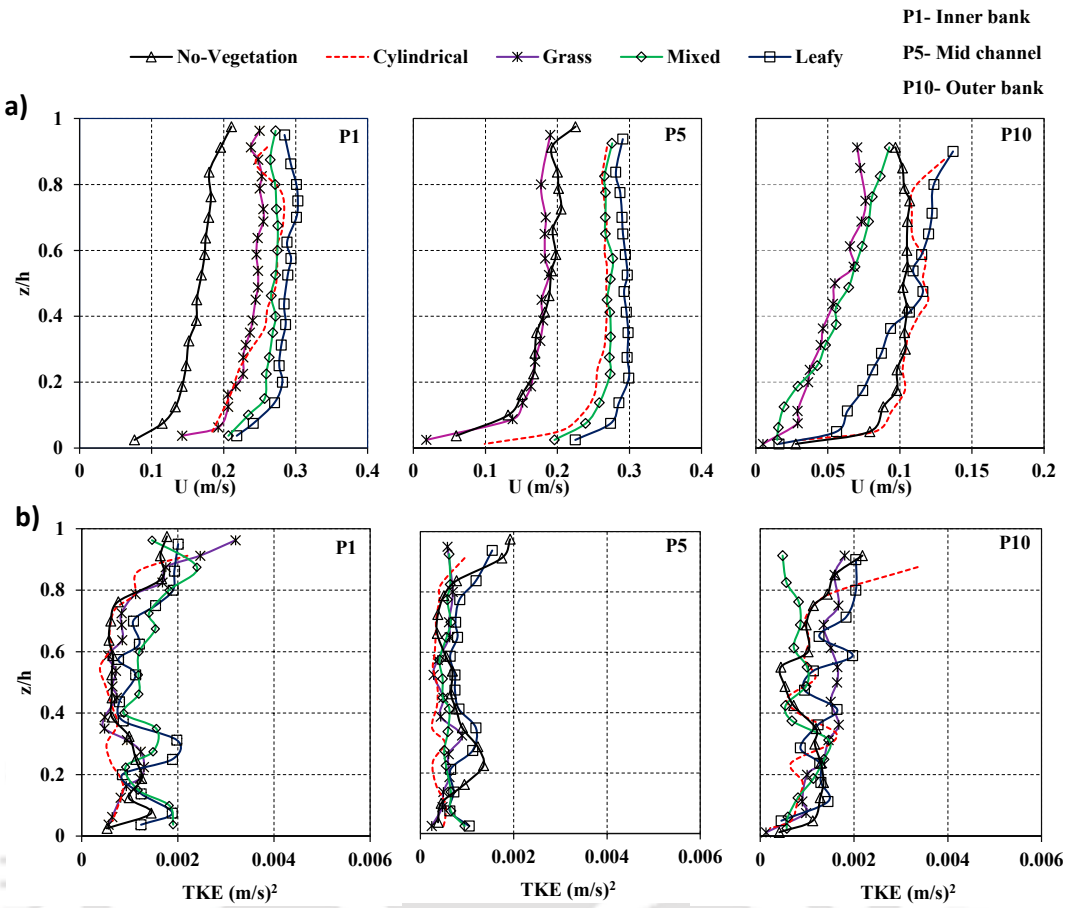


*Figure 4.4* Vertical distribution of *(a)* streamwise velocity (U), *(b)* turbulent kinetic energy (TKE)

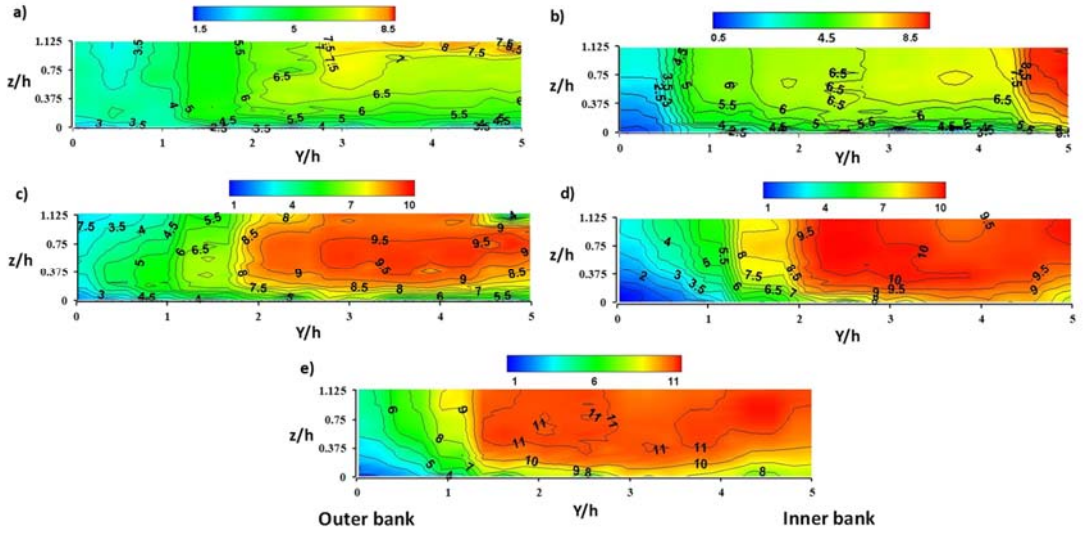


*Figure 4.5* Normalized contour plots of streamwise velocity ($u/u_*$) for *(a)* no-vegetation *(b)* cylindrical *(c)* grass *(d)* mixed *(e)* leafy vegetation conditions



TH-2690_166152105

### Secondary Velocity

The effect of different flood-plain plant forms on secondary flow behavior is investigated in this section. Figure 4.6 shows the secondary flow vector contours at apex, bend and cross-over regions for cylindrical, grasses, leafy, mixed vegetation layouts and no-vegetation conditions. In no-vegetation condition, secondary circulations were noticed at the outer bank, while in vegetation layouts there is no such specific pattern. In highly resistant leafy and mixed vegetation layouts, the secondary circulations are observed only at the apex region nearer to channel bed. Moreover, the upward inclined flows are noticed in these layouts. In the cylindrical (high canopy porosity) and grasses (flexible) vegetation layouts, the main channel cross-section is relatively free of secondary circulation patterns. The maximum magnitude of secondary velocity vectors is about 26%, 24%, 22%, 14% and 12% of the maximum streamwise velocity for leafy, mixed, grass, cylindrical and no-vegetation respectively. Further, the angle of inclination of secondary currents, which is flow angle is observed as 11°, 9°, 7.3° and 5.5° for leafy, mixed, grass and cylindrical vegetation respectively. However, the transverse flow motion and transverse surface gradient in the region of the leading edge of the outer bank is enhanced by strengthening of secondary flows. Secondary flows allow for more distinct flow mixing between low-velocity flow in the vegetated region and high-velocity flow in the open region, significantly dominating the mixing effect caused by strong horizontal secondary vortices.



TH-2690_166152105

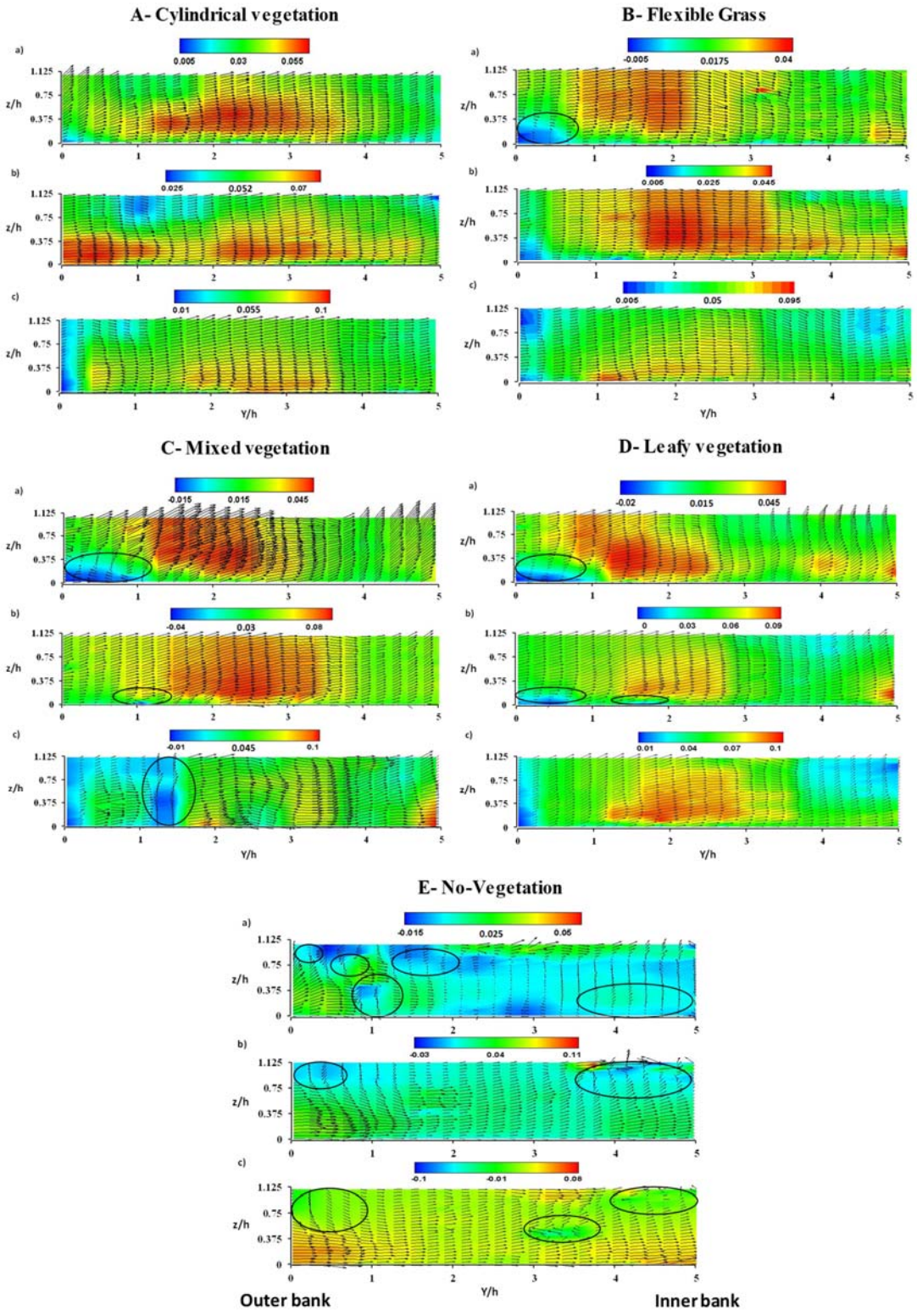


*Figure 4.6* Secondary velocity plots for vegetation with different plant forms and non-vegetated case at *a)* apex section (CS1); *b)* bend section (CS2); *c)* cross over region (CS3)



TH-2690_166152105

### 4.3.2 Flood plain vegetation patches effect on turbulence parameters:

#### Turbulence Intensity

The turbulence intensity components (i.e., streamwise $u'$, transverse $v'$, vertical $w'$) were measured in the experimental channel and examined to discuss the turbulence characteristics for transverse $v'$ further. The intensities are obtained by calculating the root mean square (RMS) of the fluctuating velocities for each direction. Figure 4.7, represents the turbulence intensities in the streamwise ($u_{rms}$), lateral ($v_{rms}$) and vertical ($w_{rms}$) directions of turbulence intensities. From the figure 4.7, the higher streamwise turbulence intensities can be observed for leafy vegetation from P1 (inner bank) to P10 (outer bank) in the main channel. This indicates the $u_{rms}$ of leafy vegetation from inner bank to outer bank is significantly dominate with other vegetation forms. Figure 4.7 (a,b) shows the streamwise and lateral turbulence intensity components, observed the highest values at the water surface, due to both the presence of the highest gradients of the averaged streamwise velocity. From the results, the magnitude of $u_{rms}$ and $v_{rms}$ are quite close to each other, the $w_{rms}$ values are relatively lower compared to the other two turbulence intensity components. In the context of vertical turbulence intensity ($w_{rms}$), the values of leafy vegetation condition are found dominating than the other vegetation forms. Figure 4.7c, for all the experimental cases the $w_{rms}$ increases with the distance from the bottom until z/h~0.05, and reaches higher at top of the water surface *i.e.,* z/h~ 1. This indicates the increase in $w_{rms}$ shows energy transfer near the surface on the vertical direction of water flow. And also, this higher intensity of $w_{rms}$ indicates that the measure of vortex rotation in the channel. The flow is sheared because of the higher velocity in the upper flow region. The vertical and streamwise turbulence intensities are increased by shear induced turbulence at the vegetation top.

As shown in Figure 4.7, the higher intensity values were observed at water surface of the channel at z/h~1 of all the vegetated floodplains. The turbulence intensity is maximum at inner bank (P1) and gradually decreases in the main river and get increased slightly to the outer bank (P10) for streamwise and lateral turbulence components. Further, the percentage increase in averaged turbulence intensities is observed as 12%, 9%, 7% and 2% for leafy, mixed vegetation, grasses and cylindrical layouts relative to no-vegetation scenario. This indicates the higher degree of turbulence occurs with effect of floodplain frond (leafy) canopy than the rod (cylindrical) canopy, at a greater level of



TH-2690_166152105

relative flow depth. The results indicate that vegetation patches significantly reduce turbulence-induced flow mixing.

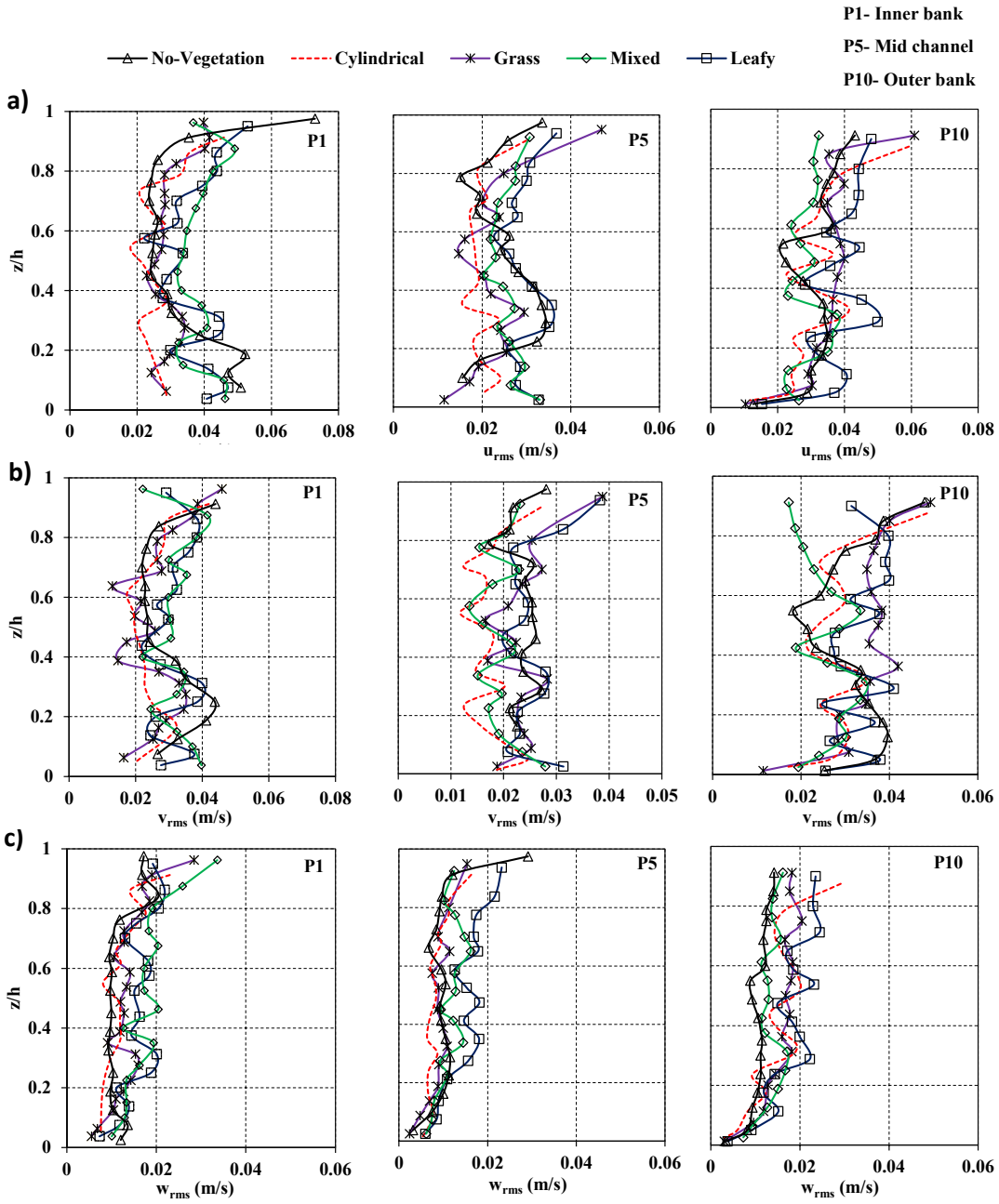


*Figure 4.7* Vertical distribution of turbulence intensity components *i.e., (a)* streamwise turbulence ($u_{rms}$), *(b)* lateral turbulence ($w_{rms}$), and *(c)* vertical turbulence ($w_{rms}$)

## Reynold's Shear Stress and Turbulent Kinetic Energy

In this section the effect of the different plant forms of the vegetation elements on the Reynolds stresses are discussed. In Figure 4.8, the variations of vertical Reynold's



TH-2690_166152105

stress for the no-vegetation, cylindrical, grass, mixed and leafy vegetation forms at the location of apex (P1, P5 and P10) are shown. The percentage increase in Reynold's shear stresses is observed as 56%, 45%, 39% and 17% for leafy, mixed vegetation, grasses and cylindrical layouts as compared with no-vegetation condition. The average Reynold's stress values are more for leafy vegetation compared to other layouts (increasing order trend with other layouts). For highly resistant leafy layout, the peak value is 2.7, 1 and 1.15 $cm^2/s^2$, which is observed at z/h ~ 0.8 to 1 (closer to top of flood-plain vegetation) of P1 (inner bank), P5 (mid) and P10 (outer bank). The near-bed (z/h= 0-0.2) values varied between -0.25 to -1.06, -0.03 to -0.7 and -0.05 to -0.87 at P1, P5 and P10 respectively. In addition, the variability of values is relatively higher above the channel-floodplain transition (from z/h ~0.4 to 1). In all other layouts (cylindrical and grasses), there is no significant changes in Reynold's stress values near to the bed across the channel cross-section. In the cylindrical layout, the vertical profile shows almost the uniform values throughout the flow depth, because of no significant interactions between flow and flood-plain vegetation unlike other plant forms. The maximum value of Reynold's stress and turbulent intensities occur near the point of inflexion in the velocity profile. From the Figure 3.8, the maximum exchange of mass and momentum at the upper vegetated layer, as evidenced by the achievement of maximum Reynold's stress near the vegetation canopy top. This is due to the additional surface area of frond vegetation type such as leafy vegetation causes larger drag forces into the main channel, the shear-generated turbulence is increased due to the inhibition of momentum exchange by the frond surface area.

Figure 4.4b shows the vertical distribution of turbulent kinetic energy (TKE) in a cross-section of apex section for different vegetation forms. In general, the patterns of Reynold's stresses ($RS_{u'v'}$) and TKE are similar throughout the cross-section. The percentage difference in turbulent kinetic energy is observed as 35%, 29%, 25% and 9% for leafy, mixed vegetation, grasses and cylindrical layouts as compared with no-vegetation condition. Similar to the Reynold's shear stress, the turbulent kinetic energy shows a maximum near the interface, which increases with increases in vegetation density. As the mean flow accelerates into apex section, curvature-induced secondary circulation moves progressively closer to the outer bank. As a result, absolute magnitudes of the $RS_{u'v'}$ and TKE increase over the entire flow depth. At these locations the maximum values of $RS_{u'v'}$ and TKE occur near the water surface and decrease evidently near the bed. The maximum turbulent kinetic energy occurs near bed at z/h ~ 0.5 for leafy vegetation.



TH-2690_166152105

From the results, it has been revealed that, the additional surface area of vegetation and heterogeneity in plant forms, have a remarkable influence on flow patterns. Due to the maximum surface area of the plant causes more the streamwise velocity and TKE values in the main channel.

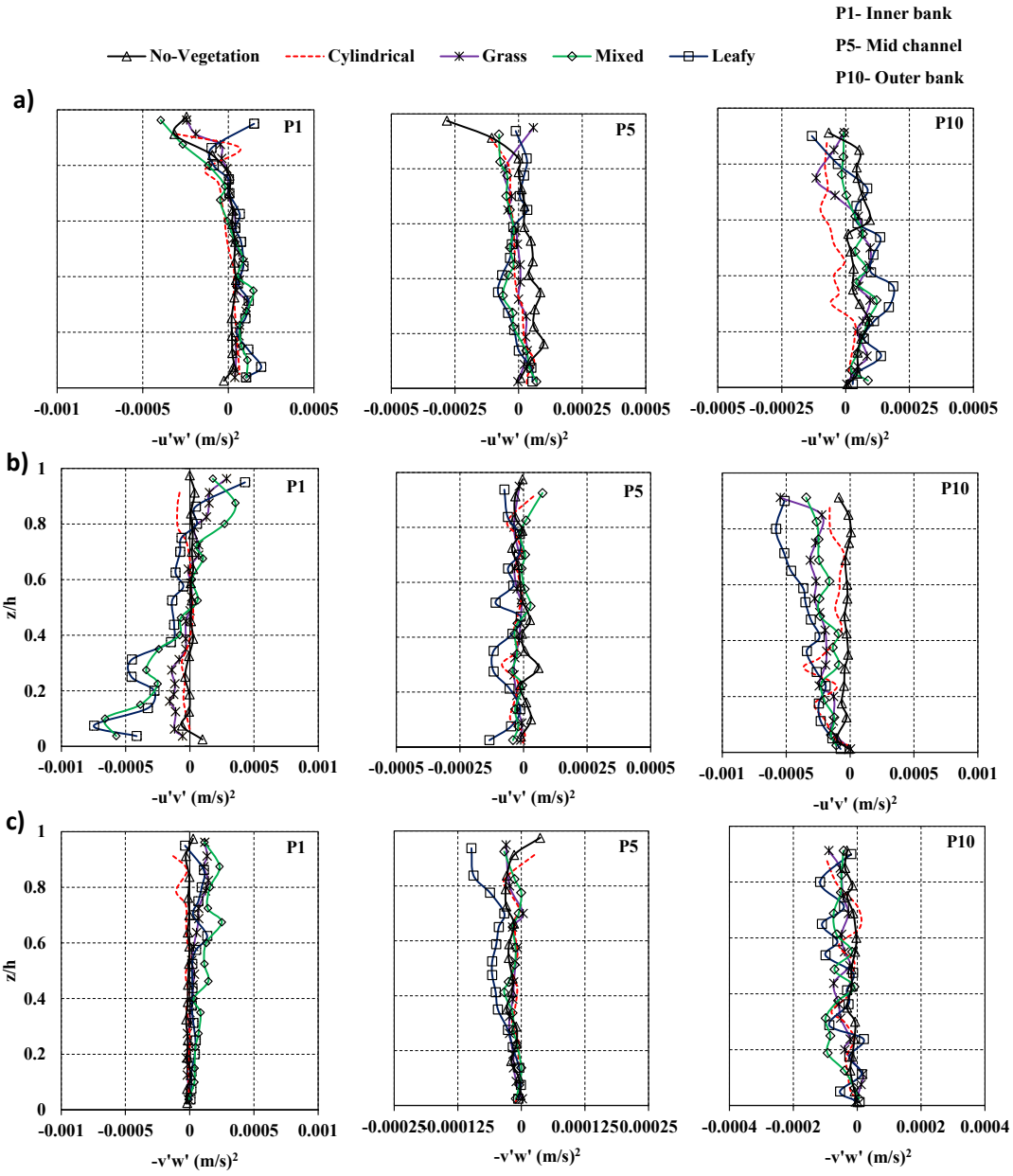


*Figure 4.8* Vertical distributions of Reynold's shear stress components *i.e., (a)* vertical Reynold stress ($RS_{u'w'}$), *(b)* lateral Reynold stress ($RS_{u'v'}$), *(c)* streamwise Reynold stress ($RS_{v'w'}$)



TH-2690_166152105

## 4.4 DISCUSSIONS

This section discusses changes in flow structure due to different floodplain vegetation layouts. Figure 4.3 illustrates the process-based mechanisms in the main channel with the effect of floodplain heterogeneous green river corridor. A large velocity gradient is generated between the vegetated and non-vegetated regions, indicating that there must be remarkable mass and momentum exchanges at the junction of the two areas. In this study, flow through different vegetation layouts significantly alters the distribution of velocity profiles due to physical features of the plant form. The velocity profiles in leafy (frond canopy) and rigid cylindrical (rod canopy) vegetation can be clearly seen based on its shape. In the lower canopy zone, velocity is constant and, at canopy level ($z/h > 0.8$) velocity profile shows accelerating trend due to shear layer interaction. Whereas, the bladed vegetation has no such difference due to flexibility of the vegetation causing velocity profile accelerating throughout the canopy zone. Due to significant difference in velocity at above and below the vegetation layer, the momentum exchange will take place to formation of shear layer at the interface or top of the vegetation. A similar observation was noticed by Wilson et al., (2003). According to Past studies, the velocity profile in the canopy zone follows a logarithmic law (Jarvela, 2005; Chen et al., 2011; Li et al., 2014). This observation can be noticed in the present study as the measurements were taken in the main channel and submerged flow condition. The results showed that the effect of plant form is significant in controlling the velocity reduction. The presence of highly resistant leafy cover and mixed vegetation forms is supporting for increased velocity in the main stream. The alteration in peak value to slightly above the canopy top was also noticed. This is may be due to the increased drag caused by the presence of leaves (additional surface area) in leafy plant form alters the momentum transfer by limiting the vertical momentum exchange between the vegetated and the over flow region. Also, negative $RS_{u'v'}$ at near bed is due to negative velocity gradient indicating upward momentum transfer (Figure 4.8). Similar phenomena were noticed by the Siniscalchi et al., 2012. According to the Jahra 2010 study, when the vegetation density grows, the streamwise velocity increases in the main channel and decreases in the vegetation, resulting in an increase in the vertical and spanwise Reynolds stresses at the vegetation interface.

Trinci et al., 2017 reported that few aquatic species prefer zones of high turbulence intensity, intermediate velocities and low TKE. Hockley et al., 2014



TH-2690_166152105

recognized the importance of heterogeneous flow conditions in rivers. Present study also shows the high turbulent intensity values were observed for the leafy vegetation. Zhang et al., 2015 reported that the higher turbulence intensity intensifies the sediment transport in the water flow. This indicates the vegetated floodplain conditions are having more capacity of sediment entrapment regions which is helpful for creating ecological zones. Reynolds shear stress expresses the momentum exchange between particles due to the flow velocity variation in turbulence. As a result, It is an vital parameter in assessing the soil erosion and sediment movement. Turbulence has been observed to be higher at the frond canopy level than the rigid cylindrical vegetation, because lateral flow deflection around the canopy top produced strong shear layers in the wake of a frond canopy leaves (Xu and Nepf 2020; Boothroyd et al., 2017; Yagci et al., 2010 and Kitsikoudis et al., 2016). Farzadkhoo et al., 2018 reported that the rigid vegetation over the floodplain can be employed as an addition parameter in river rehabilitation works for achieving of environmental management objectives. Similarly, our study also concluded that the turbulent structures are less in cylindrical (rigid stem) vegetation layout as compared with other vegetation layouts, which is helpful for river restoration schemes.

## 4.5 CHAPTER SUMMARY

Vegetation has the ability to significantly alter the time-averaged, and instantaneous flow characteristics of turbulent flow seperation, with significant implications for sediment transport and river morphology. In the present study, an analysis of laboratory experiments was conducted to investigate the effect of submerged heterogeneous vegetation patches on flow structure. For this purpose, three natural plant forms (leafy, grass and cylindrical) arranged in four different layouts (Figure 4.2), namely leafy, mixed, flexible grass, cylindrical vegetation layouts were studied. Laboratory experiments were undertaken to investigate the effect of different plant forms under submerged vegetation conditions on turbulence characteristics in a low sinuous channel. The following are the conclusions derived from the present investigation.

First, the percentage increment in primary velocities is observed as 38%, 27%, 23% and 21% for leafy, mixed vegetation, grasses and cylindrical layouts as compared with no-vegetation condition. This indicates the shear layer occupies the relatively larger portion in the main channel of the leafy vegetation than the cylindrical vegetation. Second in the case of leafy vegetation, the reduction in velocity in the channel from P1 (inner



TH-2690_166152105

bank) to P10 (outer bank) is observed as 51% at vegetation canopy height. Third the maximum magnitude of secondary velocity vectors is about 26%, 24%, 22%, 14% and 12% of the maximum streamwise velocity for leafy, mixed, grass, cylindrical and no-vegetation respectively. Fourth the vertical turbulence intensity component ($w_{rms}$) increases with the distance from the bottom until z/h~0.05, and reaches higher at top of the water surface i.e., z/h~ 1. This indicates the increase in $w_{rms}$ shows the energy transfer near the surface on the vertical direction of water flow.

This work can be further extended to study with different layouts of heterogeneous vegetation covers under varying flow conditions. To investigate further, detailed measurements on floodplain of the river can be helpful for predicting the flow processes in a river. With further improvement in knowledge, heterogeneous vegetation patches can be developed for riparian management activities in order to improve ecological behavior and sediment deposition zones.



TH-2690_166152105

# 5

# COMBINED EFFECT OF BRIDGE PIERS AND FLOODPLAIN VEGETATION ON MAIN CHANNEL HYDRAULICS

The hydrodynamics of flow around the vicinity of bridge piers in rivers are of great importance to hydraulic engineers and researchers. Scientific research in and around bridge piers and floodplain vegetation presents the multilevel fluid dynamics of a River. This allows to understand the interactions of bridge pier and heterogeneous vegetation cover on the river corridor with flow field of stream channel. This chapter addresses following questions through experimental study.

- What kind of flow structure is observed in main river with combined effect of bridge pier and floodplain vegetation?
- How can the spatial variation of turbulence characteristics with the presence of bridge piers be occurred in a low sinuous river?

## 5.1 INTRODUCTION

The flow around bridge pier is completely three-dimensional and it is quite complex to predict the coherent structures (Raudkivi and Ettema 1983; Melville and Chiew 1999; Kirkil and Constantinesu 2008). On river bars and floodplains, vegetation is ubiquitous, and it can have a major impact on flow, sediment transport rates, stream temperature, bank stability, and aquatic ecology. (e.g., Ormerod et al., 1993; McKenney

TH-2690_166152105

et al., 1995; Abernethy and Rutherfurd 1998; Simon and Collison 2002; Pollen 2007). And presence of floodplain vegetation plays an important role on river system by improving the biological characteristics (Brachet 2015). Basic physical properties of vegetation, such as variations in drag, changes in streamwise velocity, turbulence patterns, the occurrence of periodic vortices, deposition distributions, increased flow resistance, and lower conveyance capacities, were discovered in their investigations (e.g., Nepf 1999, Lopez and Garcia 2001, Bennett et al., 2002, James and Makoa 2006 and Zong and Nepf 2011).

Different flow fields are generated due to the interaction of approach flow with bridge piers, including downflow, horse-shoe vortex, wake vortices and bow waves, which result a complex flow field in the stream channel. Several authors like Kothayari et al.,1992, Koken 2008, Keshavarzi et al., 2014, Morales 2013, Lee 2019 have discussed about the turbulent flow and scour around the bridge piers. When bridge piers restrict the flow in an alluvial channel, dynamic pressure rises in front of the pier, resulting in an adverse pressure gradient from the free surface to the channel's bottom. As a result, flow separation occurs near the pier, resulting in the creation of vortices surrounding the pier (Narayana et al 2021). The three-dimensional separated flows are typically composed of a complex system of vortices. Dargahi 1989 stated that the magnitudes of the vortices present around the vicinity of the cylinder are independent of Reynold's number, and it is mainly influenced by the diameter of the pier. Goutam et al., 2019 reported that comparison of pier with and without pile cap, the flow structures such as mean velocities, turbulence intensities and Reynold's shear stresses are lower than the simple pier.

Present scenario, several studies assume rivers having a fixed width. Though, the studies did not consider the green corridor along the bank is also a part of the river. While constructing any hydraulic structures, we are disturbing the green corridor and the impact of river ecology has not been considered. Although, many studies have been carried on flow structures in the vicinity of bridge piers. This study investigated the combined effect of bridge pier and floodplain vegetation on main channel hydraulics. Experiments were conducted to obtain the contribution single and double bridge pier along with floodplain vegetation on flow behavior. Therefore, the three-dimensional analysis of velocity measurements was used to find the characteristics of turbulent flow in front of the bridge pier in association with the heterogeneous green corridor. The effect of size of bridge pier and floodplain vegetation on flow structures and their relations with erosion are presented



TH-2690_166152105

in this work. Figure 5.1 shows the downflow patterns and vortex mechanism around the bridge piers. The objectives of this work are, therefore: (a) to investigate the turbulent flow structures with the combined effect of bridge piers and floodplain vegetation; and (b) how their behavior is different from existing studies of without vegetation corridor. For these objectives, conducted laboratory experiments for four different layouts (Figure 3), such as no-vegetation, with floodplain vegetation, single bridge pier (SP) and double bridge pier (DP) along with floodplain vegetation, and detailed flow measurements were taken to determine the flow response.

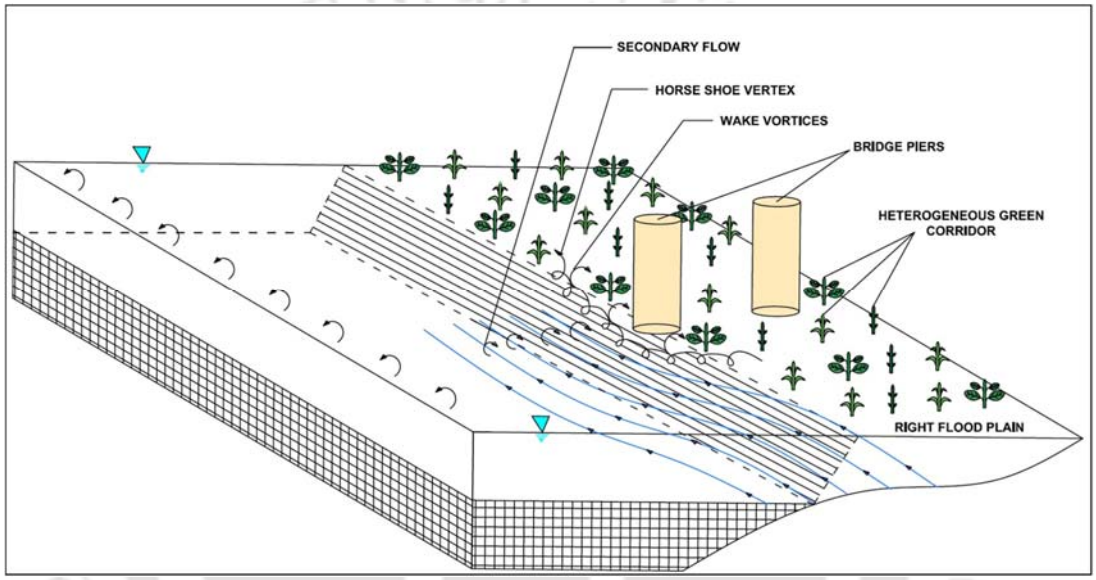


*Figure 5.1* Conceptual representation of bridge piers along with heterogeneous green river corridor

## 5.2 MATERIALS AND METHODS

### 5.2.1 Experimental Setup

Experiments were conducted in the Fluvial hydro-ecological laboratory, at IIT Guwahati. With a dimension of 18m long, 1 m wide and 0.3 m deep flume. The flume primarily consists of inlet chamber, stream channel, outlet chamber and recirculating system. A collecting chamber of 4 m long, 1.5 m wide and 1.5 m depth with concrete walls and roughness elements was placed at the upstream to diminish the turbulence and to straighten the incoming flow into the channel. The slope maintained throughout the channel is 0.001. Sinuosity has taken for the channel is 1.1. Two 15 HP pumps control flow discharge with a discharge of 15 litres/sec. The $D_{50}$ used for the median sand particle



TH-2690_166152105

size was 0.37 mm. The flume was slowly allowed the water to saturate the sand bed. After complete saturation of bed, the required discharge was established with the flow depth was gradually increased or decreased by adjusting the height of tailgate until the target flow depth was obtained. The discharge was measured using V- notch located at the entrance of the flume and the digital point gauge was used to measure the flow depth. Instantaneous velocity measurements were obtained with three-dimensional acoustic Doppler velocimeter, (4 probe, 10 MHz Vectrino ADV manufactured by Nortek) at a sampling frequency of 100 Hz. The duration of data acquisition was fixed to 2 minutes and in total 10,000 samples were collected. Accelerating threshold (Goring and Nikora, 2002; Dey et al., 2012; Devi, 2016) was used to post-process the time series velocity data for removing the spikes.

To minimize the side wall effects, maintain the width of the channel is 14 times the diameter of the pier (Raudkivi and Ettema 1983). To avoid the sediment size effects, followed the ratio of pier diameter to sediment size was 79 (Raudkivi 1998). And also, Chiew and Melville (1987) determined that pier diameter should not exceed 10% of flume width, to eliminate the wall impact on scouring. The test section is chosen an apex section of the sinuous channel. The experiments were conducted for a single and double bridge pier along with the floodplain vegetation. Figure 5.2 shows the experimental layouts of a) no-vegetation condition b) with floodplain vegetation c) single bridge pier (SP), 2-inch $\phi$ cast iron pipe surrounding with floodplain vegetation and d) double bridge pier (DP) experiment, two 1-inch $\phi$ PVC pipes surrounding with floodplain vegetation were chosen. In case of floodplain vegetation, the natural heterogeneous vegetation forms were planted with a configuration of 400 plants/$m^2$ in a staggered pattern, vegetation type were followed the section 4.2.2, and experiments were performed to analyze the turbulent characteristics.



TH-2690_166152105

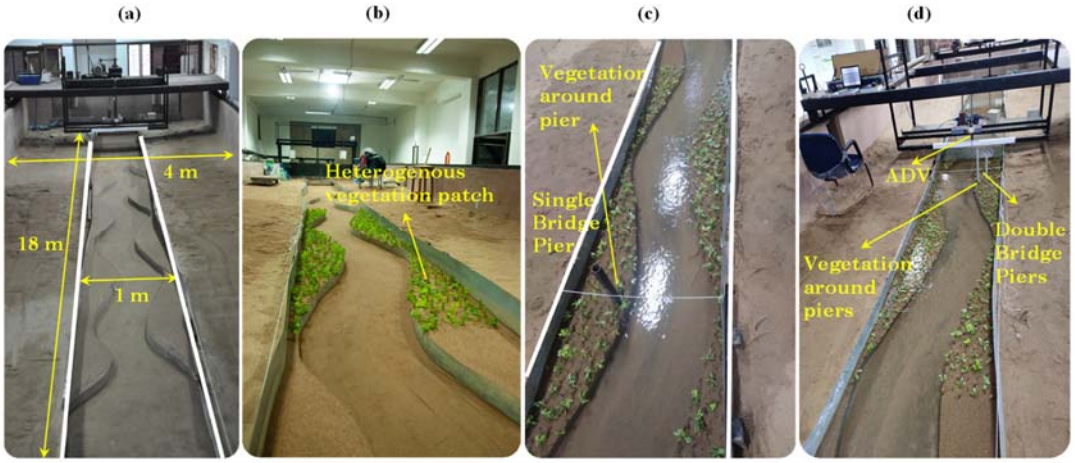


*Figure 5.2* Experimental flume setup at IIT Guwahati: *(a)* plan view showing basic components and dimensions; *(b)*, *(c)* and *(d)* front view showing test section, with floodplain vegetation, single and double bridge piers along with vegetated floodplain and measuring equipment

### 5.2.2 Flow Conditions and Measurement Locations

Experiments were conducted in submerged flow conditions in which flow depth is at the vegetation height. In the present work, considering the bed under no transport condition, the main channel depths were maintained lesser than the incipient motion depths (Devi et al., 2016). The corresponding flow depth (H) and discharge (Q) were 14 cm and 0.0153 $m^3/s$ respectively. Table 5.1 shows the hydraulic conditions maintained in the channel for single and double bridge pier experimental layouts. Measurement locations in the experiments were positioned in the main channel form P1 to P6 at apex section. Figure 5.3 shows the measurement locations along the cross-section of the channel. Instantaneous velocity components were measured with Acoustic Doppler Velocimeter (ADV) along the flow depth at increments of 1 cm from the near bed. Thus, 14 measurement points at each vertical profile were obtained.



TH-2690_166152105

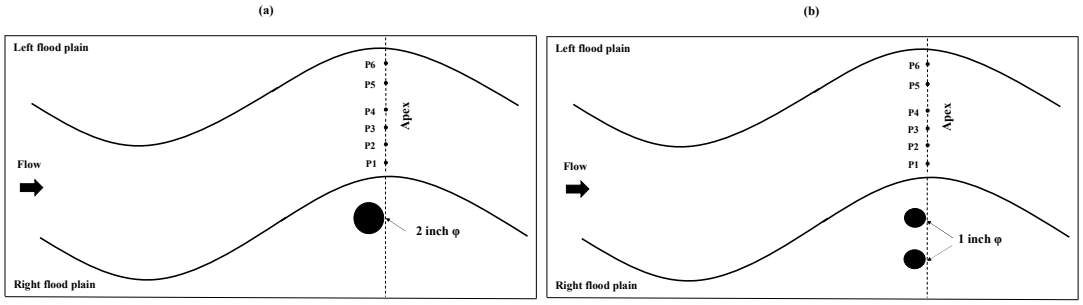


*Figure 5.3* A schematic representation of *a)* single and *b)* double bridge pier layouts and measurement locations.

*Table 5.1:* Summary of the experiments

| S. No. | Experiment layout | Pattern | Flow Depth (cm) | $F_r$ | Re |
|---|---|---|---|---|---|
| **1** | Single bridge pier with heterogeneous vegetation | Figure 5.3a | 14 | 0.245 | 20930 |
| **2** | Double bridge pier with heterogeneous vegetation | Figure 5.3b | 14 | 0.234 | 20020 |

*Table 5.2:* Trend of turbulence parameters

| Turbulence characteristics | Single Pier (SP) | Double Pier (DP) |
|---|---|---|
| Streamwise velocity (m/s) | 0.25 | 0.23 |
| Secondary Velocity | 0.011 | 0.027 |
| Turbulence Intensity ($u_{rms}$) - (m/s) | 0.053 | 0.048 |
| Reynold's shear stress ($-u'w'$) - ($m^2/s^2$) | -0.000019 | -0.000047 |
| Turbulent kinetic energy - ($m^2/s^2$) | 0.00312 | 0.00276 |



TH-2690_166152105

## 5.3 RESULTS

### 5.3.1 Main channel flow structures with effect of bridge piers and floodplain vegetation

Streamwise Velocity:

Figure 5.4(I) represents the normalized streamwise velocity contours in main channel cross-section influenced by single and double bridge piers on the floodplain surrounding with vegetation. The higher velocity zone is found at the inner bank and gradually decreasing towards the outer bank with increasing distance from the piers present on the right floodplain. The combined effect of bridge piers and flood-plain vegetation is observed by increased high velocity region with shear layer separating the low and high-velocity zones towards the outer bank. This indicates flow develops strong inward motion with in the main channel as flood-plain flow approaches the bridge pier. In the case of single- bridge pier (2-inch ϕ) condition, the length of the higher velocity region is more and lower velocity region is less, while in double piers of smaller diameters (1-inch ϕ each) condition, the length of velocity zones is opposite. This result in variability of shear layer zone in both the cases. In single pier, the shear layer is observed between Y/h: 0.7 to 2.2, and in double pier, it is observed from Y/h: 0.9 to 2.7. With the addition of bridge piers, the lateral velocity gradient increases at the interface, generating a significant shear layer at that position. The results show that the presence of other layouts in single large diameter pier with floodplain vegetation increases the velocity in the main channel up to 36% compared to no-obstruction on the floodplain.

Figure 5.4(II), represents the vertical distribution profiles showing the variation of streamwise velocity in the main channel with combined effect of bridge piers and floodplain vegetation. The velocity profiles were observed to be follow the logarithmic nature for all the conditions. The velocity magnitude in the main channel, P1(near inner bank) and P4 (mid of the channel) shows the highest velocities which is close to 0.3 m/s at water surface level. However, at P6 (near outer bank) showing that the values at the surface level 0.1 m/s and at the bed level which is 0.03 m/s. This indicates the vertical streamwise velocities were very low at outer bank which follows the streamwise contour plots (figure 5.4 I). From these vertical profiles the study did not predict much effect of the size of the pier in the main channel.



TH-2690_166152105

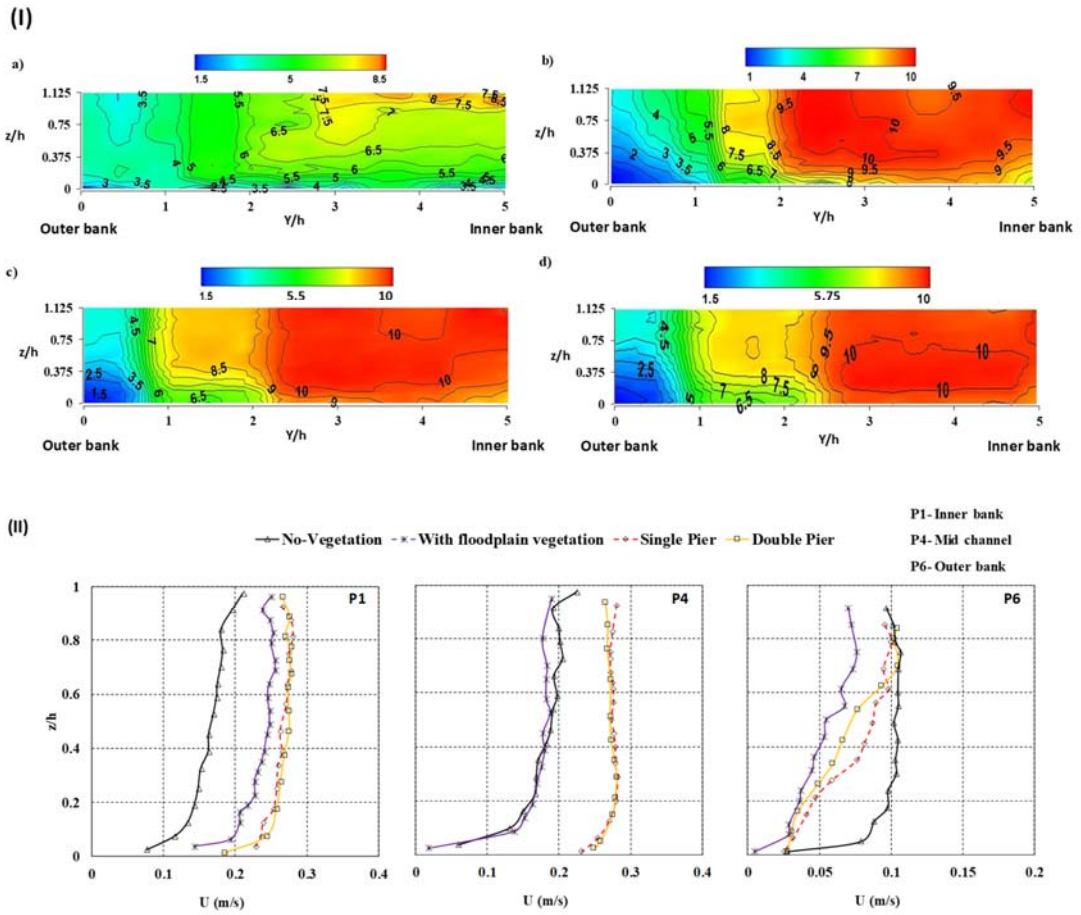


*Figure 5.4* Streamwise velocities; *I)* normalized contour plots for *a)* no-vegetation *b)* with floodplain vegetation *c)* single pier (SP) and *d)* double bridge pier (DP) conditions *II)* vertical distributions of longitudinal velocity at apex section

## Secondary Velocity:

Figure 5.5 (I), shows the secondary flow patterns in the main channel influenced by bridge pier diameter and flood-plain vegetation. For a single bridge pier (SP) (Figure 5.5 Ic), the circulation of secondary current cell is clearly visible at the mid of the channel and at a height of z/h = 0.2-0.4. The secondary flow circulations were observed over the maximum part of the channel cross-section in this case. However, for the case of double pier condition, the secondary circulations were observed close to the banks and with relatively less intensity, which is closely similar to the case of only flood-plain vegetation (Figure 5.5 Ib). This shows the secondary circulation patterns are more influenced by the larger diameter pier which is probably due to combined influence of horse-shoe vortex, curvature effects and shear zone vortex. The magnitude of secondary velocity vectors in single-pier case is 11% (at P1, inner bank), 7.5% (at P2), 7.5% (at P3), 4% (at P4), 4% (at



TH-2690_166152105

P5) and 6% (at P6, outer bank) of the streamwise velocity from near inner bank to outer bank. In double pier condition, the magnitude of secondary velocity vectors is relatively higher, which is 8% (P1), 19% (P2), 15% (P3), 12% (P4), 11% (P5) and 6% (P6) of the streamwise velocity. The results show the pier with less diameter does not influence the secondary circulations but increased the magnitude of secondary velocity. In both the cases, there is no significant effect of bridge pier on secondary velocity magnitude at outer banks.

Figure 5.5 (II), shows the vorticity contours (clock wise and anti-clock wise) for the no-vegetation, with floodplain vegetation, single pier and double pier conditions. The secondary vortex (negative and anticlockwise vortex) originated from the boundary layer separation is observed underneath the primary vortex (clockwise vortex) at Y/h= 0 to 1 (DP) and Y/h= 0 to 2 (SP). It is shown that the secondary vortex is found strong near outer bank for both the SP and DP conditions. In the single pier condition, the length of the vortex is more and its strength is 2 times more than double pier conditions. This reveals that secondary vortex grows its size and strength in case of the large diameter pier.

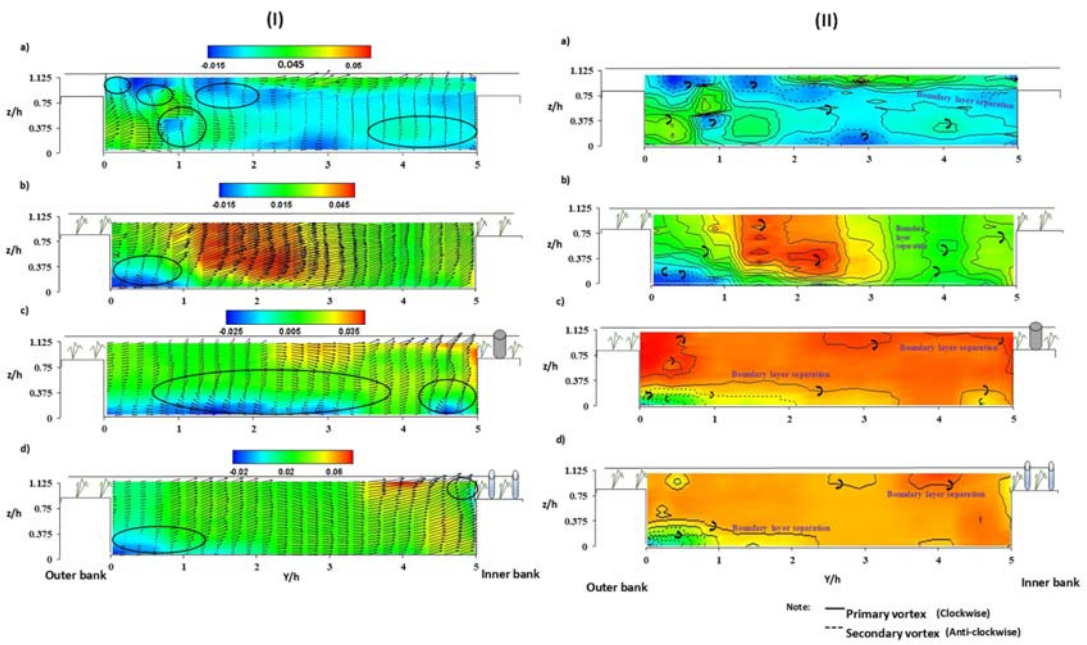


*Figure 5.5* Secondary flow and vorticity contour plots for *a)* no-vegetation *b)* with floodplain vegetation *c)* single pier and *d)* double bridge pier conditions at apex section

Turbulence Intensity:



TH-2690_166152105

Figure 5.6 shows the normalized turbulence intensity (TI) behavior in the main channel for various conditions of flood-plain vegetation and bridge pier. Figure 5.6 (I) b representing the effect of flood-plain vegetation shows the TI core region (0.04 m/s) at z/h ~ 0.375 near to outer bank and surface core region at inner bank. In comparison to Figure 5.6 (I) c, d representing the cases of combined effect of bridge pier and vegetation, the turbulence intensity is relatively higher (0.055 m/s) and the maximum value is observed at the surface towards the inner bank. This may be because of increased turbulence generated due to bridge pier in the main channel.

Figure 5.6 (II) shows vertical profiles of streamwise, lateral and vertical turbulence intensities at P1 (inner bank), P4 (mid) and P6 (outer bank). The comparative analysis of turbulence intensity in the main channel revealed significantly higher values in the channel influenced by combined effect of bridge pier and vegetation. Moreover, the larger diameter single pier has shown increased effect than smaller diameter and double number bridge piers. In almost all the cases, higher turbulence intensities are observed particularly at surface level of P1 (near inner bank), which is channel-floodplain interface and P4 (mid channel). The percentage increase in streamwise turbulence intensity ($u_{rms}$) for different cases. Such as 22% more for only vegetation, 37% more for double pier with vegetation and 40% more for single pier with vegetation as compared no vegetation case. Figure 5.6 II b shows the lateral turbulence intensity ($v_{rms}$) increases with the distance from the bottom until z/h=0.15, and higher than z/h=0.15 it decreases linearly until the floodplain elevation, reaching a minimum value at about z/h=0.3, and then increasing again upward to the water surface to form almost an S-shaped distribution at outer bank (P10). Figure 5.6 II c, for all the experimental cases the vertical turbulence intensities ($w_{rms}$) increases with the distance from the bottom until z/h~0.05, and reaches higher at top of the water surface *i.e.,* z/h~ 1. This indicates the increase in $w_{rms}$ shows energy transfer near the surface on the vertical direction of water flow.



TH-2690_166152105

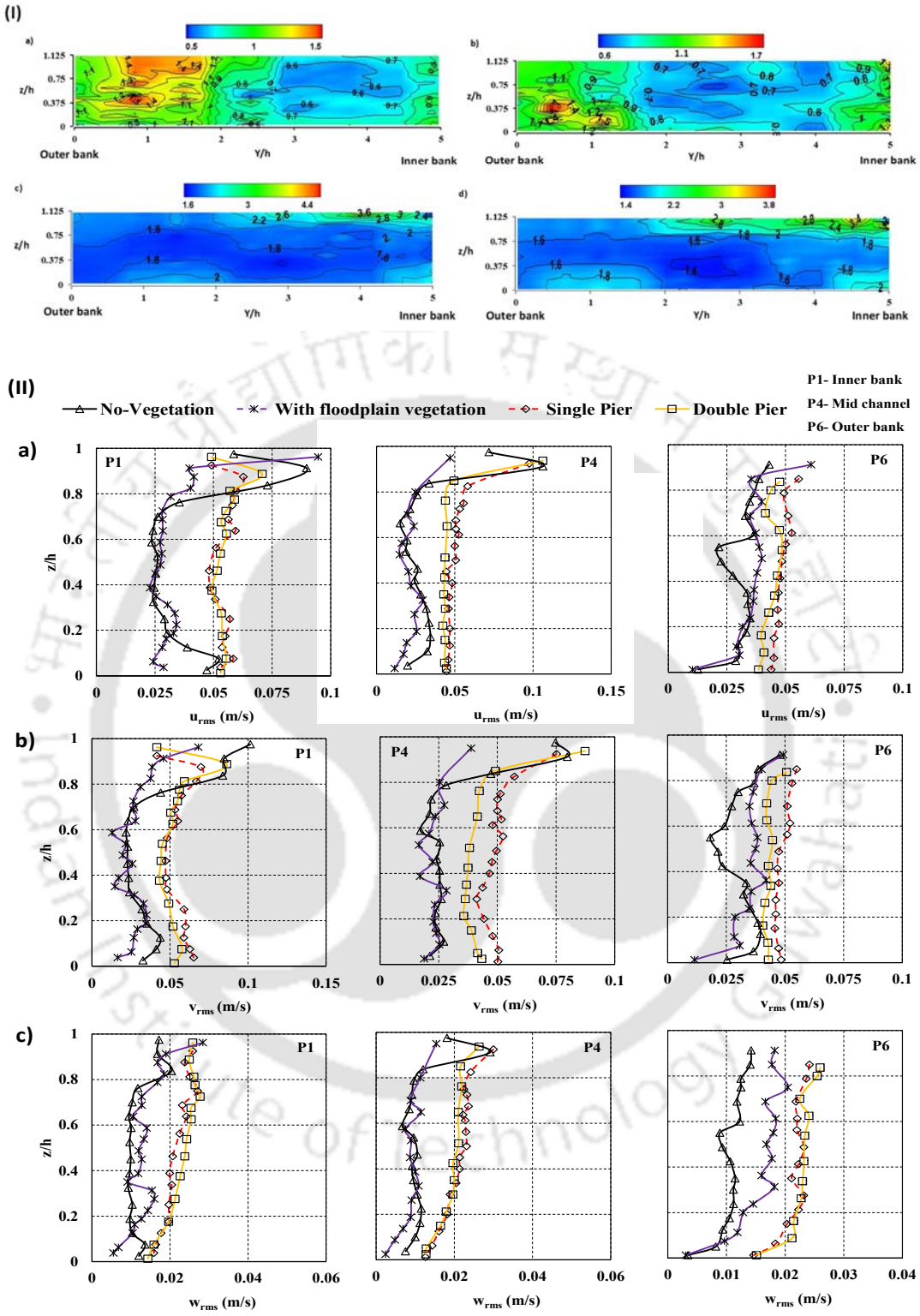


*Figure 5.6* Turbulence intensities; *I)* normalized contour plots for *a)* no-vegetation *b)* with floodplain vegetation *c)* single pier and *d)* double bridge pier conditions *II)* vertical distributions of turbulence intensity in *u*, *v* and *w* directions at apex section



TH-2690_166152105

### Reynold's Shear Stress:

Figure 5.7 (I) shows normalized Reynold's shear stress contours for different cases of flood-plain vegetation and bridge pier dimensions. The maximum positive Reynold's stresses occur at the floodplain and channel transition for all the cases except for non-vegetated condition, which indicates that the shear becomes dominant and the maximum along the inner bend apex of the main channel. The floodplain resistance cause to alter the main channel Reynold's stresses, with positive values close to the surface and negative values near to the bed. Further, zero Reynolds stress line is found along the cross-section just below the water surface. This type of behavior may also be expected from the lateral gradient of the streamwise mean velocity in Figure 5.4 (I). In single pier and double pier conditions influenced by vegetation, well-defined clusters can be seen at the near water surface of mid channel (Y/h = 2 to 4). This may be because of influence of wake regions formed due to bridge piers and the vegetation. The influence of horse-shoe vortices around the bridge pier and strong velocity gradient due to inflow-bridge pier-flood plain vegetation interactions may also be responsible for varying patterns of Reynolds stresses.

Figure 5.7 (II) shows the vertical profiles of Reynold's stresses ($RS_{u'w'}$, others) for different scenarios of flood-plain vegetation and bridge piers. The results show that the absolute values of $RS_{u'w'}$ are higher compared to $RS_{v'w'}$ and $RS_{u'v'}$. At P1 (near inner bank) for all Reynold's stress components, the mixing activity can be observed at z/h > 0.6 (floodplain-channel transition). At P4 (mid) the $RS_{u'w'}$, $RS_{u'v'}$ values were almost uniform upto the z/h > 0.8, the mixing activity can be observed at and above the z/h is 0.8. The maximum value of $RS_{u'w'}$ at P4 occurs close to the free surface and decreases to the zero at the bed. At P6 (near outer bank) of all the components of Reynold's stresses were observed almost linear and there is not much significant mixing activity. Overall, the bridge piers and vegetation cover effecting the shear layer at P1 is more significant, which can be observed from vertical profiles in all components of Reynold's Stresses.



TH-2690_166152105

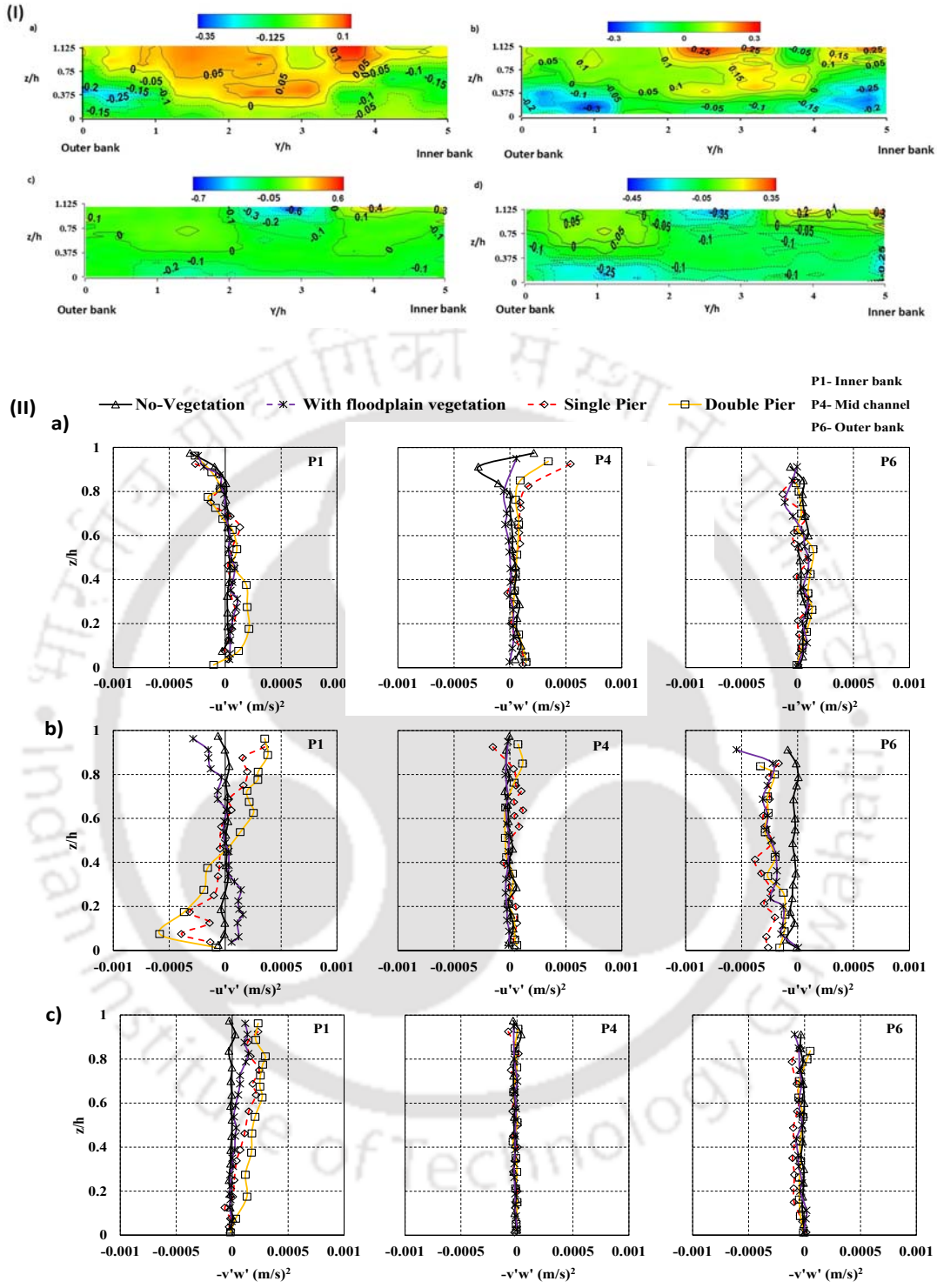


*Figure 5.7* Reynold's shear stresses; *I)* normalized contour plots for *a)* no-vegetation *b)* with floodplain vegetation *c)* single pier and *d)* double bridge pier conditions *II)* Vertical distributions of Reynold's shear stresses, *-u'w'* (vertical), *-u'v'* (lateral) and *-v'w'* (streamwise) directions at apex section



TH-2690_166152105

### Turbulent Kinetic Energy:

Figure 5.8 (I), illustrates the contour plots of normalized turbulent kinetic energy influenced by bridge pier diameter and flood-plain vegetation. The maximum value of the TKE observed at a distance about z/h~1 from bed and Y/h~ 4 from the edge. The patterns of turbulent kinetic energy confirm that values of TKE are most significant at the surface level (z/h>1) for the SP and DP conditions amongst the SP condition having the highest TKE value. The magnitude of TKE within the shear layer (Figure 5.8 (I)) weakens, as shown in figure 5.4 (I), the clustered isovels between the low-velocity region near the outer bank for streamwise velocities. In the maximum TKE region, a closed interval of isovels at the inner bank can be observed, resulting in the strong shearing flow present in the channel due to the bridge piers surrounding with vegetation.

Figure 5.8 (II), shows the combined effect of bridge pier and floodplain vegetation on turbulent kinetic energy behavior in the main channel at P1, P4 and P6 respectively. According to the figure, observed the combined effect of bridge pier and floodplain vegetation reflects in TKE at each location. The percentage increase in turbulent kinetic energy for different cases. Such as 30% more for only vegetation, 45% more for double pier with vegetation and 51% more for single pier with vegetation as compared no vegetation case.



TH-2690_166152105

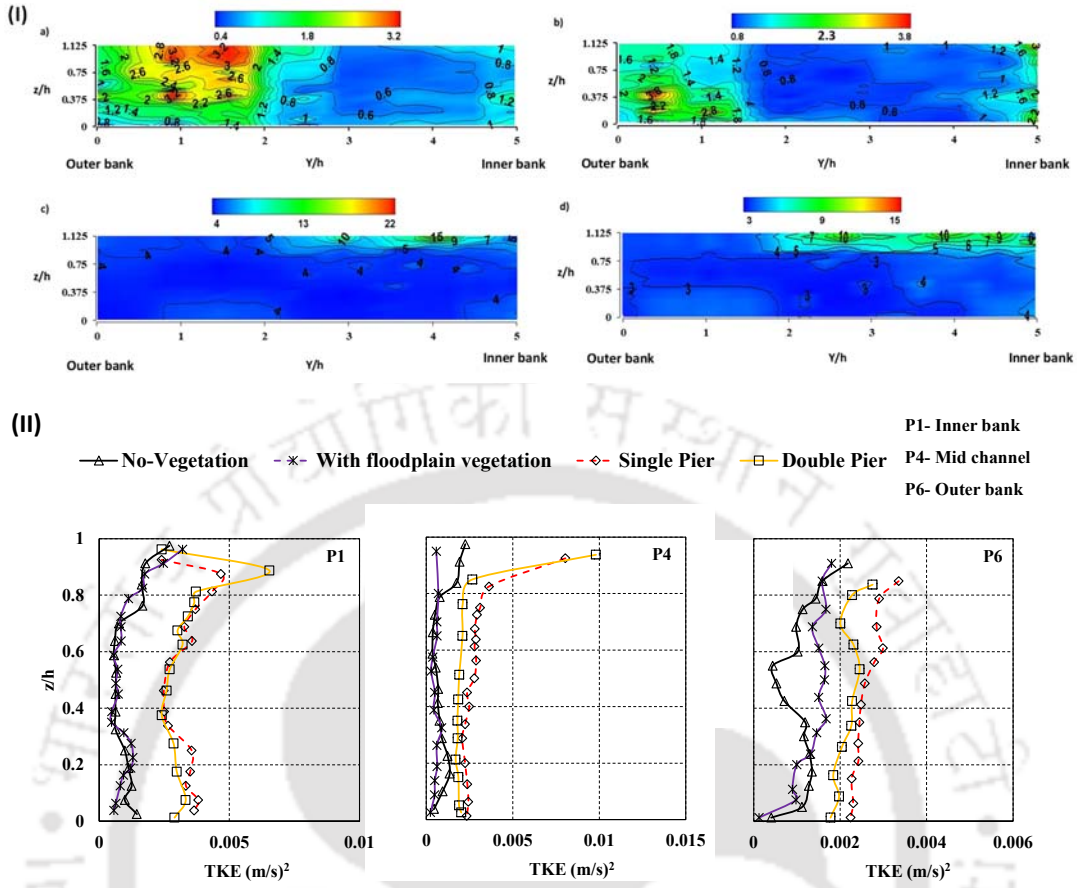


*Figure 5.8* Turbulent kinetic energy; *I)* normalized contour plots for *a)* no-vegetation *b)* with floodplain vegetation *c)* single pier and *d)* double bridge pier conditions. *II)* Vertical distributions of turbulent kinetic energy (TKE) at apex section

### 5.3.2 Flow angle with the effect of bridge piers and floodplain vegetation

The flow angle can be resolved into components with an angle Θ. Where this angle obtained by $\Theta = \tan^{-1}(\overline{v'}/\overline{u'})$. The ratio of lateral velocity ($V_{mc}$) to longitudinal velocity ($U_{mc}$) represents the intensity of secondary flow in the channel (Liu et al., 2016). The vertical distributions in the main channel of P1, P4 and P6 for SP and DP conditions are shown in the Figure 5.9, illustrating the angle between the main channel and floodplain flow induced by the curvature and roughness. At the outer bank (P6) bed level, the flow angle in SP condition is -44°and DP condition is -47°. The negative sign indicates that the sign of $V_{mc}$ and $U_{mc}$ is different. The significant effect is observed by the flow angle i.e., at P1 and P4 in both the conditions. At P1, for SP condition the angle made by the flow is 0° at (z/h ~ 0.02) and in DP condition it is Θ > 0° at bed level. On the other hand, for DP condition, at P1 at z/h> 0.6 the flow angle is less than 0°. In SP



TH-2690_166152105

condition P1 and P4 at channel-floodplain transition (z/h> 0.8) Θ > 0°. This indicates the flow becomes complex near inner bank (P1) with presence of single bridge pier (larger diameter) and floodplain vegetation.

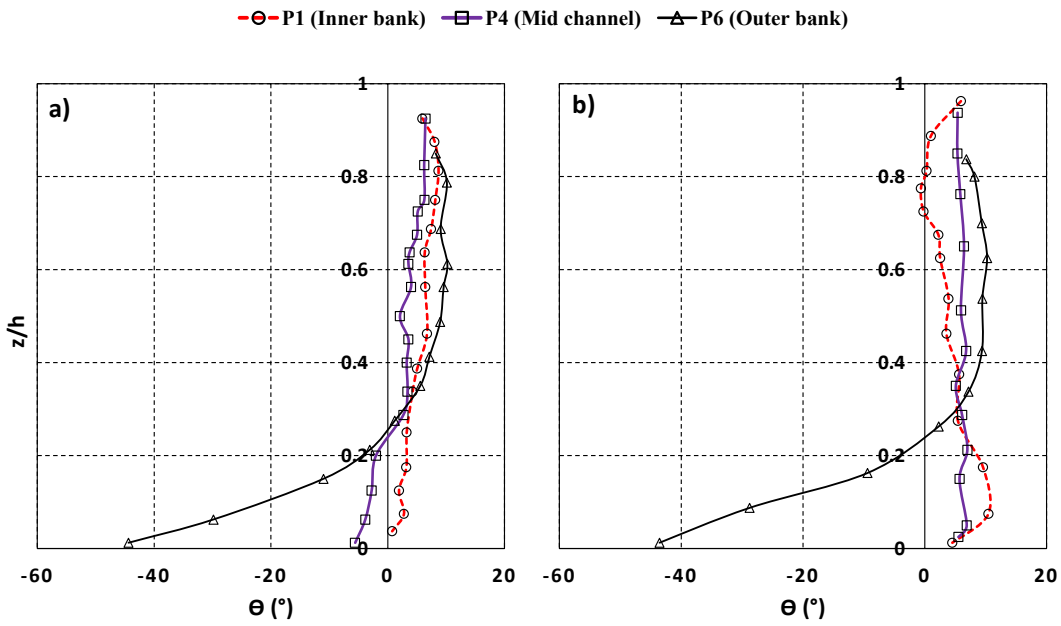


*Figure 5.9* Flow angle for *a)* single bridge pier *b)* double bridge pier along with floodplain vegetation conditions

### 5.3.3 Transverse profiles in the channel:

Figure 5.10 shows the variation of flow characteristics across the transverse section is evaluated with the combined effect of bridge pier and floodplain vegetation. Figure 5.10a shows the transverse direction of streamwise flow velocities, near to the junction of main channel and bridge piers with floodplain vegetation is high, and the values of the velocity reduces suddenly when flowing out from the bridge piers and vegetated region (i.e from the mid channel), whereas the velocities gradually increase from P1 (near inner bank) to P4 (mid channel) and declining curve is observed from P4 to P6 (near outer bank). The percentage difference between P1 to P6 for different cases such as 27% for only vegetation, 34% more for double pier with vegetation and 36% more for single pier with vegetation. Due to the presence of bridge pier surrounding vegetation on right floodplain, more flow velocity is forced into the channel causing the increase of the velocities. And there are some relatively severe fluxes from inner bank (P1) to outer bank (P6) due to the higher lateral flow velocity and momentum exchange of the transition zone between bridge pier along with vegetated region. Figure 5.10b shows that the



TH-2690_166152105

turbulence intensities in transverse direction are determined. As shown in the figure, the turbulence intensity decreases gradually in the main channel from inner bank to outer bank. The range of turbulence intensity vary approximately 0.05 to 0.06 m/s for the single bridge pier condition, therefore the turbulence intensity of the single pier case dominant significantly with double bridge pier condition.

Figure 5.10c shows the distributions of the Reynold's shear stress along the transverse section corresponding to the single and double bridge pier along with floodplain vegetation. Reynold's shear stresses show some relatively drastic fluctuations near inner bank (P1 to P4) for single bridge pier condition due to the adverse pressure gradient of the transition zone between roughness and smooth areas. Results indicate, the Reynold's shear stresses are greatly affected by the presence of large diameter pier surrounded with floodplain vegetation. As shown in the figure 5.10d, the turbulent kinetic energy gradually decreases and tend to be stable along the transverse section. However, single pier condition at P3 due to the pressure gradient after that gradually vary flow along the section is observed. Based on the above discussion, the dominance of single large diameter over all the turbulence features in the main channel is noticed. The turbulence parameters significantly showed much difference between SP and DP cases.



TH-2690_166152105

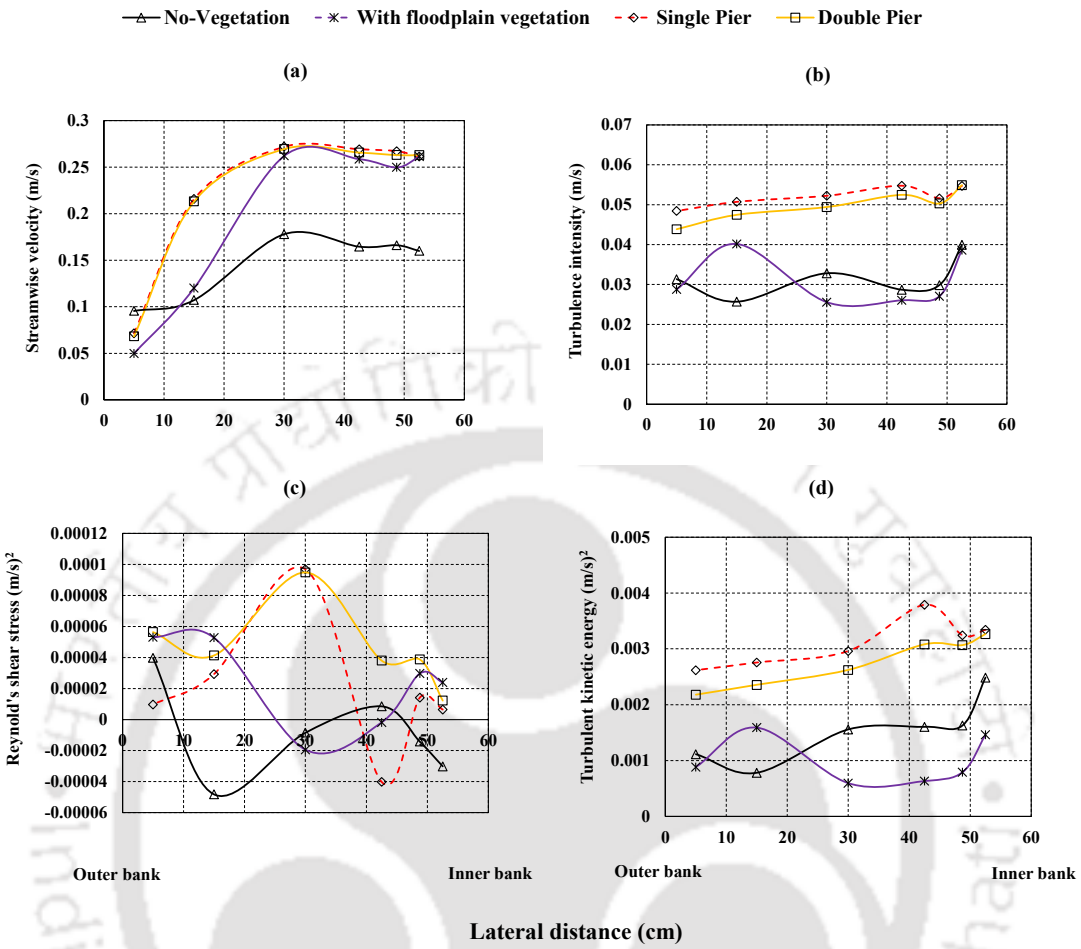


*Figure 5.10* Variation of turbulence characteristic profiles along the transverse section of apex region

## 5.4 DISCUSSIONS

This section discusses the combined effect of bridge pier diameter and floodplain vegetation on the main channel flow structures of a low sinuous compound channel. Figure 5.1 represents the conceptual understanding of mean streamwise and secondary velocity distribution due to the interactions of main channel flow-bridge pier-floodplain vegetation. Figure 5.4 (I), shows the shear layer that generates along the edge of the vegetated region is therefore extended to lateral motion upto Y/h= 2.2 from inner bank in SP case. This indicates the shear layer is pushed away from the vegetated zone along with the presence of bridge piers.

Figure 5.5 (II), secondary vortex (negative and anticlockwise vortex) originated from the boundary layer separation underneath the primary vortex (clockwise vortex) at



TH-2690_166152105

Y/h= 0 to 1 (DP) and Y/h= 0 to 2 (SP). Graf and Yulistiyanto (1998) and Beheshti (2010) reported the similar results in their study. Dargahi (1989) investigated flow structures around circular pier on rigid bed and also observed that and reported wake vortices were independent of horseshoe vortex. Figure 5.6 (II) shows that the streamwise turbulence intensity ($u_{rms}$) is larger than the vertical turbulence intensity ($v_{rms}$), while the transverse turbulence intensity ($w_{rms}$) is between the horizontal and vertical turbulence intensities. The higher turbulent intensities were found to occur close to the inner edge of the main channel z/h >0.8. Table 5.3 shows the double bridge pier condition having less values for turbulence intensity, Reynold's shear stress and turbulent kinetic energy. This indicates, the large diameter of single bridge pier condition causes more turbulence in the channel. Figure 5.6 (I) revealed a high-level pocket of Vertical Reynold's stress ($RS_{u'w'}$) component (about 2 times of corresponding values in the main channel) from contour plots near the surface level at a distance about (Y/h =4) from inner edge of the single pier condition. Figure 5.8-I, shows the magnitude of TKE within the shear layer is weakens. As shown in figure 5.4 (I) the clustered isovels between the low-velocity region near the outer bank for streamwise velocities. In this study the shear layer is pushed away from the vegetated zone along with the presence of bridge piers. This indicates the turbulent energy is more in the particular region. Similar observations are also reported by Abad et al., 2008.

## 5.5 CHAPTER SUMMARY

In this study the combined effect of bridge pier and floodplain vegetation on main channel turbulence parameters were investigated. For this purpose, conducted laboratory experiments for four different layouts (Figure 3), such as no-vegetation, with floodplain vegetation, single bridge pier (SP) and double bridge pier (DP) along with floodplain vegetation. The results are helpful to predict the flow patterns inside the channel due to presence of river engineering structures on floodplain along with vegetation. The major observations in the study lead to the following conclusions.

i) The presence of single large diameter pier with floodplain vegetation increases the main channel velocity up to 36% compared to no-obstruction on the floodplain. For the double pier condition, it is observed to be 31%.



TH-2690_166152105

ii) The variability in shear layer zone is observed to be different for different pier conditions. In the case of single pier, the shear layer is observed between Y/h: 0.7 to 2.2, while in double pier, it is observed from Y/h: 0.9 to 2.7. With the addition of bridge piers to the floodplain vegetation, the lateral velocity gradient increases at the interface generating a significant shear layer.

iii) In the single pier of larger diameter, the length of the vortex is more and its strength is 2 times more than double pier of smaller diameter. This reveals that secondary vortex grows its size and strength in case of the large diameter pier.

iv) The percentage increase in streamwise turbulence intensity ($u_{rms}$) in the main channel for different cases is 22% more for only vegetation, 37% more for double pier with vegetation and 40% more for single pier with vegetation as compared no vegetation condition.

v) The higher mixing activity can be observed at floodplain-channel interface with increase in Reynold's shear stress components at the inner bank (P1). Overall, the bridge piers and vegetation cover effecting the shear layer at inner bank is more significant, which can be observed from vertical profiles in all components of Reynolds Stresses.

vi) In both the single pier and double pier conditions, the magnitude of TKE within the shear layer is relatively less as compared to the inner bank where maximum TKE is observed at closed intervals of isovels. This is due to the strong shearing flow present in the channel with effect of bridge piers surrounded with vegetation.

The larger diameter of the pier is more susceptible to the main stream in the context of streamwise and transverse velocities. Moreover, the convergence induced contraction of curved channel along with bridge pier on its floodplain is solely affected the turbulent structures in the main stream of the channel. The experiments associated with the pier diameter and number of piers placed on floodplain will be notable addition of understanding the flow behavior. The data can potentially be used to validate and verify with numerical model in the next chapter.



TH-2690_166152105

# 6

# NUMERICAL INVESTIGATION OF EFFECT OF GREEN CORRIDOR AND BRIDGE PIERS ON RIVER TURBULENCE

The river exhibits complex hydrodynamic characteristics with different levels of interdependent processes occurring simultaneously. On the other hand, vegetation improves the river ecological condition and helps for the planform stability. The riparian zones of river are generally covered with vegetation patches and this makes important to study vegetation influence on river turbulence. This chapter addresses following question through numerical modeling.

- How the computational models like Flow-3D will predict the flow structures in a sinuous river with floodplain vegetation?
- How much the correlation between turbulence features of experimental and numerical conditions will vary?

## 6.1 INTRODUCTION

Flow structures in the meandering channel is more complex than the regular channels due to complex three-dimensional nature. Vegetation in riverine environment plays an important role by changing in the velocity distribution, turbulence structures, incidence of periodic vortices, spreading deposition, increase in flow resistance and decrease in conveyance efficiency. Several past studies have investigated the interaction

TH-2690_166152105

between flow and flexible vegetation (such as Kouwen and Unny 1973; Temple 1986; Fathi-Moghadam and Kouwen 1997; Wu et al. 1999; Kouwen and Fathi-Moghadam 2000; Jarvela 2002; Carollo et al. 2002; Jarvela 2004; Armanini et al. 2005; Carollo et al. 2005; Righetti 2008; Aberle and Jarvela 2013). Liu et al. (2008) conducted the experiments to determine the velocity distributions and turbulence properties in the vegetated channels. The experimental and numerical studies on flow through vegetation in open channels were investigated by Shimizu 1994, Nepf 1999, Nepf and Vivoni 2000, Stephan and Gutknecht 2002, Neary 2003, Erduran and Kutija 2003, Stoesser et al., 2003, Defina and Bixio 2005, Choi and Kang 2004, Stoesser et al., 2010. The turbulence structures in the main channel effected by floodplain vegetation have been examined through laboratory experiments and numerical studies.

Nikora et al., 2007 stated that the main turbulent models for hydrodynamic applications can be divided into three categories:1) no averaging Direct Numerical Simulation (DNS) models; 2) spatial averaging of the Navier-Stokes equations of Large Eddy Simulation (LES) models; and 3) Reynolds Averaged Navier-Stokes (RANS) models with temporal averaging of the Navier-Stokes equations. Their study mentioned that the DNS method is extremely expensive, particularly for complex geometries and heterogeneous cases at higher Reynolds numbers. Cui and Neary 2008 and Stoesser et al., 2009 used the LES approach to simulate flows influenced by aquatic vegetation. Huang et al., 2009 obtained the LES experimental results, which studied the effect of plant density on large-scale coherent structures inside the canopy sublayer. The k-ε turbulence model has been used to simulate flows impacted by vegetation by Choi and Kang 2004, Fischer-Antze et al., 2001, López and García 2001, and Neary 2003. These studies demonstrate the model capabilities of simulating the vegetation effects on the flow characteristics. However, due to configurable parameters and coefficients for flows with vegetation cover, the model still has some limitations.

Present study, also includes the experimental and numerical investigation on effect of bridge piers along with floodplain vegetation on main channel hydraulics. The turbulent flow around a bridge pier is quite complex and that has been analyzed both computationally and experimentally by Melville and Raudkivi 1977; Dargahi 1990; Ahmed and Rajarantnam 1998; Ettema et al., 2006; Unger and Hager 2006; Dey and Raikar 2007; Kirkil et al., 2008. Chang et al., 1999 solved the flow equations around a bridge pier with a fixed bed and no scour using a large-eddy simulation (LES) model. Tseng et al., 2000



TH-2690_166152105

used LES to run a numerical simulation for square and circular type piers. The flow patterns around a bridge pier with and without the scour hole were modelled by Richardson et al., 1998. They discovered that the FLOW-3D fluid dynamic model accurately predicts the complicated flow patterns around the bridge pier when they analyzed the simulated and experimental data. They discovered that the down flow originates at the pier's front face, which has an impact on the formation of the horseshoe vortex. They also compared the experimental results to simulated turbulence structures, lift coefficient, and drag coefficient and the agreements were found satisfactory.

Considering the importance of vegetation for the flow phenomena of a river, in this objective hydrodynamic change due to presence of vegetation cover on floodplain is studied using three-dimensional computational fluid dynamic model, FLOW-3D. This study provides the assessment between the simulation and experimental data by conducting the range of comparisons. Present study asses the simulation of experimental sinuous channel for analyzing the flow features like velocity distribution and turbulent structures in the apex, bend and cross-over regions by the turbulence modelling such as Renormalization-Group (RNG) model in the FLOW-3D [FLOW-3D V.12, FLOW-3D HYDRO v1.0 u 1]. In the present work, the results are presented through an experimental investigation related to the case of flexible submerged vegetation that has been modeled by placing cylindrical (rigid vegetation) rods due to limitation of the model. And also in this study, numerical simulations were conducted to investigate the effect on turbulence structures due to bridge pier and floodplain vegetation. The CFD software FLOW-3D was used to predict the 3D flow patterns in the main channel due to bridge piers and floodplain vegetation. The turbulence modelling by FLOW-3D was satisfactorily tested against experimental data of turbulence in the main channel due to the effect of bridge pier surrounded with vegetation. Effects of bridge pier and floodplain vegetation on turbulence flow were investigated by comparing different results obtained from the experiments with numerical models.

## 6.2 METHODOLOGY

### 6.2.1 Experimental conditions

A series of experiments were conducted in the fluvial tray contains the dimensions of 18m long and 1m wide of low sinuous channel. Median sand particle diameter used ($D_{50}$) 0.37mm for the bed in the fluvial hydro-ecological laboratory at IIT Guwahati.



TH-2690_166152105

Instantaneous velocity measurements were obtained with three-dimensional Acoustic Doppler Velocimeter (ADV), (4 probes, 10 MHz Vectrino ADV manufactured by Nortek) at a sampling frequency of 100 Hz with data collection up to 2 minute duration at each point. Accelerating threshold method was used to post-process the time series velocity data for removing the spikes (Goring and Nikora, 2002; Dey et al., 2012; Devi, 2016). The signal-to-noise ratio of the measurements is maintained above 15, to ensure the quality of the data collected. To carry out the experiments, test section of 1.2 m length was chosen. By measuring the velocity profiles at various cross-sections on the main channel, it is concluded that the flow at a distance 10.6 m from the inlet of flume, the flow becomes fully developed. Hence, the vegetation patch is located on the floodplain of the channel and with a distance of 8.95 m from the beginning of the flume. Figure 6.1 shows the representation of the vegetation in the model geometry as well as replicate the experimental flume.

### 6.2.2 Flow conditions and measurement locations

Experiments were conducted in submerged flow conditions in which flow depth is at the vegetation height. In the present work, considering the bed under no transport condition, the main channel depths were maintained lesser than the incipient motion depths (Devi et al., 2016). The corresponding flow depth (H) and discharge (Q) were 14 cm and 0.0153 m3/s respectively. Instantaneous velocity components were measured with ADV along the flow depth at increments of 1 cm from the near bed. Thus, 14 measurement points at each vertical profile were obtained. The experimental parameters were discussed in the table 6.1 and 6.2 for different cases.



TH-2690_166152105

*Table 6.1:* Summary of the experiments with and without floodplain vegetation

| | H(cm) | h(cm) | α | β | Q (cumecs) | $A_{mc}$ ($m^2$) | $R_{mc}$ (m) | $U_*$ (m/s) | $U_m$ (m/s) | $F_r$ | Re |
|---|---|---|---|---|---|---|---|---|---|---|---|
| **No-Vegetation** | 14 | 8 | 1.88 | 0.43 | 0.01536 | 0.07 | 0.09 | 0.029 | 0.17 | 0.18 | 15470 |
| **100 Plants/$m^2$** | 14 | 8 | 1.88 | 0.43 | 0.01536 | 0.07 | 0.09 | 0.029 | 0.19 | 0.20 | 16926 |

*Table 6.2* Summary of the experimental conditions for bridge pier with floodplain vegetation cases

| S. No. | Experiment layout | Flow Depth (cm) | Q (cumecs) | $U_*$ (m/s) | $U_m$ (m/s) | $F_r$ | Re |
|---|---|---|---|---|---|---|---|
| **1** | Single bridge pier with heterogeneous vegetation | 14 | 0.01536 | 0.029 | 0.25 | 0.245 | 20930 |
| **2** | Double bridge pier with heterogeneous vegetation | 14 | 0.01536 | 0.029 | 0.23 | 0.234 | 20020 |

## 6.3 COMPUTATIONAL MODELLING

### 6.3.1 Flow 3D modelling and approaches

The Computational fluid dynamic (CFD) solver used in this study is Flow3D model, where employs specially developed numerical techniques to solve the equations of motion for fluids to obtain transient, three-dimensional solutions to multi-scale, multi-physics flow problems. This study considered the free surface and can be included in the one-fluid incompressible mode. The Volume of Fluid (VOF) method is deployed in the Flow3D model. The RNG equations for steady, incompressible flow have been solved by CFD software to quantify the interaction between flow and vegetation in a laboratory channel. The flow region is subdivided into a mesh of fixed rectangular cells by varying of suitable grid size (e.g., 0.05m, 0.04m, 0.03m, 0.02m, 0.01m, 0.005m and 0.0025m).

The full unsteady non-hydrostatic Reynolds-averaged Navier-Stokes equations that describe the flow physics are solved by the FLOW-3D hydrodynamic model. The Two-Equation Renormalization-Group (RNG) turbulence model has been used in this study. The selection of mesh sizes was chosen based on mesh size optimization. The model was simulated for two different cases: (a) floodplain vegetation with the density of 100 plants/$m^2$; (b) no floodplain vegetation condition; (c) single pier with floodplain vegetation;



TH-2690_166152105

and (d) double pier with floodplain vegetation. In all the cases the model simulations were carried out for flow depth 14cm, and turbulence parameters were analyzed. The hydrodynamic performance evaluation of the model was carried for no-vegetation and with vegetation condition by comparing with observed velocity data. The CFD model geometry is a simplified 3D rectangular cube, as shown in Figure 6.1. The vegetation, which has been modelled as a rigid cylinder, has 3.6 m length on both sides of the floodplain.

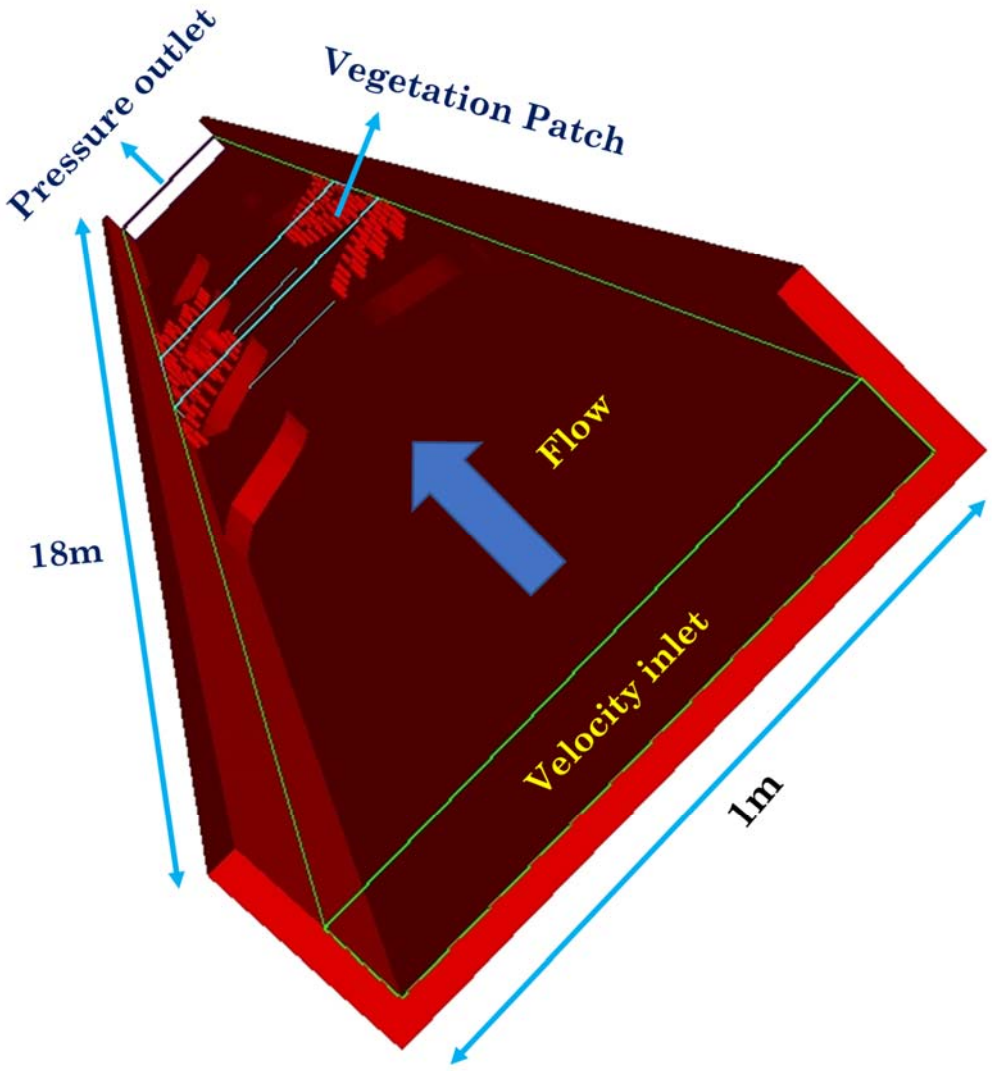


*Figure 6.1* FLOW-3D model geometry and boundary conditions.

### 6.3.2 Governing equations

FLOW-3D solves the Reynolds Averaged Navier-Stokes (RANS) equation with a finite volume approach, using the Fractional Area/Volume Obstacle Representation



TH-2690_166152105

(FAVOR) technique to define problem geometry, and a free-gridding technique for mesh generation (Flow Science Inc. 2018). The equations are continuity and RANS equations with FAVOR variables that are applied for incompressible flows.

$$\frac{\partial}{\partial X_i}(u_i A_i) = 0$$

$$\frac{\partial u_i}{\partial t} + \frac{1}{V_F}\left(u_j A_j \frac{\partial u_i}{\partial x_j}\right) = \frac{1}{\rho}\frac{\partial p}{\partial x_i} + g_i + f_i$$

where $u_i$ is the velocity in $x_i$ direction, t is the time, $A_i$ is the fractional area open to flow in the subscript directions, $V_F$ is the volume fraction of fluid in each cell, p is the hydrostatic pressure, ρ is the density, $g_i$ is the gravitational force in subscript directions and $f_i$ is the Reynolds stresses.

The most popular turbulence models include Zero-equation models, One-equation models, Two-equation models, Reynold's stress/Flux models, and Algebraic Stress/Flux models. The FLOW-3D software's formulation differs slightly from other formulations in that it incorporates the FAVOR™ method's fractional areas/volumes and generalizes the turbulence creation (or decay) related with buoyancy forces.

### 6.3.3 Turbulence Model

The available turbulence models in FLOW-3D software are the Prandtl Mixing Length Model, the One-Equation Turbulent Energy Model, the Two-Equation Standard *k-ε* Model, the Two-Equation Renormalization-Group (RNG) Model and large Eddy Simulation Model (Flow Science Inc. 2018). In general, the RNG model is classified as a more widely-used application than the standard *k-ε* model. And in particular, the RNG model is more accurate in flows that have strong shear regions than the standard *k-ε* model and it is defined to describe low intensity turbulent flows.
The 3D governing equations could be expressed as follows:

The general mass continuity equation is:

$$V_F \frac{\partial \rho}{\partial t} + \frac{\partial}{\partial x}(\rho u A_x) + R\frac{\partial}{\partial y}(\rho v A_y) + \frac{\partial}{\partial z}(\rho w A_Z) + \xi \frac{\rho u A_x}{x} = R_{DIF} + R_{SOR}$$

where $V_F$ is the fractional volume open to flow, ρ is the fluid density, $R$ is a turbulent diffusion term, and $R$ is a mass source. The velocity components ($u$, $v$, $w$) are in the



TH-2690_166152105

coordinate directions ($x, y, z$) or ($r, \theta, z$). $A_x$ is the fractional area open to flow in the x-direction, $A_y$ and $A_z$ are similar area fractions for flow in the y and $z$ directions, respectively.

### 6.3.4 Boundary Conditions

In this study, a structured and uniform block of mesh was used to simulate the main and floodplain channels. The meshes were finer at the vicinity of the fluid-structure interaction to increase the accuracy of computations. Boundary conditions included inflow discharge for the main channel and the lateral channel entrance, constant level outflow for the main channel outlet, wall for bed, right and left boundaries of the main channel, and atmospheric pressure for the top free surface. Other required wall conditions were produced using solid components. As per the restrictions in the available processing configuration, the study area mesh block is considered with more finer mesh block in order to increase the accuracy at the study section and reducing the number of mesh cells in less important areas like total channel mesh block. Considering the limitations in processing power (Xeon (R) CPU of 4.10 GHz), a mesh size optimization process was performed to find a proper balance between the consumed simulation time and the resulted accuracy of the simulations. Different mesh sizes were tested; to reduce the severe increase in computational time. Thus, a mesh domain, with 18 m length, 1 m width, and 0.14 m height and consisting of 4,424,000 cells, was opted to simulate the channels. As mentioned above, the cell sizes were reduced throughout the channel except at study area of the channel. Besides, the same cell size was identified at the corners of the interface and the space of flow mixing in order to increase the accuracy of the calculations. The front view of the all the simulated cases in this study is shown in Figure 6.2.



TH-2690_166152105

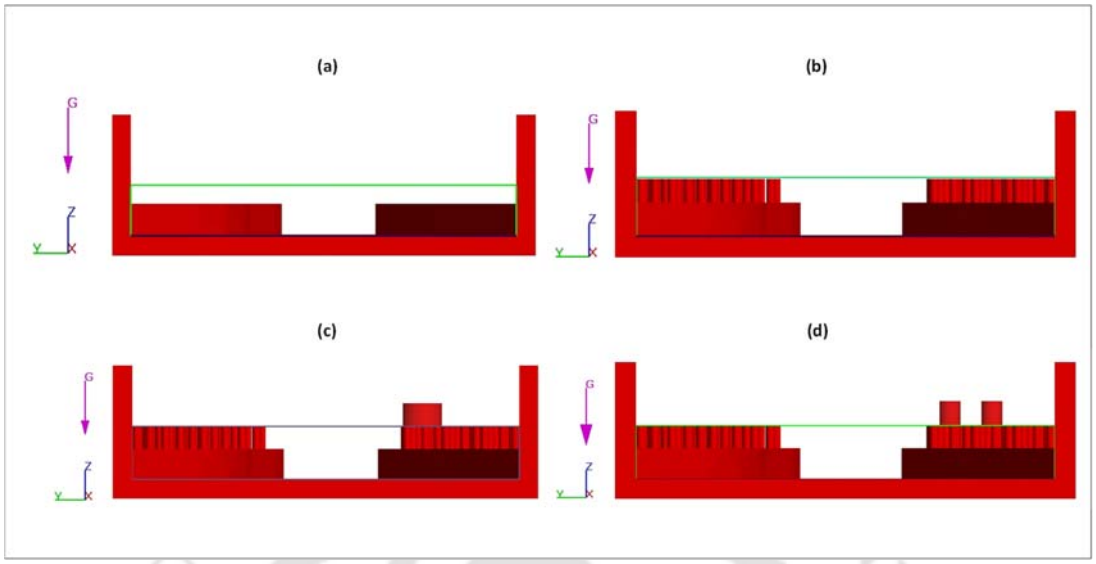


*Figure 6.2* Front view of *(a)* no-vegetation *(b)* with floodplain vegetation *(c)* single bridge pier and *(d)* double bridge pier with vegetation of submerged simulated conditions.

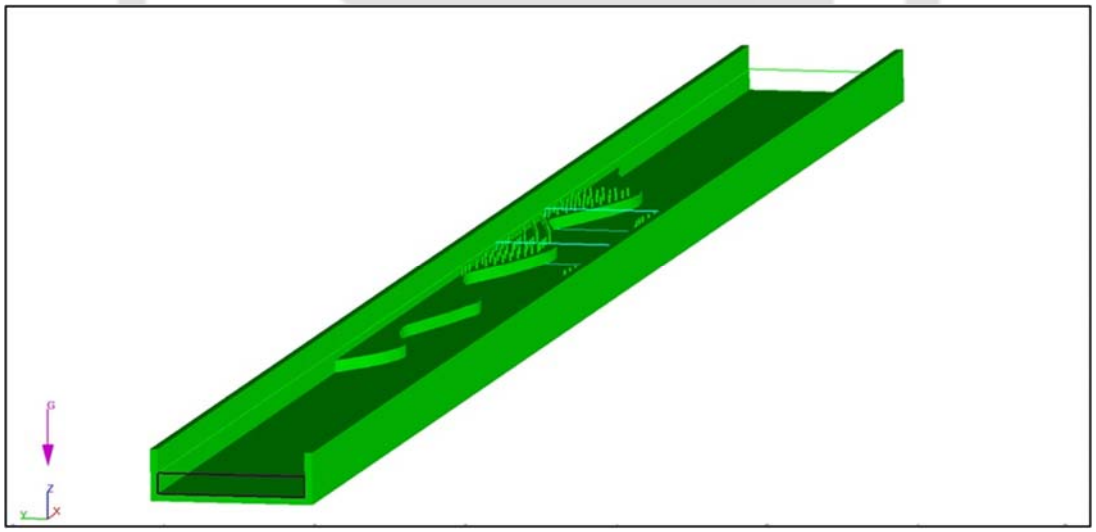

*Figure 6.3* Side view of model geometry for floodplain vegetation condition



TH-2690_166152105

*Table 6.3* Boundary condition for the experimental flume

| Geometry | Type of boundary condition |
|---|---|
| Flow inlet | Volume flow rate |
| Flow outlet | outflow |
| Right sidewall | Wall |
| Left sidewall | Wall |
| Bed of the channel | Wall |
| Surface of the channel | Atmospheric pressure |

*Table 6.4* Boundary conditions for the study area

| Geometry | Type of boundary condition |
|---|---|
| Flow inlet of the study section | Symmetry |
| Flow outlet of the study section | Symmetry |
| Right sidewall | Wall |
| Left sidewall | Wall |
| Bed of the channel | Wall |
| Top Surface of the channel | Atmospheric pressure |

### 6.3.5 Meshing and grid size of the channel

The mesh process is a very important stage that requires a lot of attention in CFD modeling. The domain had to be divided into smaller cells to analyze the fluid flow in which the governing equations would be solved as shown in Figure 6.12. The number and size of the cells are significant factors for numerical model simulation and limit the accuracy of the findings as well as the simulation time. An appropriate solution to determine the optimum mesh size is to begin with a relatively large mesh and then reducing it until the desired efficiency is reached; further mesh size reductions have no significant effect on the results. The same procedure has followed in the Figure 6.4. The mesh in the FLOW-3D numerical model divides the flow domain into tiny areas. The flow properties such as velocity, fluid fraction, and dynamic pressure are estimated in cells, which are the smallest component of the mesh. The accuracy of the results and simulation time depends directly on the mesh block size. Orthogonal mesh was used in cartesian coordinate systems. The main setup was the same for all models although floodplain vegetation density differs for each case. Each run applied one fluid, incompressible flow, and a free surface. The



TH-2690_166152105

water was set to 20 °C for all simulations. The gravity option was activated with gravitational acceleration in the *z*-direction set to (-9.81 m/s$^2$). The viscosity and turbulence options were also activated with Newtonian viscosity being applied to the flow along with a selection of appropriate turbulence. The turbulence option used in this study, the two equations RNG (Renormalization-Group) model. Non-slip or partial slip was used for wall shear boundary conditions. A numerical model geometry was prepared by drawing flume channel models using 3D SolidWorks tool. These were exported into the stereo lithography (STL) format and then directly imported into FLOW-3D where the appropriate mesh was generated.

Figure 6.1 shows the 3D computational domain model of a channel, consists of 18.0 m length, 1 m width and 0.35 m height. In the model has study area section of 1.2 m length, 1 m width and 0.14 m height and the size of meshes in *X*, *Y*, and *Z* directions for total channel and study area mesh sizes were taken as 0.01 m and 0.005 m respectively (Figure 6.4). For the total channel model, the number of cells were 2,520,000 and for the study area, the number of cells were 1,904,000. The total number of cells equal to 4,424,000 (used for solving the flow equations).

Boundary conditions should be used while solving the Navier-Stokes equation and continuous equations. Boundary conditions most significant task is to produce flow conditions that are equivalent to physical status. The FLOW-3D software has many categories of boundary condition; each type can be used for the specific condition of the models. The boundary conditions in FLOW-3D are symmetry, wall, pressure, velocity, volume flow rate, continuative, outflow, wave, periodic, and grid overlay. In the FLOW-3D tool, there are two ways to enter a finite flow rate, either for the system's inlet discharge or the domain's outlet discharge: defined velocity and volume flow rate. In the present study, for the X-minimum boundary condition the volume flow rate has been chosen. For X-maximum boundary condition, the outflow was selected because there is nothing to be calculated at the end of the flume. The volume flow rate and the elevation of surface water was set for Q= 0.01534 m3/s and 0.14 m respectively. These results showed further investigation on turbulence characteristics in depth for understanding the interaction of main channel and floodplain flow on simulation ground.



TH-2690_166152105

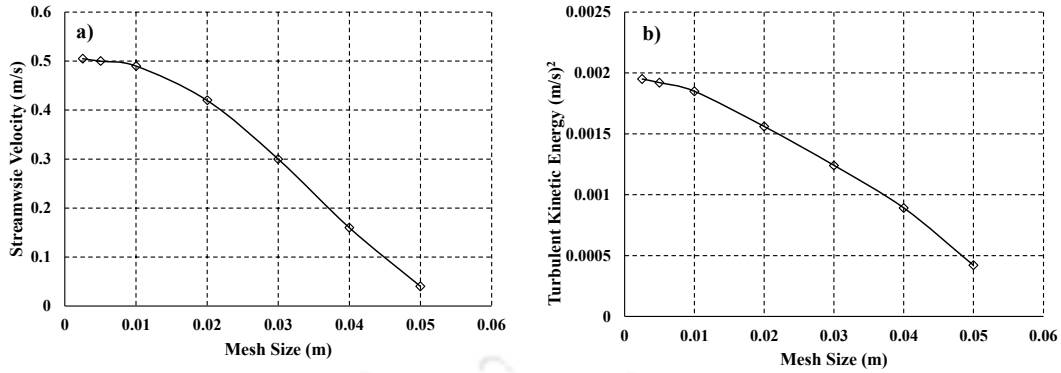


*Figure 6.4* The variation of turbulence parameters with different mesh sizes

## 6.4 RESULTS

### 6.4.1 Experimental and Model results of with and without floodplain vegetation

#### Case 1: Without Vegetation Cover over the Floodplain

Figure 6.5-6.7 represent the comparison between experimental (left panel) and model (right panel) data for without floodplain vegetation condition. Figure 6.5 compares the measured stream wise velocity profiles with the simulated ones of different cross-sections in the main channel such as apex, bend and cross-over sections. Figure shows the experimental velocity values were almost close to the simulated data as the streamwise velocity is observed as 0.24 m/s at apex section. The result indicates the reasonable agreement between simulated and experimental contour plots. From the results, the averaged streamwise velocities at the apex section in the simulated data ($U_{sim}$ = 0.17m/s) were approximately 1.2 times of the experimental result ($U_{exp}$ = 0.14m/s). The mean velocity of streamwise velocity is around $5u_*$ for experimental condition and for simulated case is $5.9u_*$. The percentage increase for streamwise velocity of no-vegetated condition for experimental to simulated condition is estimated to be approximately 15%.

Figure 6.6 represents the secondary flow comparison between measured and modeled data. The secondary flow structure is well defined in the simulated case at the apex section. The maximum magnitude of secondary velocity vectors at apex, bend and COR is about 7.5%, 11.5%, 12% respectively of the maximum streamwise velocity for experimental condition. The maximum magnitude of secondary velocity vectors at apex, bend and COR is about 3.6%, 12%, 16% respectively of the maximum streamwise velocity for simulation condition. The angle of inclination of secondary currents at apex bend and COR sections are about 2°, 7° and 9° respectively for experimental condition. The angle



TH-2690_166152105

of inclination of secondary currents at apex bend and COR sections are about 1°, 5° and 9° respectively for simulation condition. In Figure 6.6, secondary flow circulations in the simulated case at the outer bank ($4 \leq Y / h \leq 5$) is visible. Moreover, a weak main channel vortices in the no-vegetated condition at apex section throughout the channel is visible for the experimental plot (Figure 6.6(I)). At the inner bank, the circulations were strong that it reached from bed to the free surface as also shown in the experimental results. To understand the similarity index of both simulated and experimental results, at outer bank of no-vegetated condition is the better example (Figure 6.6). In the simulated results of no vegetation on the floodplain, the velocity distributions along the transverse direction have circulations at outer bank due to the curvature effect. Figure 6.7 shows the contour plots for the TKE of no-vegetation condition for both the experimental and simulated conditions, the maximum TKE observed at near bed surface in the simulated run which is not following the experimental patterns. The percentage increase in turbulent kinetic energy for experimental as 0.11% more at apex, 0.13% more at bend and 0.21% more at COR as compared to simulation case.

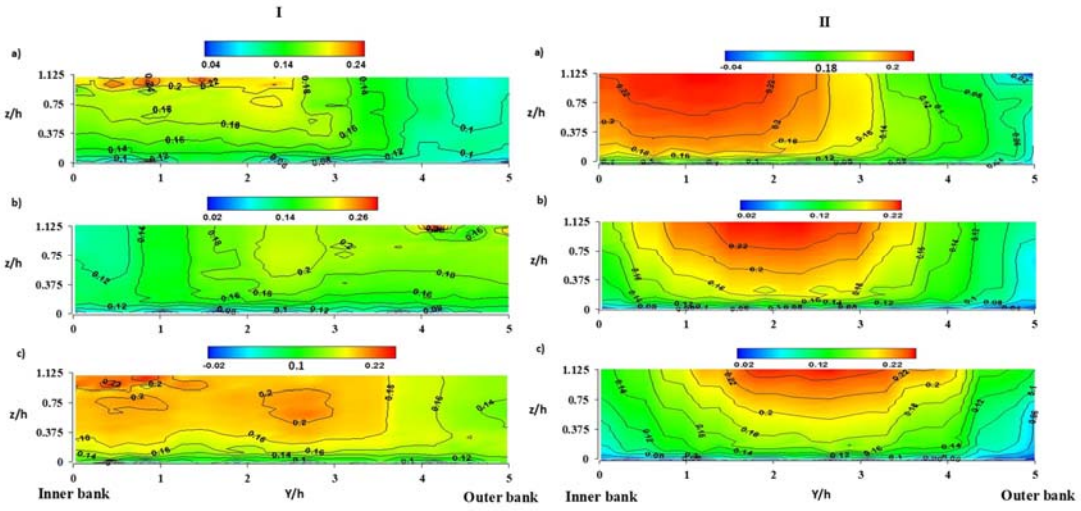


*Figure 6.5* Streamwise velocity contour plots for experimental *(I)* and simulated *(II)* conditions of no-vegetation condition at *a)* apex *b)* bend *c)* cross-over sections



TH-2690_166152105

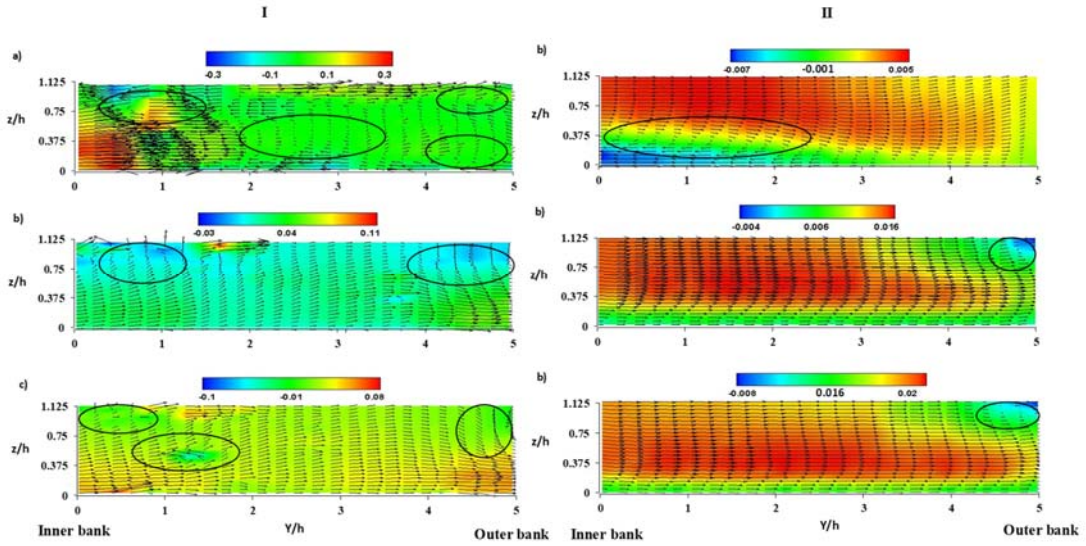


*Figure 6.6* Secondary velocity contour plots for experimental *(I)* and simulated *(II)* conditions of no-vegetation condition at *a)* apex *b)* bend *c)* cross-over sections

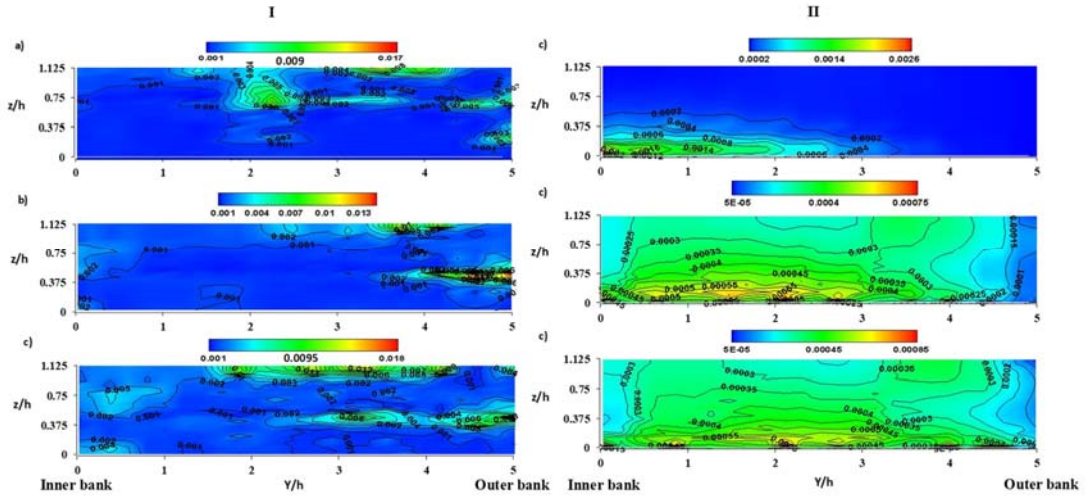


*Figure 6.7* Turbulent kinetic energy contour plots for experimental *(I)* and simulated *(II)* conditions of no-vegetation condition at *a)* apex *b)* bend *c)* cross-over sections

## Case 2: Vegetation Patch Density of 100 Plants/m$^2$ over the Floodplain

Figure 6.8-6.10 compares the experimental (left panel) with the simulated (right panel) results in an open channel with a low sinuosity of vegetation density 100 Plants/m$^2$ is considered. Figure 6.8 compares the measured stream wise velocity profiles with the simulated ones of different cross-sections in the main channel. From the results, the averaged streamwise velocities in the simulated data ($U_{sim}$ = 0.32m/s) were approximately 1.5 times of the experimental result ($U_{exp}$ = 0.2m/s). The mean velocity of streamwise velocity is around 7$u_*$ for experimental condition and for simulated case is 11$u_*$. However,



TH-2690_166152105

the apex and cross-over section in the main channel, measured locations show the reasonable results in the view of velocity core region between simulated and experimental contour plots. At the bend section the plot is relatively different indicating simulated one was not following the experimental observations. The percentage increase of mean streamwise velocity for floodplain vegetated condition for simulated condition is estimated to be approximately at apex is 47%, bend is 49.8%, and COR is 44% compared to experimental condition.

Figure 6.9 represents the secondary flow comparison between measured and modeled data of floodplain vegetated condition, the secondary flow structure is well defined in the simulated one at apex section is observed. The maximum magnitude of secondary velocity vectors at cross-sections of apex, bend and COR is about 12%, 26%, and 37% respectively of the maximum streamwise velocity for experimental condition. The maximum magnitude of secondary velocity vectors at apex, bend and COR is about 5%, 12%, and 21% respectively of the maximum streamwise velocity for simulation condition. The angle of inclination of secondary currents at apex bend and COR sections are about 3°, 7.5° and 11° respectively for experimental condition. The angle of inclination of secondary currents at apex bend and COR sections are about 2.2°, 7° and 12° respectively for simulation condition. In Figure 6.9, the secondary flow structure is well defined in the simulated one at apex section is observed. Due to the effect of floodplain vegetation, the secondary flow circulations were predicted well in the simulation case than experimental one. In Figure 6.8 (II), as $z/h < 0.75$, the distinct effect of secondary cell circulation in the main channel increased significantly in the simulated condition. The region of secondary flow circulation was shown at the apex between approximately $3 \leq Y / h \leq 5$ which is near outer bank as seen in the simulation. These secondary cells were easily recorded in the simulated results, but were absent from the experimental results due to the data's inability to missed out the wake regions. Similar observations were also made out by Singh et al., 2020. The wavy isovel lines are deepens as the vegetation introduces on the floodplain and these lines were occurred due to strong secondary currents. As the secondary circulation strength increases at outer bank, it is helpful to restrict the wavy isovel lines extended to outer bank in the vegetated condition (Figure 6.8). In such cases, the velocity distribution in the channel appears to be uniform in the lateral direction unlike that in the non-vegetated zone (Figure 6.5).



TH-2690_166152105

Figure 6.10 shows the contour plots for TKE of floodplain vegetated condition. The percentage increase in turbulent kinetic energy for experimental as 46% more at apex, 72% more at bend and 67% more at COR as compared to simulation case. The flow structures simulated by the CFD model presents an agreement with the measured data in our experimental channel. The results show some deviation between the model and the experimental data, particularly for the turbulent kinetic energy characteristics. This deviation might be related to the inability of the CFD model to simulate the micro-turbulence structures occurs in the main stream and the flow separation.

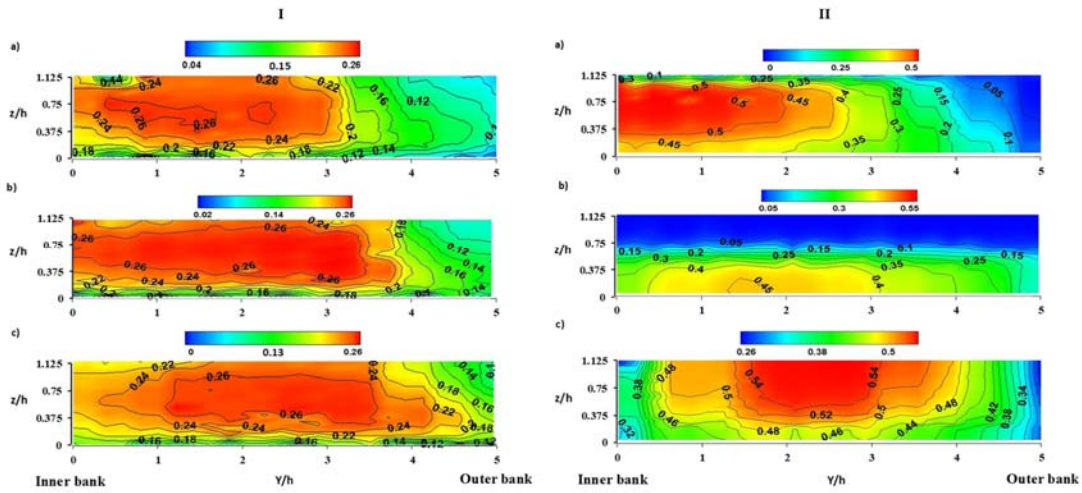


*Figure 6.8* Streamwise velocity contour plots for *I)* experimental and *II)* simulated results of floodplain vegetation density of 100 plants/m$^2$ *a)* apex *b)* bend and *c)* cross-over sections



TH-2690_166152105

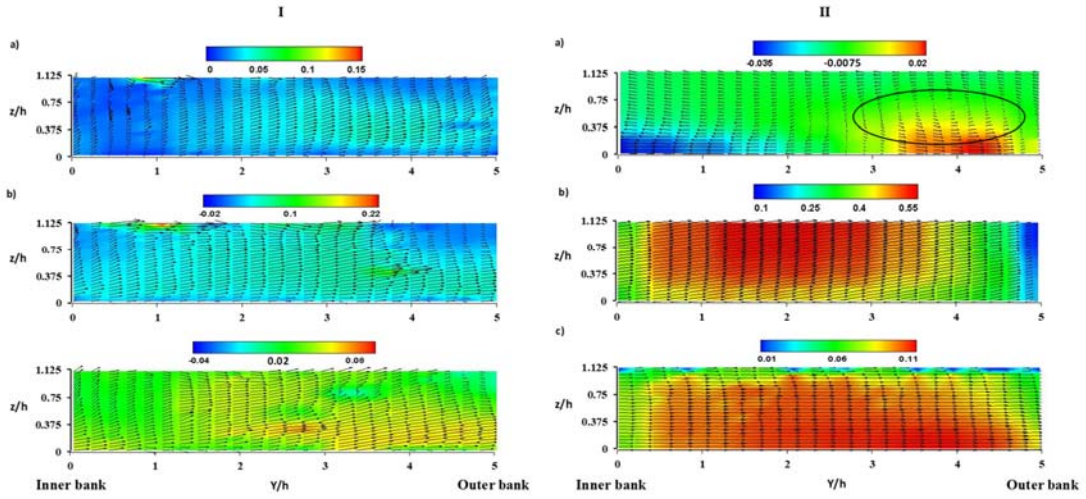


*Figure 6.9* Secondary velocity contour plots for *I)* experimental and *II)* simulated results of floodplain vegetation density of 100 plants/m$^2$ *a)* apex *b)* bend and *c)* cross-over sections

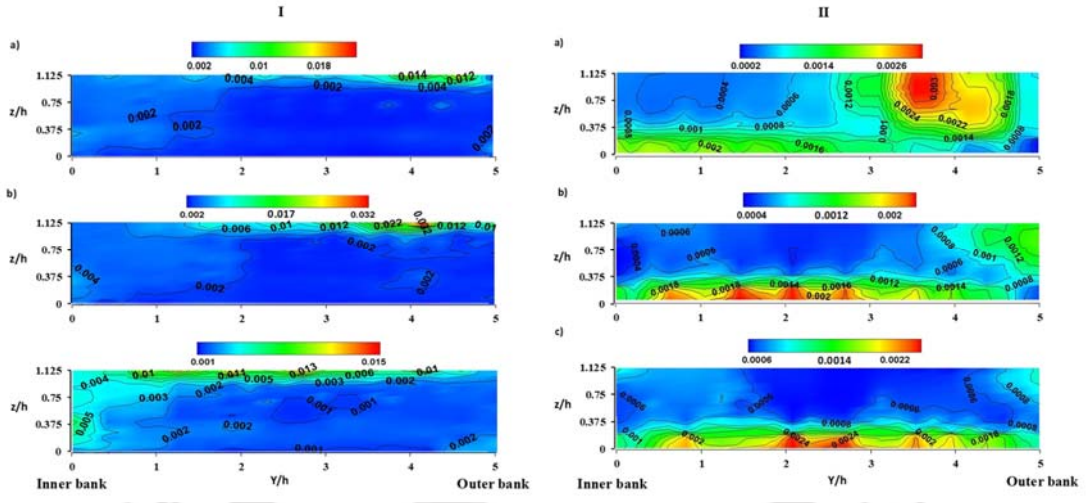


*Figure 6.10* Turbulent kinetic energy contour plots for *I)* experimental and *II)* simulated results of floodplain vegetation density of 100 plants/m$^2$ *a)* apex *b)* bend and *c)* cross-over sections

## Model Performance

This study enumerates the numerical investigation of green river corridor effect on the hydrodynamics of a low sinuous river. Laboratory experiments and numerical modeling is to investigate flows in with and without floodplain vegetation. Figure 6.11, shows the result comparison between experimental and model data for no-vegetation case. And it represents that the good correlation between the model and experimental data of without



TH-2690_166152105

floodplain vegetation condition with $R^2$ value of 0.87, 0.89 and 0.67 at apex section near inner bank (P1), mid channel (P5) and outer bank (P10) respectively. In Figure 6.10, the difference in correlation coefficient can be noticed. And from the experimental and model data, evaluated the standard error estimate (SEE) and n (sample size), Figure 6.10 at apex section near inner bank (channel- floodplain transition) i.e., 0.0078, 0.01 and 16.

Figure 6.12 represents the comparison between experimental and model data of vegetation density of 100 plants/$m^2$ condition. The results showed that the correlation between the model and experimental data of $R^2$ =0.83 in leaving of surface values and it shows $R^2$ =0.7 inclusion of surface level values. In experimental condition, the vegetation blades are flexible. whereas, in modelling the vegetation is considered as rigid. So, the values at the surface level difference could have observed. The prediction from correlation data at apex and COR is good but for the bend section it is quite different. According to Figure 6.11, it is observed that the streamwise velocity at the apex section along the vegetation patch reaches a maximum value close to the crest of vegetation, which is caused by the high-velocity gradient in this region. In figure 6.12 (a,b), the difference in correlation coefficient can be noticed. And from the experimental and model data, evaluated the standard error estimate (SEE) and n (sample size), For Figure 6.12 a) at crest of vegetation i.e., 0.00029, 0.00075 and 14, b) just below the surface level i.e., 0.0006 and 0.00053 and 14 respectively. The result provides the useful insights into laboratory and numerical investigation of flow structures of a sinuous channel.

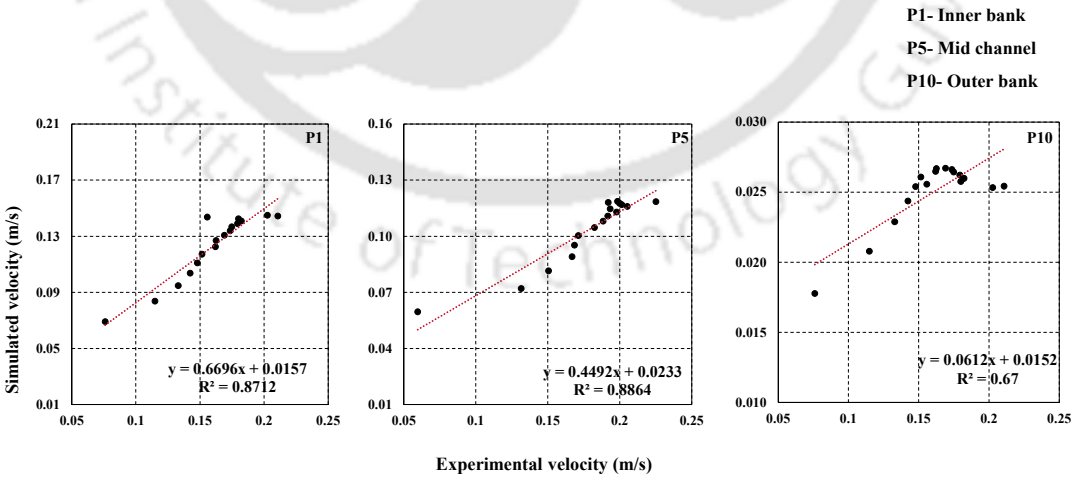


*Figure 6.11* Comparison of streamwise velocities between simulation and experimental data of no-vegetation condition at apex section



TH-2690_166152105

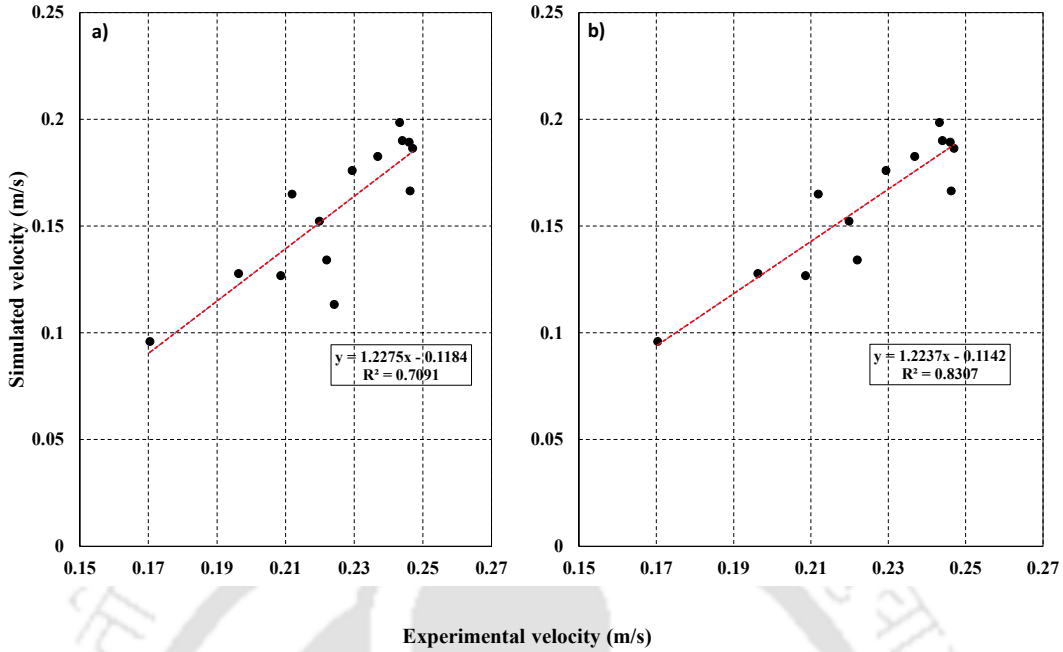


*Figure 6.12* Comparison of streamwise velocities between simulation and experimental data of floodplain vegetation density *i.e.,* 100 plants/m$^2$ a) at crest of vegetation b) just below the surface level

### 6.4.2 Experimental and Model results of Bridge Piers with Floodplain Vegetation

This section discusses the effect of bridge piers surrounded with floodplain vegetation on main channel flow structures. Figure 6.13 shows the simulated conditions of single and double bridge piers surrounded with floodplain vegetation. The plan and side view of the mesh domain, are showed in Figure 6.13. Turbulent kinetic energy behavior around the bridge pier can be observed in Figure 6.14.



TH-2690_166152105

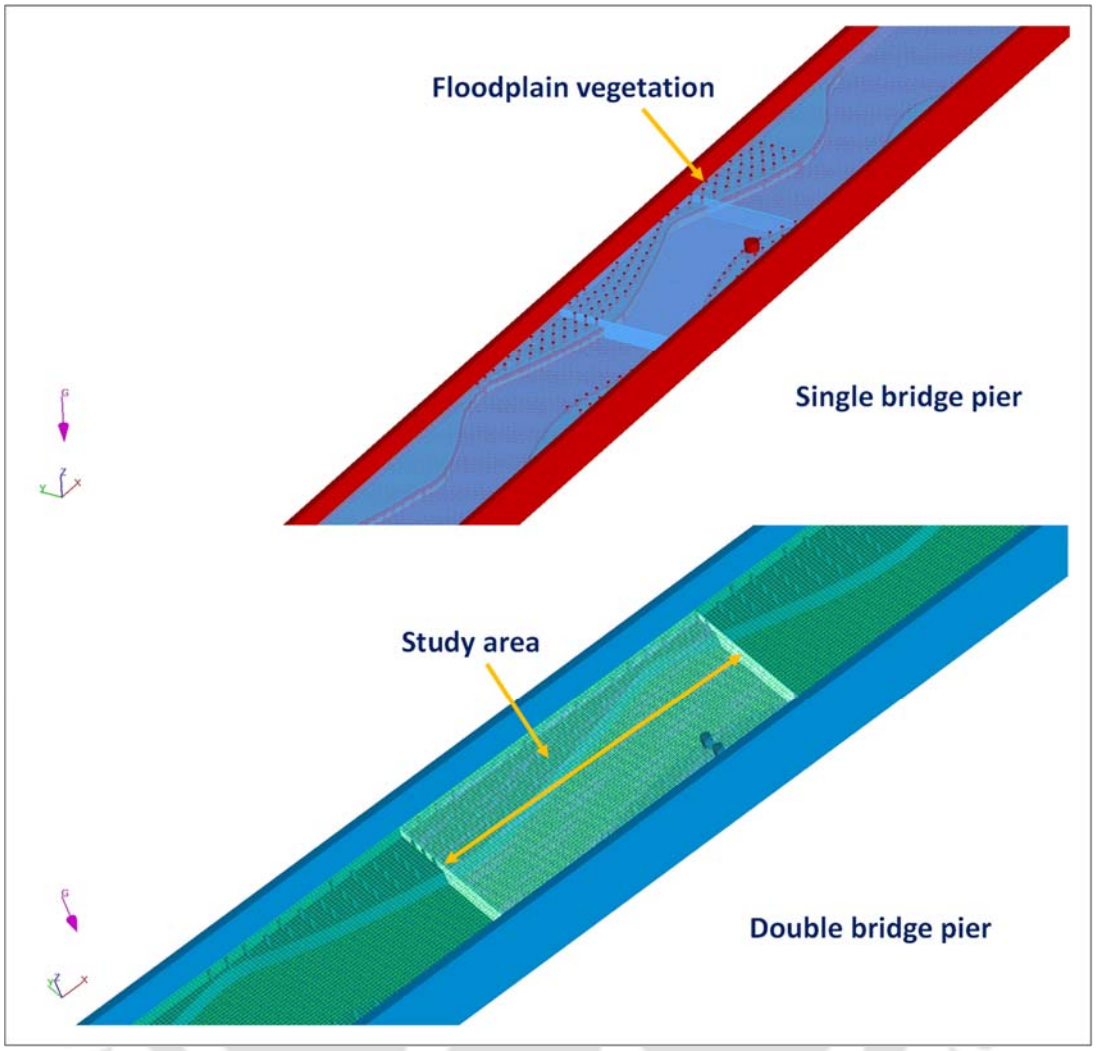


*Figure 6.13* Simulated layouts of single and double bridge pier conditions



TH-2690_166152105

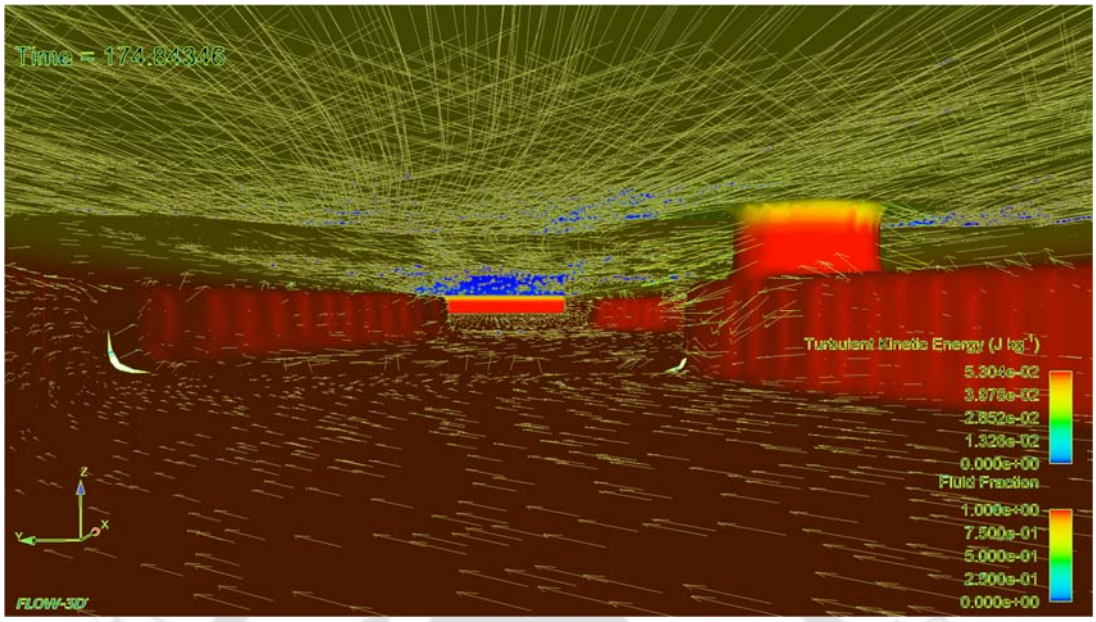


*Figure 6.14* Simulated results for turbulent kinetic energy at bridge pier location

### Case 1: Single Bridge Pier Surrounding with floodplain vegetation

Laboratory experiments and numerical modeling is to investigate flows in single bridge pier surrounded with floodplain vegetation condition. Figure 6.15 compares the experimental (left panel) with the simulated (right panel) results in an open channel of single pier with floodplain vegetation is considered. Figure 6.15a compares the measured stream wise velocity profiles with the simulated ones at apex in the main channel. From the results, the averaged streamwise velocities in the simulated data ($U_{sim}$ = 0.33m/s) were approximately 1.32 times of the experimental result ($U_{exp}$ = 0.25m/s). The mean velocity of streamwise velocity is around $9u_*$ for experimental condition and for simulated case is $11u_*$. However, the apex section in the main channel measured locations shows the reasonable results in the view of velocity core region between simulated and experimental contour plots. The percentage increase of mean streamwise velocity for single pier with floodplain vegetation condition for simulated to experimental condition is estimated to be approximately at the apex section is 27%.

Figure 6.15b represents the secondary flow comparison between measured and modeled data of single pier surrounding with floodplain vegetated condition, the secondary flow structure is well defined in the simulated one at apex section is observed. The maximum magnitude of secondary velocity vectors at the apex section is about 22%, of the maximum streamwise velocity for experimental condition. The maximum magnitude of



TH-2690_166152105

secondary velocity vectors at apex is about 5% of the maximum streamwise velocity for simulation condition. The angle of inclination of secondary currents at apex is about 7° for experimental condition. The angle of inclination of secondary currents at apex section is about 3° for simulation condition. In Figure 6.14(II)b, secondary flow circulations in the simulated case at the outer bank ($2 \leq Y / h \leq 5$) is visible. Moreover, a larger span of vortex in the single pier surrounding vegetated condition at apex section for the region between ($0.5 \leq Y / h \leq 3.5$) is visible for the experimental plot (Figure 6.15(I)). And at the outer bank, a small circulation is visible at the bottom due to the curvature effect shown in the experimental results. The stronger secondary vortex is visible at outer bank in the simulated condition, due to the combined effect of bridge pier and vegetation along with curvature effect. To understand the similarity index of both simulated and experimental results, the parameters variability at outer bank is the better example (Figure 6.15).

Figure 6.15c shows the contour plots for TKE of single pier surrounding with floodplain vegetation condition. The percentage increase in turbulent kinetic energy for experimental as 63% more at apex section as compared to simulation case.

### Case 2: Double Bridge Pier Surrounding with floodplain vegetation

Laboratory experiments and numerical modeling is to investigate flows in double pier with floodplain vegetation condition. Figure 6.16 compares the experimental (left panel) with the simulated (right panel) results in an open channel of double bridge piers with floodplain vegetation is considered. Figure 6.16a compares the measured stream wise velocity profiles with the simulated ones at apex in the main channel. From the results, the averaged streamwise velocities in the simulated data ($U_{sim}$ = 0.3m/s) were approximately 1.3 times of the experimental result ($U_{exp}$ = 0.23m/s). The mean velocity of streamwise velocity is around $8u_*$ for experimental condition and for simulated case is $10u_*$. However, the apex section in the main channel measured locations shows the reasonable results in the view of velocity core region between simulated and experimental contour plots. The percentage increase of mean streamwise velocity for double pier with floodplain vegetated condition for simulated to experimental condition is estimated to be approximately at apex is 25%.

Figure 6.16b represents the secondary flow comparison between measured and modeled data of single pier surrounding with floodplain vegetated condition, the secondary flow structure is well defined in the simulated one at apex section is observed. The maximum magnitude of secondary velocity vectors at apex is about 18%, of the maximum



TH-2690_166152105

streamwise velocity for experimental condition. The maximum magnitude of secondary velocity vectors at apex is about 5% of the maximum streamwise velocity for simulation condition. The angle of inclination of secondary currents at apex is about 5°, for experimental condition. The angle of inclination of secondary currents at apex section is about 2.6° for simulation condition. In Figure 6.16(II)b, secondary flow circulations in the simulated case at the outer bank ($3 \leq Y / h \leq 5$) is visible. In compared to single bridge pier the length of the vortex is lesser for double pier with vegetation condition. Moreover, smaller vortices in the single pier surrounding vegetated condition at apex section near inner bank top and near outer bank bottom are visible for the experimental plot (Figure 6.16(I)). The longitudinal vortex, at the outer bank is visible due to the curvature effect showed in the experimental and simulated results. To understand the similarity index of both simulated and experimental results, at outer bank is the better example (Figure 6.16).

Figure 6.16c shows the contour plots for TKE of single pier surrounding with floodplain vegetation condition. The percentage increase in turbulent kinetic energy for experimental is 66% more at apex as compared to simulation case. The distribution of turbulent kinetic energy shows an increase in anisotropy near the outer bank of the apex section, as demonstrated in the experimental investigation and compared with the simulation result.

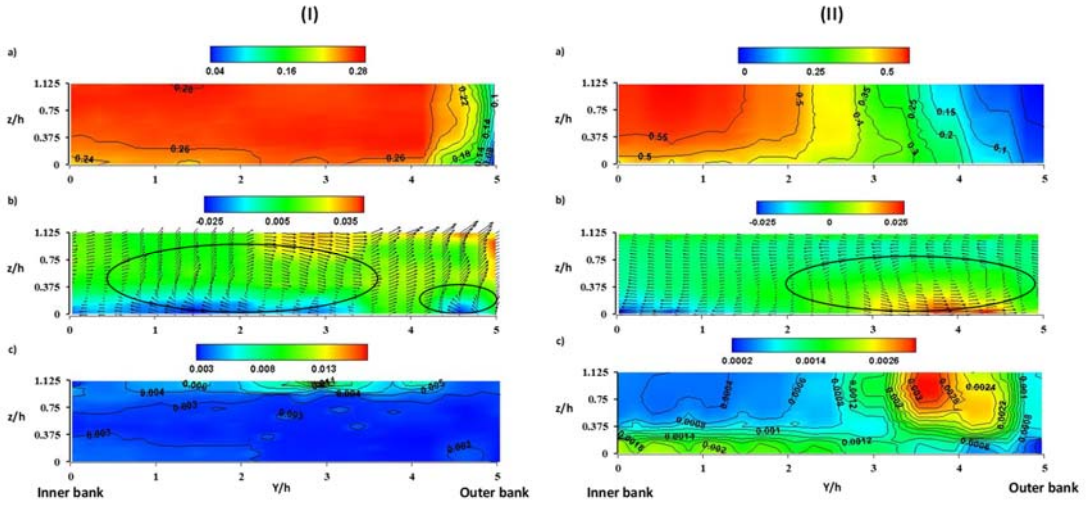


*Figure 6.15* Contour plots for single bridge pier with floodplain vegetation for *I)* experimental *II)* simulation conditions of *a)* streamwise velocity *b)* secondary velocity and *c)* turbulent kinetic energy



TH-2690_166152105

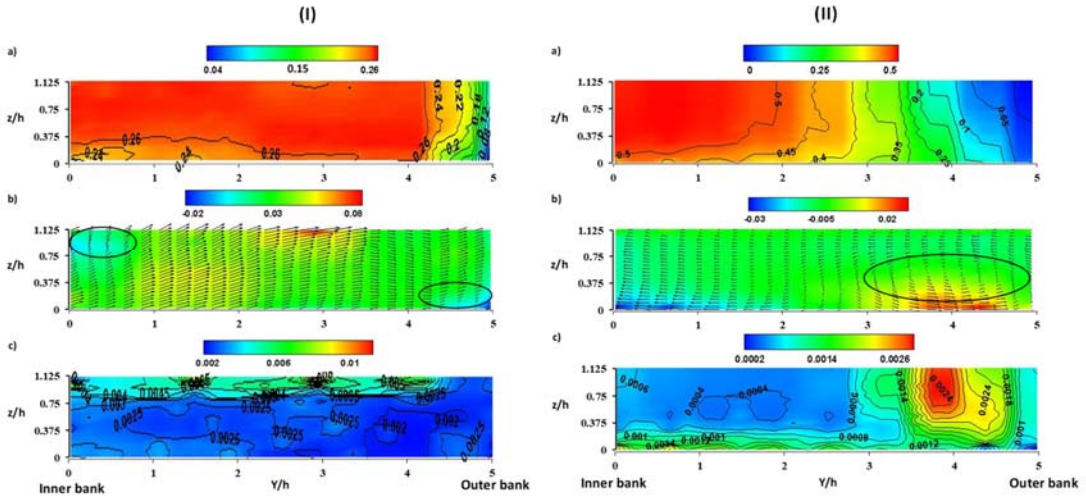


*Figure 6.16* Contour plots for double bridge pier with floodplain vegetation of *I)* experimental *II)* simulation conditions of *a)* streamwise velocity *b)* secondary velocity and *c)* turbulent kinetic energy

## Model Performance

Figure 6.17 shows the comparison between experimental and model data of single and double bridge pier along with floodplain vegetation. The plot representing laboratory and numerical studies provide useful insights into investigation of streamwise flow velocities at apex section of the channel. Figure 6.17 (I), shows the correlation between the model and experimental data for single bridge pier condition of $R^2$ =0.86, 0.70 and 0.64 at P1 (inner bank), P4 (mid channel) and P6 (outer bank) respectively. Figure 6.17 (II), shows the correlation between the model and experimental data for double bridge pier condition of $R^2$ =0.92, 0.75 and 0.77 at P1 (inner bank), P4 (mid channel) and P6 (outer bank) respectively.

Figure 6.17 shows the correlation coefficient plots for the measuring locations of P1 (inner bank), P4 (mid channel) and P6 (outer bank), the difference in correlation coefficient can be noticed. And from the experimental and model data, evaluated the standard error estimate (SEE) and n (sample size), Figure 6.17 I) single bridge pier condition i.e., 0.00042, 0.0096 and 15, b) double bridge pier condition i.e., 0.0091, 0.0063 and 15 respectively.



TH-2690_166152105

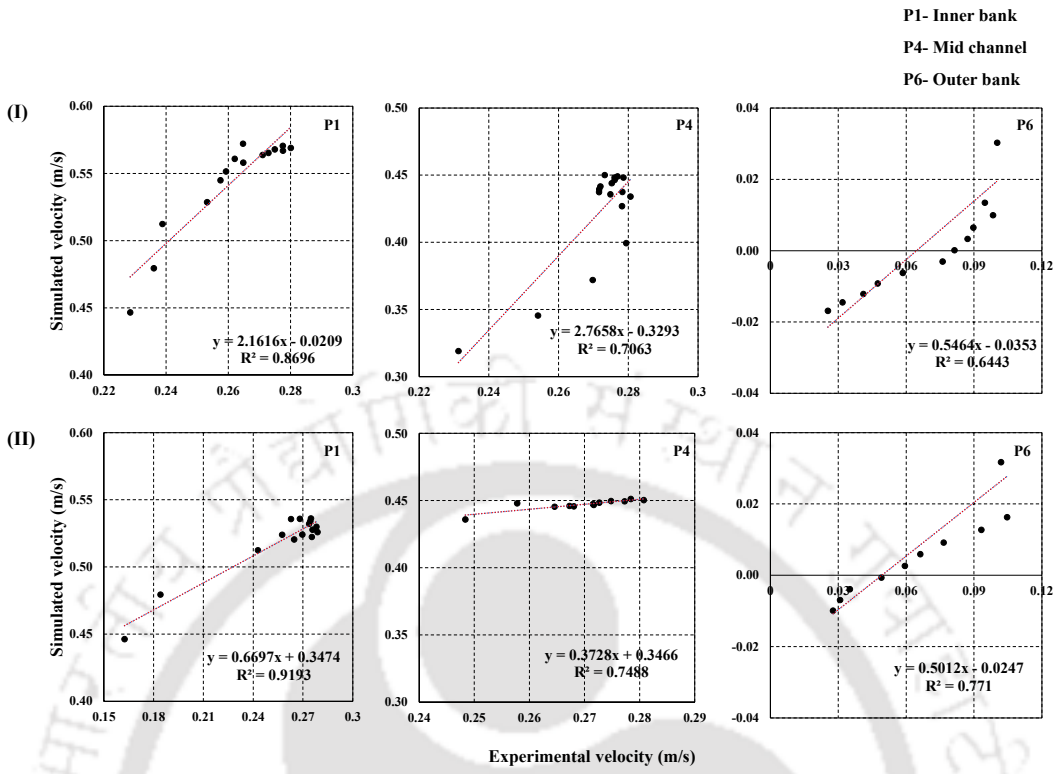


*Figure 6.17* Comparison of streamwise velocities between experimental and simulation data of *(I)* single pier and *(II)* double pier along with floodplain vegetation conditions

## 6.5 DISCUSSIONS

This section focuses on interprets the results of numerical analysis to understand the interaction between the main channel and floodplain. From the Figure 6.5, 6.8, 6.15a and 6.16a, the results of simulation and experimental plots of No-vegetation, with floodplain vegetation, single and double bridge pier with the vegetation showed that the velocity isovel lines bulging along the bed of the channel and outer bank of the river, due to high-momentum transfer by secondary current. The similar trend has also been noticed by Singh et al., 2020. In the above Figures, the characterization of shear layer (*i.e.,* the width of shear layer) due to the velocity gradients effected by the main channel and different floodplain roughness result in formation of secondary vortices and this effect significantly implicated on other turbulence parameters in the channel. Jahra 2010 also observed similar kind of observations in their study.

According to Figures 6.6 (I) and 6.6 (II), there is a slight discrepancy between the measured and the simulated values at the top of vegetation and just below the water surface



TH-2690_166152105

of it. This may be due to the effect of flexibility of vegetation in experimental modeling and rigid vegetation elements in numerical model. Although Flow3D model is not able to simulate the flexible vegetation, it helps to show the shear layer mechanism and the strong circulation in the main channel of all the cases with the rigid vegetation. Sonnenwald et al., 2016 reported that minor disagreement between the measured and simulated observations at the top of vegetation by using porous zone model due to its inability to capture the flow separation and secondary circulation near the vegetation patch. Sinsicalchi et al., 2012 and Jahadi et al., 2020 discussed in their study the maximum velocities were observed at top of vegetation. According to Liu et al. (1996) the predicted turbulent kinetic energy was 100% larger than their experimental observations. Present study noticed that the turbulent kinetic energy is high in the vicinity of the interface (*i.e.,* channel floodplain transition) near inner bank and the contour lines near the junction bulge towards the free surface due to secondary currents. The same feature is observed by Kang and Choi 2006 in their turbulence study. However, the results overpredicted in the simulated results than the observed results. Although, from the figures 6.11, 6.12 and 6.17, the correlation trend between the experimental and model simulations is found satisfactory.

## 6.6 CHAPTER SUMMARY

In this study the numerical modelling is carried out for low sinuous channel with different cases of floodplain vegetation and bridge piers to evaluate the CFD model performance with the experimental. The hydraulic parameters such as primary and secondary flow velocities, and turbulent kinetic energy behavior in the main channel were analysed by FLOW3D solver using RNG turbulence model. The major observations in the study lead to the following conclusions.

i) The averaged streamwise velocities in the no-vegetation condition at the apex section, the simulated data were approximately 1.2 times of the experimental result.
ii) The percentage increase of mean streamwise velocity for floodplain vegetated condition, the simulated condition is estimated to be approximately at apex is 47%, bend is 49.8%, and COR is 44% compared to experimental condition.
iii) For floodplain vegetation density of 100 plants/$m^2$ condition, the correlation between the model and experimental data is $R^2$ 0.75. This is due to the difference in vegetation representation in laboratory experiments (flexible) and numerical simulation (rigid).



TH-2690_166152105

iv) The secondary flow circulations in the simulated case in the single pier surrounding vegetated condition at apex section at the outer bank ($2 \leq Y / h \leq 5$) is noticeable. Moreover, a larger span of vortex for the region between ($0.5 \leq Y / h \leq 3.5$) is evident in the experimental plot.

v) The correlation between the model and experimental data for double bridge pier condition of $R^2$ =0.92, 0.75 and 0.77 at P1 (inner bank), P4 (mid channel) and P6 (outer bank) respectively.

These results obtained from the study have shown the capability of the RNG model to captured the shear layer mechanism and momentum transfer phenomenon at the floodplain channel transition. However, extrapolation of turbulence characteristics has been noticed over the main channel and interface regions. The overall simulation results showed the shear layer mechanism and secondary circulation patterns followed the experimental results. Furthermore, the secondary circulations near the outer bank were significant in the simulated results, which are not noticeable in the experimental analysis, because these regions near the boundaries were identified and typically sometimes neglected as wake regions in the experimental analysis. we emphasize the disagreements in aspects of turbulent kinetic energy.



TH-2690_166152105

# 7

# SUMMARY AND FUTURE SCOPE

## 7.1 SUMMARY

The present research aims to understand the hydrodynamic behavior of a low sinuous river. The flow structures in a curved channel are more complex than the regular channels due to complex three-dimensional nature. This study attempted to investigate river hydrodynamic behavior and the physics by analyzing the flow-vegetation interaction mechanisms. For this work, we conducted a series of experiments in Fluvial hydro-ecological laboratory. This study comprises of different vegetation layouts and varying flow conditions for different cross-sections of the sinuous channel, suits best for studying the river main channel behavior. The following sub-sections are the brief summary of the work done and findings made in the present research.

### 7.1.1 Flow Through Green River Corridor

In this objective, an analysis of laboratory experiments was conducted to investigate the effect of emergent and submerged homogeneous green corridor on flow structures. For this purpose, Oryza Sativa (young rice plants) of 400, 200, 150, 100 plants/$m^2$ were arranged in four different layouts (Figure 3.3). The results of the study provided the understanding of effect of homogeneous green corridor on flow characteristics.

TH-2690_166152105

The major observations in the study lead to the following conclusions.

1. A strong velocity gradient is observed in the high vegetation density scenario i.e., 400 plants/$m^2$ because of flow diversion from floodplain to the main channel, which resulted in increases the main channel velocity by 23% compared to the no-vegetation scenario.
2. The angle of inclination of secondary currents in higher floodplain flow condition are about 2°, 6°, 6.5° and 7.3° for 100, 150, 200 and 400 plants/$m^2$, respectively. This indicates the arrangement of vegetation on the floodplain has significant influence on the flow distribution in the channel.
3. The turbulence core region is mainly observed towards the inner bank (Y/h ~ 4 to 5) and z/h is 0.375. Further, this core region is deeper in the main channel which may be due to more surface area occupied by the higher density of vegetation compared to other vegetation configurations.
4. The maximum positive Reynold's stresses occur at the interface of main channel and vegetated zone in between the range of z/h~0.75 to 1.125 (h is floodplain depth), which indicates that the shear becomes dominant and the maximum along the inner bend apex of the main channel.
5. The findings showed the floodplain vegetation affects the Reynold's shear stresses in the main channel, producing strong lateral shear stresses at a higher floodplain flow depth condition. Thus, the floodplain vegetation shifts the flow structure into the main stream, creates the more turbulence and alters the distribution of velocity profiles that play an important role in stabilizing the bank and ecological regeneration.

### 7.1.2 Effect on Main Channel Flow Structures Due to Floodplain Vegetation Patches

In this present study, an analysis of laboratory experiments was conducted to investigate the effect of submerged heterogeneous vegetation patches on flow structure. For this purpose, three natural plant forms (leafy, grass and cylindrical) arranged in four different layouts (Figure 4.2), namely leafy, mixed, flexible grass, cylindrical vegetation layouts were studied. Laboratory experiments were undertaken to investigate the effect of different plant forms under submerged vegetation conditions on turbulence characteristics



TH-2690_166152105

in a low sinuous channel. The following are the conclusions derived from the present investigation.

First, the percentage increment in primary velocities is observed as 38%, 27%, 23% and 21% for leafy, mixed vegetation, grasses and cylindrical layouts as compared with no-vegetation condition. This indicates the shear layer occupies the relatively larger portion in the main channel of the leafy vegetation than the cylindrical vegetation. Second in the case of leafy vegetation, the reduction in velocity in the channel from P1 (inner bank) to P10 (outer bank) is observed as 51% at vegetation canopy height. Third the maximum magnitude of secondary velocity vectors is about 26%, 24%, 22%, 14% and 12% of the maximum streamwise velocity for leafy, mixed, grass, cylindrical and no-vegetation respectively. Fourth the vertical turbulence intensity component ($w_{rms}$) increases with the distance from the bottom until z/h~0.05, and reaches higher at top of the water surface i.e., z/h~ 1. This indicates the increase in $w_{rms}$ shows the energy transfer near the surface on the vertical direction of water flow.

### 7.1.3 Combined Effect of Bridge Piers and Floodplain Vegetation on Flow Characteristics

This objective, the combined effect of bridge pier and floodplain vegetation on main channel turbulence parameters were investigated. For this purpose, conducted laboratory experiments for four different layouts (Figure 3), such as no-vegetation, with floodplain vegetation, single bridge pier (SP) and double bridge pier (DP) along with floodplain vegetation. The results are helpful to predict the flow patterns inside the channel due to presence of river engineering structures on floodplain along with vegetation. The major observations in the study lead to the following conclusions.

1. The presence of single large diameter pier with floodplain vegetation increases the main channel velocity up to 36% compared to no-obstruction on the floodplain. For the double pier condition, it is observed to be 31%.

2. The variability in shear layer zone is observed to be different for different pier conditions. In the case of single pier, the shear layer is observed between Y/h: 0.7 to 2.2, while in double pier, it is observed from Y/h: 0.9 to 2.7. With the addition of bridge piers to the floodplain vegetation, the lateral velocity gradient increases at the interface generating a significant shear layer.



TH-2690_166152105

3. In the single pier of larger diameter, the length of the vortex is more and its strength is 2 times more than double pier of smaller diameter. This reveals that secondary vortex grows its size and strength in case of the large diameter pier.

4. The percentage increase in streamwise turbulence intensity ($u_{rms}$) in the main channel for different cases is 22% more for only vegetation, 37% more for double pier with vegetation and 40% more for single pier with vegetation as compared no vegetation condition.

5. The higher mixing activity can be observed at floodplain-channel interface with increase in Reynold's shear stress components at the inner bank (P1). Overall, the bridge piers and vegetation cover effecting the shear layer at inner bank is more significant, which can be observed from vertical profiles in all components of Reynolds Stresses.

6. In both the single pier and double pier conditions, the magnitude of TKE within the shear layer is relatively less as compared to the inner bank where maximum TKE is observed at closed intervals of isovels. This is due to the strong shearing flow present in the channel with effect of bridge piers surrounded with vegetation.

### 7.1.4 Numerical Investigation of Different Floodplain Roughness Layouts

In this objective, the numerical modelling is carried out for low sinuous channel with different cases of floodplain vegetation and bridge piers to evaluate the CFD model performance with the experimental. The hydraulic parameters such as primary and secondary flow velocities, and turbulent kinetic energy behavior in the main channel were analysed by FLOW3D solver using RNG turbulence model. The major observations in the study lead to the following conclusions.

1. The averaged streamwise velocities in the no-vegetation condition at the apex section, the simulated data were approximately 1.2 times of the experimental result.
2. The percentage increase of mean streamwise velocity for floodplain vegetated condition, the simulated condition is estimated to be approximately at apex is 47%, bend is 49.8%, and COR is 44% compared to experimental condition.



TH-2690_166152105

3. For floodplain vegetation density of 100 plants/$m^2$ condition, the correlation between the model and experimental data is $R^2$ 0.75. This is due to the difference in vegetation representation in laboratory experiments (flexible) and numerical simulation (rigid).
4. The secondary flow circulations in the simulated case in the single pier surrounding vegetated condition at apex section at the outer bank ($2 \leq Y / h \leq 5$) is noticeable. Moreover, a larger span of vortex for the region between ($0.5 \leq Y / h \leq 3.5$) is evident in the experimental plot.
5. The correlation between the model and experimental data for double bridge pier condition of $R^2$ =0.92, 0.75 and 0.77 at P1 (inner bank), P4 (mid channel) and P6 (outer bank) respectively.

These results obtained from the study have shown the capability of the RNG model to captured the shear layer mechanism and momentum transfer phenomenon at the floodplain channel transition. However, extrapolation of turbulence characteristics has been noticed over the main channel and interface regions. The overall simulation results showed the shear layer mechanism and secondary circulation patterns followed the experimental results. Furthermore, the secondary circulations near the outer bank were significant in the simulated results, which are not noticeable in the experimental analysis, because these regions near the boundaries were identified and typically sometimes neglected as wake regions in the experimental analysis. we emphasize the disagreements in aspects of turbulent kinetic energy.

## 7.2 FUTURE SCOPE

The present research has provided better insights to understand the hydrodynamic behavior of a sinuous channel. However, there are many other important aspects to be looked in detail for process-form based understanding of this river. The present work can be extended further with prime focus to following aspects

- Experimental study for different sinuosity of the channel to find out the interactions of flow structures with vegetation.
- To better understanding the turbulence behavior of a river, the experimental investigation should extend to the floodplain of a curved channel.
- Interlinking of flow-vegetation-turbulence interactions to aquatic life behaviour can be helpful for management of ecological zones of a river.



TH-2690_166152105

# APPENDIX A

# PUBLICATIONS

## A.1 UNDER REVIEW

Modalavalasa, S., Chembolu, V., Kulkarni, V., Dutta, S. The combined effect of bridge piers and floodplain vegetation on main channel hydraulics. (Submitted)

Modalavalasa, S., Chembolu, V., Kulkarni, V., Dutta, S. Influence of floodplain green corridor on turbulent structure in a low sinuous River. (Submitted)

## A.2 UNDER PREPARATION

Modalavalasa, S., Chembolu, V., Kulkarni, V., Dutta, S. Role of heterogeneous plant forms of riparian vegetation on fluvial Hydrodynamics of a sinuous channel.

Modalavalasa, S., Chembolu, V., Kulkarni, V., Dutta, S. Numerical Investigation of effect of green corridor on River hydraulics.

## A.3 CONFERENCES

Modalavalasa, S., Chembolu, V., Nandi, K.K., Kulkarni, V. and Dutta, S. 2021, April. “Effect of bridge pier induced turbulence on vegetated meander river morphology”. In EGU General Assembly Conference Abstracts (pp. EGU21-1465).

Modalavalasa. S., Dutta, S. 2021, February. “Analysis of flow at the vicinity of bridge pier in the floodplain of a sinuous channel”. International Conference on River Corridor Research and Management (RCRM 2021), IIT Jammu (pp. RCRM-34 page)

TH-2690_166152105

## PUBLICATIONS

Modalavalasa, S.; Pradhan, C.; Siddharth, A.; Dutta, S. 2019, November. “National Symposium on Innovations in geospatial technology for sustainable development with special emphasis on NER”. ISG-ISRS, 2019, Shillong, India.

Modalavalasa, S; Pradhan, C; Kulkarni, V; Dutta, S. 2019, August. “Flow Structure in Meandering Channel with Vegetation”. Conference Paper: 16th Annual Meeting, AOGS 2019, Singapore.

भारतीय प्रौद्योगिकी संस्थान गुवाहाटी • Indian Institute of Technology Guwahati •



TH-2690_166152105

# APPENDIX B

# HOMOGENEOUS GREEN CORRIDOR-EMERGENT CONDITION

## B.1 EMERGENT VEGETATION CONDITION

Flow through emergent condition, Figure B-1 and B-2 shows the trend between the turbulence parameters and vegetation densities. All the turbulence characteristics such as streamwise velocity, secondary velocity, turbulence intensity, Reynold's shear stresses and turbulent kinetic energy are showing the trend is almost linear with respect to vegetation densities (i.e., 0, 100, 150, 200 and 400 Plants/m$^2$). This indicated the turbulence parameters in emergent condition not much significant effect among the different densities of vegetation.

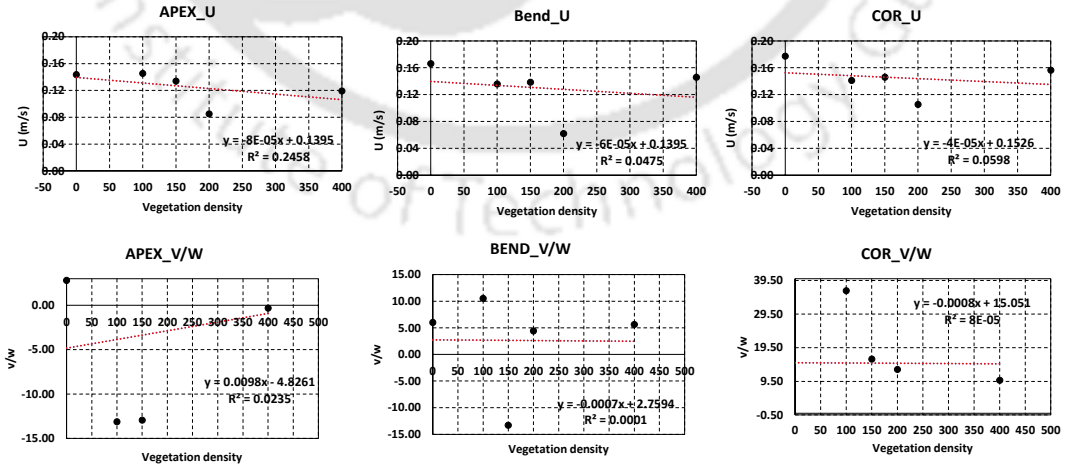


*Figure B-1* Streamwise and secondary flow velocities trend between the different configurations of vegetation densities (i.e., 0, 100, 150, 200 and 400 Plants/m$^2$).

TH-2690_166152105

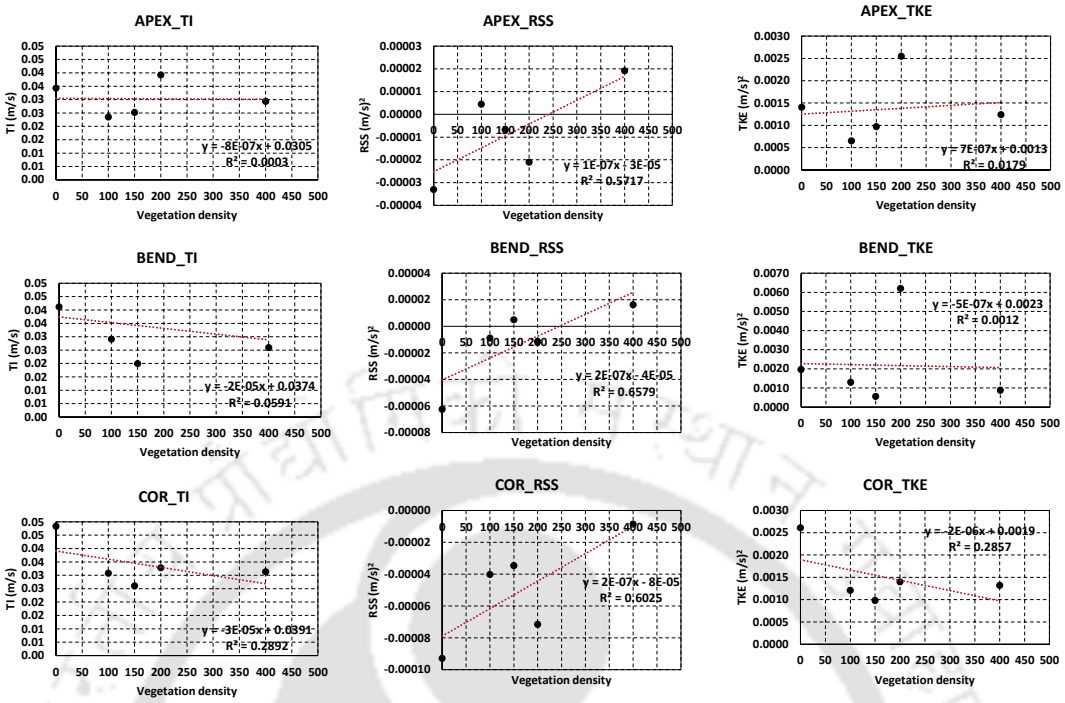


*Figure B-2* Turbulence intensity (TI), Reynold's shear stress (RSS) and turbulent kinetic energy (TKE) trend between the different configurations of vegetation densities (i.e., 0, 100, 150, 200 and 400 Plants/$m^2$).



TH-2690_166152105

# REFERENCES


Abad, J.D., Rhoads, B.L., Güneralp, İ. and García, M.H., 2008. Flow structure at different stages in a meander-bend with bendway weirs. Journal of Hydraulic Engineering, 134(8), pp.1052-1063.

Aberle, J. and Järvelä, J., 2013. Flow resistance of emergent rigid and flexible floodplain vegetation. Journal of Hydraulic Research, 51(1), pp.33-45.

Abernethy, B. and Rutherfurd, I.D., 1998. Where along a river's length will vegetation most effectively stabilise stream banks? Geomorphology, 23(1), pp.55-75.

Abernethy, B. and Rutherfurd, I.D., 2001. The distribution and strength of riparian tree roots in relation to riverbank reinforcement. Hydrological processes, 15(1), pp.63-79.

Ackerman, J.D. and Okubo, A., 1993. Reduced mixing in a marine macrophyte canopy. Functional Ecology, pp.305-309.

Afzalimehr, H., Maddahi, M.R., Sui, J. and Rahimpour, M., 2019. Impacts of vegetation over bedforms on flow characteristics in gravel-bed rivers. Journal of Hydrodynamics, 31(5), pp.986-998.

Ahmed, F. and Rajaratnam, N., 1998. Flow around bridge piers. Journal of Hydraulic Engineering, 124(3), pp.288-300.

Al-Turki, A.M., Ibrahim, H.M. and Spalevic, V., 2015. Impact of land use changes on soil erosion intensity in Wadi Jazan watershed in southwestern Saudi Arabia.

Armanini, A., Righetti, M. and Grisenti, P., 2005. Direct measurement of vegetation resistance in prototype scale. Journal of Hydraulic Research, 43(5), pp.481-487.

Asbjornsen, H., Goldsmith, G.R., Alvarado-Barrientos, M.S., Rebel, K., Van Osch, F.P., Rietkerk, M., Chen, J., Gotsch, S., Tobon, C., Geissert, D.R. and Gomez-Tagle, A., 2011. Ecohydrological advances and applications in plant–water relations research: a review. Journal of Plant Ecology, 4(1-2), pp.3-22.

Azevedo, R., Roja-Solórzano, L.R. and Leal, J.B., 2017. Turbulent structures, integral length scale and turbulent kinetic energy (TKE) dissipation rate in compound channel flow. Flow Measurement and Instrumentation, 57, pp.10-19.

Baptist, M.J., 2003, February. A flume experiment on sediment transport with flexible, submerged vegetation. In International workshop on riparian forest vegetated channels: hydraulic, morphological and ecological aspects, RIPFOR, Trento, Italy.




TH-2690_166152105

Beheshti, A.A. and Ataie-Ashtiani, B., 2010. Experimental study of three-dimensional flow field around a complex bridge pier. Journal of engineering mechanics, 136(2), pp.143-154.

Benavente, J., Gracia, F.J., Anfuso, G. and Lopez-Aguayo, F., 2005. Temporal assessment of sediment transport from beach nourishments by using foraminifera as natural tracers. Coastal Engineering, 52(3), pp.205-219.

Bennett, S.J. and Simon, A., 2004. Riparian vegetation and fluvial geomorphology (Vol. 8). American Geophysical Union.

Bennett, S.J., Pirim, T. and Barkdoll, B.D., 2002. Using simulated emergent vegetation to alter stream flow direction within a straight experimental channel. Geomorphology, 44(1-2), pp.115-126.

Boothroyd, R.J., Hardy, R.J., Warburton, J. and Marjoribanks, T.I., 2017. Modeling complex flow structures and drag around a submerged plant of varied posture. Water Resources Research, 53(4), pp.2877-2901.

Bornette, G. and Puijalon, S., 2011. Response of aquatic plants to abiotic factors: a review. Aquatic sciences, 73(1), pp.1-14.

Bousmar, D., 2002. Flow modelling in compound channels. Unire de Genie Civil et Environnemental.

Brachet, C., 2015. The Handbook for Management and Restoration of Aquatic Ecosystems in river and lake basins.

Brookes, A., 1996. Floodplain restoration and rehabilitation. Floodplain processes, pp.553-576.

Cameron, S.M., Nikora, V.I., Albayrak, I., Miler, O., Stewart, M. and Siniscalchi, F., 2013. Interactions between aquatic plants and turbulent flow: a field study using stereoscopic PIV. Journal of Fluid Mechanics, 732, pp.345-372.

Carollo, F.G., Ferro, V. and Termini, D., 2005. Flow resistance law in channels with flexible submerged vegetation. Journal of hydraulic engineering, 131(7), pp.554-564.

Carollo, F.G., Ferro, V.I.T.O. and Termini, D., 2002. Flow velocity measurements in vegetated channels. Journal of Hydraulic Engineering, 128(7), pp.664-673.

Chang, W.Y., Lai, J.S. and Yen, C.L., 1999. Simulation of Scour Depth Evolution at Pier Nose. In Proceedings of the 1999 International Water Resources Engineering Conference, August, Session BS-05, Water Resources Publications, LLC, Highlands Ranch, CO.

Chembolu, V., Kakati, R. and Dutta, S., 2019. A laboratory study of flow characteristics in natural heterogeneous vegetation patches under submerged conditions. Advances in Water Resources, 133, p.103418.

Chen, S.C., Kuo, Y.M. and Li, Y.H., 2011. Flow characteristics within different configurations of submerged flexible vegetation. Journal of Hydrology, 398(1-2), pp.124-134.

Chen, Y.C. and Kao, S.P., 2011. Velocity distribution in open channels with submerged aquatic plant. Hydrological Processes, 25(13), pp.2009-2017.

Chiew, Y.M. and Melville, B.W., 1987. Local scour around bridge piers. Journal of hydraulic research, 25(1), pp.15-26.

Chin, W.W. and Todd, P.A., 1995. On the use, usefulness, and ease of use of structural equation modeling in MIS research: A note of caution. MIS quarterly, pp.237-246.



TH-2690_166152105

Choi, S.U. and Kang, H., 2004. Reynolds stress modeling of vegetated open-channel flows. Journal of Hydraulic Research, 42(1), pp.3-11.

Cui, J. and Neary, V.S., 2008. LES study of turbulent flows with submerged vegetation. Journal of Hydraulic Research, 46(3), pp.307-316.

D'Ippolito, A., Ferrari, E., Iovino, F., Nicolaci, A. and Veltri, A., 2013. Reforestation and land use change in a drainage basin of southern Italy. iForest-Biogeosciences and Forestry, 6(4), p.175.

Dargahi, B., 1990. Controlling mechanism of local scouring. Journal of Hydraulic Engineering, 116(10), pp.1197-1214.

Dargahi, B., 1989. The turbulent flow field around a circular cylinder. Experiments in fluids, 8(1), pp.1-12.

De Cacqueray, N., Hargreaves, D.M. and Morvan, H.P., 2009. A computational study of shear stress in smooth rectangular channels. Journal of Hydraulic Research, 47(1), pp.50-57.

Defina, A. and Bixio, A.C., 2005. Mean flow and turbulence in vegetated open channel flow. Water Resources Research, 41(7).

Devi, T.B. and Kumar, B., 2016. Flow characteristics in an alluvial channel covered partially with submerged vegetation. Ecological Engineering, 94, pp.478-492.

Devi, T.B., Daga, R., Mahto, S.K. and Kumar, B., 2016. Drag and turbulent characteristics of mobile bed channel with mixed vegetation densities under downward seepage. Journal of Fluids Engineering, 138(7).

Dey, S. and Raikar, R.V., 2007. Characteristics of horseshoe vortex in developing scour holes at piers. Journal of Hydraulic Engineering, 133(4), pp.399-413.

Dey, S., Das, R., Gaudio, R. and Bose, S.K., 2012. Turbulence in mobile-bed streams. Acta Geophysica, 60(6), pp.1547-1588.

Dosskey, M.G., Vidon, P., Gurwick, N.P., Allan, C.J., Duval, T.P. and Lowrance, R., 2010. The role of riparian vegetation in protecting and improving chemical water quality in streams 1. JAWRA Journal of the American Water Resources Association, 46(2), pp.261-277.

Dufour, S., Rodríguez-González, P.M. and Laslier, M., 2019. Tracing the scientific trajectory of riparian vegetation studies: Main topics, approaches and needs in a globally changing world. *Science of the total environment*, *653*, pp.1168-1185.

Erduran, K.S. and Kutija, V., 2003. Quasi-three-dimensional numerical model for flow through flexible, rigid, submerged and non-submerged vegetation. Journal of Hydroinformatics, 5(3), pp.189-202.

Ervine, D.A., Willetts, B.B., Sellin, R.H.J. and Lorena, M., 1993. Factors affecting conveyance in meandering compound flows. Journal of Hydraulic Engineering, 119(12), pp.1383-1399.

Ettema, R., Kirkil, G. and Muste, M., 2006. Similitude of large-scale turbulence in experiments on local scour at cylinders. Journal of Hydraulic Engineering, 132(1), pp.33-40.

Faafeng, B.A. and Mjelde, M., 1998. Clear and turbid water in shallow Norwegian lakes related to submerged vegetation. In *The structuring role of submerged macrophytes in lakes* (pp. 361-368). Springer, New York, NY.

Farzadkhoo, M., Keshavarzi, A., Hamidifar, H. and Javan, M., 2018. A comparative study of longitudinal dispersion models in rigid vegetated compound meandering channels. Journal of environmental management, 217, pp.78-89.



TH-2690_166152105

Fathi-Maghadam, M. and Kouwen, N., 1997. Nonrigid, nonsubmerged, vegetative roughness on floodplains. Journal of Hydraulic Engineering, 123(1), pp.51-57.

Ferziger, J.H. and Perić, M., 2002. Properties of numerical solution methods. Computational methods for fluid dynamics, 3(2), pp.31-35.

Fischer-Antze, T., Stoesser, T., Bates, P. and Olsen, N.R.B., 2001. 3D numerical modelling of open-channel flow with submerged vegetation. Journal of Hydraulic Research, 39(3), pp.303-310.

Fleri, J.R., Lera, S., Gerevini, A., Staver, L. and Nardin, W., 2019. Empirical observations and numerical modelling of tides, channel morphology, and vegetative effects on accretion in a restored tidal marsh. Earth Surface Processes and Landforms, 44(11), pp.2223-2235.

FLOW-3D® Version 12.0 Users Manual (2018). *FLOW-3D* [Computer software]. Santa Fe, NM: Flow Science, Inc. https://www.flow3d.com (or) Flow Science, Inc., Santa Fe, NM, USA. *FLOW-3D*® Version 12.0 Users Manual (2018) [Online]. Accessed on: Feb. 3, 2019.

Gambi, M.C., Nowell, A.R. and Jumars, P.A., 1990. Flume observations on flow dynamics in Zostera marina (eelgrass) beds. Marine ecology progress series, pp.159-169.

Garcia, M.H., López, F., Dunn, C. and Alonso, C.V., 2013. Flow, turbulence, and resistance in a flume with simulated vegetation. In Riparian vegetation and fluvial geomorphology (pp. 11-27). American Geophysical Union.

Gautam, P., Eldho, T.I., Mazumder, B.S. and Behera, M.R., 2019. Experimental study of flow and turbulence characteristics around simple and complex piers using PIV. Experimental Thermal and Fluid Science, 100, pp.193-206.

Gentès, S., Coquery, M., Vigouroux, R., Hanquiez, V., Allard, L. and Maury-Brachet, R., 2019. Application of the European Water Framework Directive: Identification of reference sites and bioindicator fish species for mercury in tropical freshwater ecosystems (French Guiana). Ecological Indicators, 106, p.105468.

Ghisalberti, M. and Nepf, H.M., 2002. Mixing layers and coherent structures in vegetated aquatic flows. Journal of Geophysical Research: Oceans, 107(C2), pp.3-1.

Goring, D.G. and Nikora, V.I., 2002. Despiking acoustic Doppler velocimeter data. Journal of hydraulic engineering, 128(1), pp.117-126.

Gorrick, S. and Rodríguez, J.F., 2014. Flow and force-balance relations in a natural channel with bank vegetation. Journal of hydraulic research, 52(6), pp.794-810.

Gorrick, S. and Rodríguez, J.F., 2014. Scaling of sediment dynamics in a laboratory model of a sand-bed stream. Journal of Hydro-Environment Research, 8(2), pp.77-87.

Grabowski, R.C., Surian, N. and Gurnell, A.M., 2014. Characterizing geomorphological change to support sustainable river restoration and management. Wiley Interdisciplinary Reviews: Water, 1(5), pp.483-512.

Graf, W.H. and Yulistiyanto, B., 1998. Experiments on flow around a cylinder; the velocity and vorticity fields. Journal of Hydraulic Research, 36(4), pp.637-654.

Gunawan, B., Sun, X., Sterling, M., Shiono, K., Tsubaki, R., Rameshwaran, P., Knight, D.W., Chandler, J.H., Tang, X. and Fujita, I., 2012. The application of LS-PIV to a small irregular river for inbank and overbank flows. Flow Measurement and Instrumentation, 24, pp.1-12.



TH-2690_166152105

Gurbisz, C., Kemp, W.M., Cornwell, J.C., Sanford, L.P., Owens, M.S. and Hinkle, D.C., 2017. Interactive effects of physical and biogeochemical feedback processes in a large submersed plant bed. Estuaries and Coasts, 40(6), pp.1626-1641.

Gurbisz, C., Kemp, W.M., Sanford, L.P. and Orth, R.J., 2016. Mechanisms of storm-related loss and resilience in a large submersed plant bed. Estuaries and Coasts, 39(4), pp.951-966.

Gurnell, A., 2014. Plants as river system engineers. Earth Surface Processes and Landforms, 39(1), pp.4-25.

Gurnell, A.M., Bertoldi, W. and Corenblit, D., 2012. Changing river channels: The roles of hydrological processes, plants and pioneer fluvial landforms in humid temperate, mixed load, gravel bed rivers. Earth-Science Reviews, 111(1-2), pp.129-141.

Gurnell, A.M., Corenblit, D., García de Jalón, D., González del Tánago, M., Grabowski, R.C., O'hare, M.T. and Szewczyk, M., 2016. A conceptual model of vegetation–hydrogeomorphology interactions within river corridors. River research and applications, 32(2), pp.142-163.

Hockley, F.A., Wilson, C.A.M.E., Brew, A. and Cable, J., 2014. Fish responses to flow velocity and turbulence in relation to size, sex and parasite load. Journal of the Royal Society Interface, 11(91), p.20130814.

Hu, Z., Yu, G., Fu, Y., Sun, X., Li, Y., Shi, P., Wang, Y. and Zheng, Z., 2008. Effects of vegetation control on ecosystem water use efficiency within and among four grassland ecosystems in China. Global Change Biology, 14(7), pp.1609-1619.

Huai, W.X., Zeng, Y.H., Xu, Z.G. and Yang, Z.H., 2009. Three-layer model for vertical velocity distribution in open channel flow with submerged rigid vegetation. Advances in Water Resources, 32(4), pp.487-492.

Huang, J., Cassiani, M. and Albertson, J.D., 2009. The effects of vegetation density on coherent turbulent structures within the canopy sublayer: A large-eddy simulation study. Boundary-layer meteorology, 133(2), pp.253-275.

Hughes, F.M., Adams, W.M., Muller, E., Nilsson, C., Richards, K.S., Barsoum, N., Decamps, H., Foussadier, R., Girel, J., Guilloy, H. and Hayes, A., 2001. The importance of different scale processes for the restoration of floodplain woodlands. Regulated Rivers: Research & Management: An International Journal Devoted to River Research and Management, 17(4-5), pp.325-345.

Hupp, C.R., 2000. Hydrology, geomorphology and vegetation of Coastal Plain rivers in the south-eastern USA. Hydrological processes, 14(16-17), pp.2991-3010.

Ibrahim, M., Suzuki, A., Yamada, K., Takahashi, S., Yasuda, H., Dohzono, S., Koike, T. and Nakamura, H., 2015. The relationship between cervical and lumbar spine lesions in rheumatoid arthritis with a focus on endplate erosion. Clinical Spine Surgery, 28(3), pp.E154-E160.

Jahadi, M., Afzalimehr, H., Ashrafizaadeh, M. and Kumar, B., 2020. A numerical study on hydraulic resistance in flow with vegetation patch. ISH Journal of Hydraulic Engineering, pp.1-8.

Jahadi, M., Afzalimehr, H. and Rowinski, P.M., 2019. Flow structure within a vegetation patch in a gravel-bed river. Journal of Hydrology and Hydromechanics, 67(2), pp.154-162.

Jahra, F., Yamamoto, H., Hasegawa, F. and Kawahara, Y., 2010. Turbulent flow structure in meandering vegetated open channel. River Flow 2010, pp.153-162.



TH-2690_166152105

James, C.S. and Makoa, M.J., 2006, December. Conveyance estimation for channels with emergent vegetation boundaries. In Proceedings of the Institution of Civil Engineers-Water Management (Vol. 159, No. 4, pp. 235-243). Thomas Telford Ltd.

Jansson, R., Backx, H., Boulton, A.J., Dixon, M., Dudgeon, D., Hughes, F.M.R., Nakamura, K., Stanley, E.H. and Tockner, K., 2005. Stating mechanisms and refining criteria for ecologically successful river restoration: a comment on Palmer et al.(2005). Journal of applied Ecology, 42(2), pp.218-222.

Järvelä, J., 2005. Effect of submerged flexible vegetation on flow structure and resistance. Journal of hydrology, 307(1-4), pp.233-241.

Järvelä, J., 2004. Determination of flow resistance caused by non-submerged woody vegetation. International Journal of River Basin Management, 2(1), pp.61-70.

Järvelä, J., 2002. Flow resistance of flexible and stiff vegetation: a flume study with natural plants. Journal of hydrology, 269(1-2), pp.44-54.

Jordanova, A.A. and James, C.S., 2003. Experimental study of bed load transport through emergent vegetation. Journal of Hydraulic Engineering, 129(6), pp.474-478.

Kang, H. and Choi, S.U., 2006. Reynolds stress modelling of rectangular open-channel flow. International journal for numerical methods in fluids, 51(11), pp.1319-1334.

Kang, H. and Choi, S.U., 2006. Turbulence modeling of compound open-channel flows with and without vegetation on the floodplain using the Reynolds stress model. Advances in Water Resources, 29(11), pp.1650-1664.

Keshavarzi, A., Melville, B. and Ball, J., 2014. Three-dimensional analysis of coherent turbulent flow structure around a single circular bridge pier. Environmental Fluid Mechanics, 14(4), pp.821-847.

Khatua, K.K., Patra, K.C. and Mohanty, P.K., 2012. Stage-discharge prediction for straight and smooth compound channels with wide floodplains. Journal of hydraulic Engineering, 138(1), pp.93-99.

Khatua, K.K., Patra, K.C. and Nayak, P., 2011. Meandering effect for evaluation of roughness coefficients in open channel flow. WIT Transactions on Ecology and the Environment, 146, pp.213-224.

King, A.T., Tinoco, R.O. and Cowen, E.A., 2012. A k–ε turbulence model based on the scales of vertical shear and stem wakes valid for emergent and submerged vegetated flows. Journal of Fluid Mechanics, 701, pp.1-39.

Kirkil, G., Constantinescu, S.G. and Ettema, R., 2008. Coherent structures in the flow field around a circular cylinder with scour hole. Journal of Hydraulic Engineering, 134(5), pp.572-587.

Kitsikoudis, V., Yagci, O., Kirca, V.O. and Kellecioglu, D., 2016. Experimental investigation of channel flow through idealized isolated tree-like vegetation. Environmental Fluid Mechanics, 16(6), pp.1283-1308.

Klopstra, D., Barneveld, H.J., Van Noortwijk, J.M. and Van Velzen, E.H., 1996. Analytical model for hydraulic roughness of submerged vegetation. In Proceedings of the congress-international association for hydraulic research (pp. 775-780). LOCAL ORGANIZING COMMITTEE OF THE XXV CONGRESS.

Koken, M. and Constantinescu, G., 2008. An investigation of the flow and scour mechanisms around isolated spur dikes in a shallow open channel: 1. Conditions corresponding to the initiation of the erosion and deposition process. Water Resources Research, 44(8).



TH-2690_166152105

Kondolf, G.M., Podolak, K. and Grantham, T.E., 2013. Restoring mediterranean-climate rivers. Hydrobiologia, 719(1), pp.527-545.

Kordi, H., Amini, R., Zahiri, A. and Kordi, E., 2015. Improved Shiono and Knight method for overflow modeling. Journal of Hydrologic Engineering, 20(12), p.04015041.

Kothyari, U.C., Garde, R.C.J. and Ranga Raju, K.G., 1992. Temporal variation of scour around circular bridge piers. Journal of Hydraulic Engineering, 118(8), pp.1091-1106.

Kothyari, U.C., Hashimoto, H. and Hayashi, K., 2009. Effect of tall vegetation on sediment transport by channel flows. Journal of Hydraulic Research, 47(6), pp.700-710.

Kouwen, N. and Fathi-Moghadam, M., 2000. Friction factors for coniferous trees along rivers. Journal of hydraulic engineering, 126(10), pp.732-740.

Kouwen, N. and Unny, T.E., 1973. Flexible roughness in open channels. Journal of the Hydraulics Division, 99(5), pp.713-728.

KUBRAK, E., Kubrak, J. and ROWIŃSKI, P.M., 2008. Vertical velocity distributions through and above submerged, flexible vegetation. Hydrological sciences journal, 53(4), pp.905-920.

Laxmi Narayana, P., Timbadiya, P.V. and Patel, P.L., 2021. Vorticity fields around a pier on rigid and mobile bed channels. ISH Journal of Hydraulic Engineering, pp.1-10.

Lee, S.O. and Hong, S.H., 2019. Turbulence characteristics before and after scour upstream of a scaled-down bridge pier model. Water, 11(9), p.1900.

Lee, T.W., 2019. Maximum entropy method for solving the turbulent channel flow problem. Entropy, 21(7), p.675.

Lera, S., Nardin, W., Sanford, L., Palinkas, C. and Guercio, R., 2019. The impact of submersed aquatic vegetation on the development of river mouth bars. Earth Surface Processes and Landforms, 44(7), pp.1494-1506.

Li, S., Liang, W., Fu, B., Lü, Y., Fu, S., Wang, S. and Su, H., 2016. Vegetation changes in recent large-scale ecological restoration projects and subsequent impact on water resources in China's Loess Plateau. Science of the Total Environment, 569, pp.1032-1039.

Li, Y., Wang, Y., Anim, D.O., Tang, C., Du, W., Ni, L., Yu, Z. and Acharya, K., 2014. Flow characteristics in different densities of submerged flexible vegetation from an open-channel flume study of artificial plants. Geomorphology, 204, pp.314-324.

Liu, C., Shan, Y., Liu, X., Yang, K. and Liao, H., 2016. The effect of floodplain grass on the flow characteristics of meandering compound channels. Journal of Hydrology, 542, pp.1-17.

Liu, C., Wright, N., Liu, X. and Yang, K., 2014. An analytical model for lateral depth-averaged velocity distributions along a meander in curved compound channels. Advances in water resources, 74, pp.26-43.

Liu, D., Diplas, P., Fairbanks, J.D. and Hodges, C.C., 2008. An experimental study of flow through rigid vegetation. Journal of Geophysical Research: Earth Surface, 113(F4).

Liu, D., Diplas, P., Hodges, C.C. and Fairbanks, J.D., 2010. Hydrodynamics of flow through double layer rigid vegetation. Geomorphology, 116(3-4), pp.286-296.

Liu, J., Piomelli, U. and Spalart, P.R., 1996. Interaction between a spatially growing turbulent boundary layer and embedded streamwise vortices. Journal of Fluid Mechanics, 326, pp.151-179.



TH-2690_166152105

López, F. and García, M., 1998. Open-channel flow through simulated vegetation: Suspended sediment transport modeling. Water resources research, 34(9), pp.2341-2352.

López, F. and García, M.H., 2001. Mean flow and turbulence structure of open-channel flow through non-emergent vegetation. Journal of Hydraulic Engineering, 127(5), pp.392-402.

McKenney, R., Jacobson, R.B. and Wertheimer, R.C., 1995. Woody vegetation and channel morphogenesis in low-gradient, gravel-bed streams in the Ozark Plateaus, Missouri and Arkansas. Geomorphology, 13(1-4), pp.175-198.

Melville, B.W. and Chiew, Y.M., 1999. Time scale for local scour at bridge piers. Journal of Hydraulic Engineering, 125(1), pp.59-65.

Melville, B.W. and Raudkivi, A.J., 1977. Flow characteristics in local scour at bridge piers. Journal of Hydraulic Research, 15(4), pp.373-380.

Moncho-Esteve, I.J., Folke, F., García-Villalba, M. and Palau-Salvador, G., 2017. Influence of the secondary motions on pollutant mixing in a meandering open channel flow. Environmental Fluid Mechanics, 17(4), pp.695-714.

Moncho-Esteve, I.J., García-Villalba, M., Muto, Y., Shiono, K. and Palau-Salvador, G., 2018. A numerical study of the complex flow structure in a compound meandering channel. Advances in Water Resources, 116, pp.95-116.

Morales, R. and Ettema, R., 2013. Insights from depth-averaged numerical simulation of flow at bridge abutments in compound channels. Journal of Hydraulic Engineering, 139(5), pp.470-481.

Morvan, H.P., 2005. Channel shape and turbulence issues in flood flow hydraulics. Journal of Hydraulic Engineering, 131(10), pp.862-865.

Morvan, H., Pender, G., Wright, N.G. and Ervine, D.A., 2002. Three-dimensional hydrodynamics of meandering compound channels. Journal of Hydraulic Engineering, 128(7), pp.674-682.

Muto, Y. and Ishigaki, T., 1999. Secondary flow in compound sinuous/meandering channels. In Engineering Turbulence Modelling and Experiments 4 (pp. 511-520). Elsevier Science Ltd.

Myers, J.K. and Oas, T.G., 2001. Preorganized secondary structure as an important determinant of fast protein folding. Nature structural biology, 8(6), pp.552-558.

Myers, W.R.C., 1978. Momentum transfer in a compound channel. Journal of Hydraulic Research, 16(2), pp.139-150.

Myers, W.R.C., Lyness, J.F. and Cassells, J., 2001. Influence of boundary roughness on velocity and discharge in compound river channels. Journal of Hydraulic Research, 39(3), pp.311-319.

Neary, V.S., 2003. Numerical solution of fully developed flow with vegetative resistance. Journal of engineering mechanics, 129(5), pp.558-563.

Neary, V.S., Constantinescu, S.G., Bennett, S.J. and Diplas, P., 2012. Effects of vegetation on turbulence, sediment transport, and stream morphology. Journal of Hydraulic Engineering, 138(9), pp.765-776.

Nepf, H. and Ghisalberti, M., 2008. Flow and transport in channels with submerged vegetation. Acta Geophysica, 56(3), pp.753-777.

Nepf, H.M. and Vivoni, E.R., 2000. Flow structure in depth-limited, vegetated flow. Journal of Geophysical Research: Oceans, 105(C12), pp.28547-28557.



TH-2690_166152105

Nepf, H.M., 1999. Drag, turbulence, and diffusion in flow through emergent vegetation. Water resources research, 35(2), pp.479-489.

Newson, M.D., Boon, P.J., Calow, P. and Petts, G.E., 1992. River conservation and catchment management: a UK perspective. In Unknown Host Publication Title. John Wiley & Sons Ltd, Chichester, UK.

Nezu, I. and Sanjou, M., 2008. Turburence structure and coherent motion in vegetated canopy open-channel flows. Journal of hydro-environment research, 2(2), pp.62-90.

Nikora, V., McEwan, I., McLean, S., Coleman, S., Pokrajac, D. and Walters, R., 2007. Double-averaging concept for rough-bed open-channel and overland flows: Theoretical background. Journal of hydraulic Engineering, 133(8), pp.873-883.

Ormerod, S.J., Rundle, S.D., Lloyd, E.C. and Douglas, A.A., 1993. The influence of riparian management on the habitat structure and macroinvertebrate communities of upland streams draining plantation forests. Journal of applied ecology, pp.13-24.

Orth, R.J., Dennison, W.C., Lefcheck, J.S., Gurbisz, C., Hannam, M., Keisman, J., Landry, J.B., Moore, K.A., Murphy, R.R., Patrick, C.J. and Testa, J., 2017. Submersed aquatic vegetation in Chesapeake Bay: sentinel species in a changing world. Bioscience, 67(8), pp.698-712.

Perucca, E., Camporeale, C. and Ridolfi, L., 2009. Estimation of the dispersion coefficient in rivers with riparian vegetation. Advances in Water Resources, 32(1), pp.78-87.

Petryk, S. and Bosmajian III, G., 1975. Analysis of flow through vegetation. Journal of the Hydraulics Division, 101(7), pp.871-884.

Pollen, N., 2007. Temporal and spatial variability in root reinforcement of streambanks: accounting for soil shear strength and moisture. Catena, 69(3), pp.197-205.

Pradhan, C., Bharti, R. and Dutta, S., 2017, July. Assessment of post-impoundment geomorphic variations along Brahmani River using remote sensing. In 2017 IEEE International Geoscience and Remote Sensing Symposium (IGARSS) (pp. 5598-5601). IEEE.

Pujol, D., Colomer, J., Serra, T. and Casamitjana, X., 2010. Effect of submerged aquatic vegetation on turbulence induced by an oscillating grid. Continental Shelf Research, 30(9), pp.1019-1029.

Rahimi, H.R., Tang, X. and Singh, P., 2020. Experimental and numerical study on impact of double layer vegetation in open channel flows. Journal of Hydrologic Engineering, 25(2), p.04019064.

Raudkivi, A.J. and Ettema, R., 1983. Clear-water scour at cylindrical piers. Journal of hydraulic engineering, 109(3), pp.338-350.

Raudkivi, A.J., 1998. Loose boundary hydraulics, Balkema, Rotterdam. The Netherland.

Richardson, J.E. and Panchang, V.G., 1998. Three-dimensional simulation of scour-inducing flow at bridge piers. Journal of Hydraulic Engineering, 124(5), pp.530-540.

Righetti, M., 2008. Flow analysis in a channel with flexible vegetation using double-averaging method. Acta Geophysica, 56(3), pp.801-823.

Robertson, K.M. and Augspurger, C.K., 1999. Geomorphic processes and spatial patterns of primary forest succession on the Bogue Chitto River, USA. Journal of Ecology, 87(6), pp.1052-1063.

Rozovskii, I.L., 1961. Flow of water in bends of open channels: Israel Program for Scientific Translations. Jerusalem, 233p.



TH-2690_166152105

Sand-Jensen, K. and Pedersen, O., 1999. Velocity gradients and turbulence around macrophyte stands in streams. Freshwater Biology, 42(2), pp.315-328.

Sanjou, M., Komatsu, T. and Nezu, I., 2011. Experimental study on secondary currents in wind-induced water waves by stereoscopic PIV. Journal of Japan Society of Civil Engineers, Ser. A2 (Applied Mechanics (AM)), 67(2), pp.I_589-I_598.

Sawyer, J.A., Stewart, P.M., Mullen, M.M., Simon, T.P. and Bennett, H.H., 2004. Influence of habitat, water quality, and land use on macro-invertebrate and fish assemblages of a southeastern coastal plain watershed, USA. Aquatic Ecosystem Health & Management, 7(1), pp.85-99.

Schiavo, L.A., Wolf, W.R. and Azevedo, J.L.F., 2017. Turbulent kinetic energy budgets in wall bounded flows with pressure gradients and separation. Physics of fluids, 29(11), p.115108.

Shan, Y., Liu, C. and Luo, M., 2015. Simple analytical model for depth-averaged velocity in meandering compound channels. Applied Mathematics and Mechanics, 36(6), pp.707-718.

Shimizu, Y., 1994. Numerical analysis of turbulent open-channel flow over a vegetation layer using a κ-ε turbulence model. Journal of Hydroscience and Hydraulic Engineering, JSCE, 11(2), pp.57-67.

Shiono, K. and Knight, D.W., 1991. Turbulent open-channel flows with variable depth across the channel. Journal of fluid mechanics, 222, pp.617-646.

Shiono, K., Muto, Y., Knight, D.W. and Hyde, A.F.L., 1999. Energy losses due to secondary flow and turbulence in meandering channels with overbank flows. Journal of Hydraulic Research, 37(5), pp.641-664.

Shucksmith, J.D., Boxall, J.B. and Guymer, I., 2010. Effects of emergent and submerged natural vegetation on longitudinal mixing in open channel flow. Water Resources Research, 46(4).

Simon, A. and Collison, A.J., 2002. Quantifying the mechanical and hydrologic effects of riparian vegetation on streambank stability. Earth surface processes and landforms, 27(5), pp.527-546.

Singh, P.K., Khatua, K.K. and Banerjee, S., 2021. Flow resistance in straight gravel bed inbank flow with analytical solution for velocity and boundary shear distribution. ISH Journal of Hydraulic Engineering, 27(1), pp.9-22.

Singh, P.K., Tang, X. and Rahimi, H., 2020. A Computational Study of Interaction of Main Channel and Floodplain: Open Channel Flows. Journal of Applied Mathematics and Physics, 8(11), pp.2526-2539.

Siniscalchi, F. and Nikora, V.I., 2012. Flow-plant interactions in open-channel flows: A comparative analysis of five freshwater plant species. Water Resources Research, 48(5).

Siniscalchi, F., Nikora, V.I. and Aberle, J., 2012. Plant patch hydrodynamics in streams: Mean flow, turbulence, and drag forces. Water Resources Research, 48(1).

Solari, L., Van Oorschot, M., Belletti, B., Hendriks, D., Rinaldi, M. and Vargas-Luna, A., 2016. Advances on modelling riparian vegetation—hydromorphology interactions. River Research and Applications, 32(2), pp.164-178.

Sonnenwald, F., Stovin, V. and Guymer, I., 2016. Feasibility of the porous zone approach to modelling vegetation in CFD. In Hydrodynamic and mass transport at freshwater aquatic interfaces (pp. 63-75). Springer, Cham.



TH-2690_166152105

Stephan, U. and Gutknecht, D., 2002. Hydraulic resistance of submerged flexible vegetation. Journal of Hydrology, 269(1-2), pp.27-43.

Stewart, R., Hotopf, M., Dewey, M., Ballard, C., Bisla, J., Calem, M., Fahmy, V., Hockley, J., Kinley, J., Pearce, H. and Saraf, A., 2014. Current prevalence of dementia, depression and behavioural problems in the older adult care home sector: the South East London Care Home Survey. Age and ageing, 43(4), pp.562-567.

Stoesser, T., Kim, S.J. and Diplas, P., 2010. Turbulent flow through idealized emergent vegetation. Journal of Hydraulic Engineering, 136(12), pp.1003-1017.

Stoesser, T., Salvador, G.P., Rodi, W. and Diplas, P., 2009. Large eddy simulation of turbulent flow through submerged vegetation. Transport in porous media, 78(3), pp.347-365.

Stoesser, T., Wilson, C.A.M.E., Bates, P.D. and Dittrich, A., 2003. Application of a 3D numerical model to a river with vegetated floodplains. Journal of Hydroinformatics, 5(2), pp.99-112.

Stone, B.M. and Shen, H.T., 2002. Hydraulic resistance of flow in channels with cylindrical roughness. Journal of hydraulic engineering, 128(5), pp.500-506.

Sun, W., Song, X., Mu, X., Gao, P., Wang, F. and Zhao, G., 2015. Spatiotemporal vegetation cover variations associated with climate change and ecological restoration in the Loess Plateau. Agricultural and Forest Meteorology, 209, pp.87-99.

Sun, X. and Shiono, K., 2009. Flow resistance of one-line emergent vegetation along the floodplain edge of a compound open channel. Advances in Water Resources, 32(3), pp.430-438.

Tanino, Y. and Nepf, H.M., 2008. Laboratory investigation of mean drag in a random array of rigid, emergent cylinders. Journal of Hydraulic Engineering, 134(1), pp.34-41.

Temple, D.M., 1986. Velocity distribution coefficients for grass-lined channels. Journal of Hydraulic Engineering, 112(3), pp.193-205.

Tennekes, H. and Lumley, J.L., 1972. Spectral dynamics.

Tennekes, H. and Lumley, J.L., 2018. A first course in turbulence. MIT press.

Tominaga, A. and Nezu, I., 1991. Turbulent structure in compound open-channel flows. Journal of Hydraulic Engineering, 117(1), pp.21-41.

Trinci, G., Harvey, G.L., Henshaw, A.J., Bertoldi, W. and Hölker, F., 2017. Life in turbulent flows: interactions between hydrodynamics and aquatic organisms in rivers. Wiley interdisciplinary reviews: Water, 4(3), p.e1213.

Tseng, M.H., Yen, C.L. and Song, C.C., 2000. Computation of three-dimensional flow around square and circular piers. International journal for numerical methods in fluids, 34(3), pp.207-227.

Türker, U., Yagci, O. and Kabdaşlı, M.S., 2006. Analysis of coastal damage of a beach profile under the protection of emergent vegetation. Ocean Engineering, 33(5-6), pp.810-828.

Unger, J. and Hager, W.H., 2007. Down-flow and horseshoe vortex characteristics of sediment embedded bridge piers. Experiments in Fluids, 42(1), pp.1-19.

Vargas-Luna, A., Crosato, A., Anders, N., Hoitink, A.J., Keesstra, S.D. and Uijttewaal, W.S., 2018. Morphodynamic effects of riparian vegetation growth after stream restoration. *Earth Surface Processes and Landforms*, *43*(8), pp.1591-1607.



TH-2690_166152105

Vargas-Luna, A., Crosato, A., Hoitink, A., Groot, J. and Uijttewaal, W., 2016. Effects of riparian vegetation development in a restored lowland stream. In River Flow.

Velasco, D., Bateman, A. and Medina, V., 2008. A new integrated, hydro-mechanical model applied to flexible vegetation in riverbeds. Journal of Hydraulic Research, 46(5), pp.579-597.

Wang, C., Zheng, S.S., Wang, P.F. and Hou, J., 2015. Interactions between vegetation, water flow and sediment transport: A review. Journal of Hydrodynamics, 27(1), pp.24-37.

Wang, Y., Li, S. and Luo, D., 2009. Seasonal response of Asian monsoonal climate to the Atlantic Multidecadal Oscillation. Journal of Geophysical Research: Atmospheres, 114(D2).

Wilson, C.A.M.E., 2007. Flow resistance models for flexible submerged vegetation. Journal of Hydrology, 342(3-4), pp.213-222.

Wilson, C.A.M.E., Stoesser, T., Bates, P.D. and Pinzen, A.B., 2003. Open channel flow through different forms of submerged flexible vegetation. Journal of Hydraulic Engineering, 129(11), pp.847-853.

Wilson, J.R., Ajuonu, O., Center, T.D., Hill, M.P., Julien, M.H., Katagira, F.F., Neuenschwander, P., Njoka, S.W., Ogwang, J., Reeder, R.H. and Van, T., 2007. The decline of water hyacinth on Lake Victoria was due to biological control by Neochetina spp. Aquatic Botany, 87(1), pp.90-93.

Wu, F.C., Shen, H.W. and Chou, Y.J., 1999. Variation of roughness coefficients for unsubmerged and submerged vegetation. Journal of hydraulic Engineering, 125(9), pp.934-942.

Xu, Y. and Nepf, H., 2020. Measured and predicted turbulent kinetic energy in flow through emergent vegetation with real plant morphology. Water Resources Research, 56(12), p.e2020WR027892.

Yagci, O., Tschiesche, U. and Kabdasli, M.S., 2010. The role of different forms of natural riparian vegetation on turbulence and kinetic energy characteristics. Advances in water Resources, 33(5), pp.601-614.

Yang, K., Cao, S. and Knight, D.W., 2007. Flow patterns in compound channels with vegetated floodplains. Journal of Hydraulic Engineering, 133(2), pp.148-159.

Zhang, C., Miorini, R. and Katz, J., 2015. Integrating Mach–Zehnder interferometry with TPIV to measure the time-resolved deformation of a compliant wall along with the 3D velocity field in a turbulent channel flow. Experiments in Fluids, 56(11), pp.1-22.

Zhang, J., Tian, H., Yao, Z., Hao, P. and Jiang, N., 2015. Mechanisms of drag reduction of super hydrophobic surfaces in a turbulent boundary layer flow. Experiments in Fluids, 56(9), pp.1-13.

Zhang, H., Wang, Z., Dai, L. and Xu, W., 2015. Influence of vegetation on turbulence characteristics and reynolds shear stress in partly vegetated channel. Journal of Fluids Engineering, 137(6).

Zhang, Y., Lai, X., Zhang, L., Song, K., Yao, X., Gu, L. and Pang, C., 2020. The influence of aquatic vegetation on flow structure and sediment deposition: A field study in Dongting Lake, China. Journal of Hydrology, 584, p.124644.

Zong, L. and Nepf, H., 2011. Spatial distribution of deposition within a patch of vegetation. Water Resources Research, 47(3).



TH-2690_166152105